Effective field theories in a finite volume and lattice QCD

Akaki Rusetsky

(儒赛斯基, 阿卡基)

Helmholtz-Institut für Strahlen- und Kernphysik (Theorie) and

Bethe Center for Theoretical Physics,
Universität Bonn, Nussallee 14-16, D-53115 Bonn, Germany

and

High Energy Physics Institute, Tbilisi State University,
10, G. Danelia str., 0186 Tbilisi, Georgia

Lecture course, 9-11 April 2024, ITP, CAS (Beijing)

Disclaimer: These are working notes, may still contain typos.

1 Introduction: what will be addressed in the lectures?

Nowadays, it is commonly accepted that the fundamental theory of strong interactions is Quantum Chromodynamics (QCD), which describes interactions between quarks and gluons. The quarks are spin-1/2 particles carrying 6 different flavors u, d, s, c, b, t, with the masses ranging approx. from 2 MeV to 173 GeV. The interactions between quarks is mediated by gluons, which are the (massless) gauge bosons of unbroken $SU(3)_c$ local symmetry (the corresponding quantum number is called color).

$SU(3)$ is a non-Abelian group, implying that, even in the absence of the quark fields, the gluons interact with each other. These self-interactions lead to the confinement: the observed spectrum of QCD contains only colorless objects – hadrons – which are made of quarks and gluons. In the naive quark models, all existing mesons are made up of a quark and an antiquark, and baryons consist of three quarks, everything bound together by gluons (of course, more complex objects, which are not covered by the naive quark model, can and do exist in Nature, like tetra- and pentaquarks, glueballs, etc.). The gluon interactions grow very strong at large distances (equivalently, as small momentum scales), so that a colored object cannot escape into the asymptotic state. On the contrary, at short distances (at large momenta), the quark-gluon interactions are weak and can be handled in perturbation theory. This is shown in Fig 1, where the dependence of the renormalized strong coupling constant on the momentum scale is shown.

In the following, we shall be exclusively concentrated at the physics at small momentum scales, of order of the dynamically generated QCD scale Λ_{QCD} (for this reason, we can safely neglect the presence of heavy quarks with $m_c, m_b, m_t \gg \Lambda_{QCD}$ and consider QCD with light u, d, s quark flavors only). At these scales, QCD becomes a strongly coupled non-local field theory, for which the perturbation theory cannot be applied. How does one calculate the characteristics of light hadrons from the underlying theory in this case?

In my lectures, I shall consider two very powerful tools which can be used to systematically deal with QCD at low energy. The first is an approach based on the effective chiral Lagrangians, which makes use of the so-called chiral symmetry of QCD in the light quark sector. This symmetry is spontaneously broken in the QCD vacuum and an octet of almost massless pseudoscalar Goldstone bosons (π-, K- and η-mesons) emerges, dominating the physical processes at low energy. The chiral symmetry of the underlying theory imposes severe constraints on the form of the possible operators that can enter the Lagrangian describing these Goldstone bosons and their interactions with other hadrons, and this fact renders predictive power to the effective theory. However, this approach does not completely solve the problem – the values of the couplings in the effective Lagrangian are not fixed by the symmetry requirements and should be determined independently.

Another approach, the so-called lattice QCD, is based on the formulation of QCD

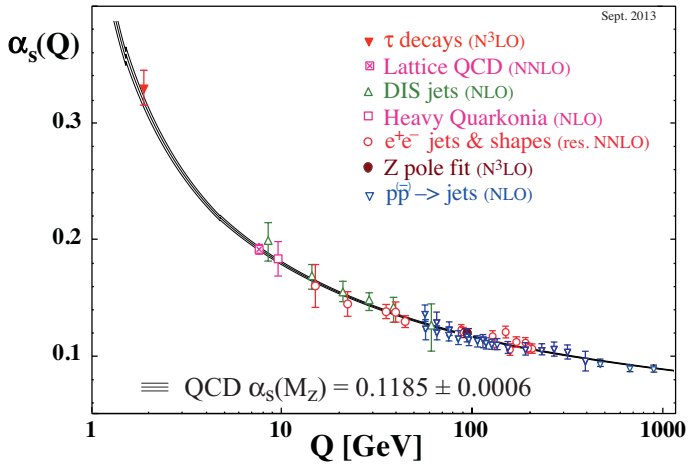

Figure 1: The running coupling constant in QCD (figure from: arXiv:1506.05407).

in terms of Euclidean path integrals. The latter are defined as ordinary multiple integrals on a discretized space-time grid (lattice) and are calculated numerically by using various Monte-Carlo algorithms. The continuum limit emerges, when the lattice spacing is taken very small, and its volume very large, both in the physical units characterizing strong interactions at low energy. Potentially, this approach has capability to describe all low-energy sector of QCD in terms of the parameters of the underlying QCD Lagrangian only (in particular, it can address the calculation of the low-energy effective couplings, mentioned in the previous paragraph). In practice, it is a fascinating approach facing numerous conceptual and calculational challenges. One of these challenges forms the main topic of the present lectures.

As mentioned above, the lattice used in the calculations is always finite. This means that the hadrons, which are simulated on the lattice, are always confined to a box, whose size in physical units, on the present-day lattices, is not even very large. Thus, finite-volume artifacts emerge in the physical observables, calculated on the lattice. Moreover, the hadron scattering processes are absent in a finite volume from the beginning, because asymptotic states cannot be defined. Then, how does one extract the physical quantities in the scattering sector (say, the phase shifts or the cross sections) from the lattice QCD calculations?

It turns out that effective field theory methods and the lattice methods beautifully complement each other, when it comes to the study of the finite-volume effects. In these lectures I shall demonstrate that, using effective field theories in a finite volume, it is possible to find a systematic solution of the problems mentioned above.

I tried to make the presentation self-contained, as far as it was possible. In the beginning, I give a very brief introduction to the path integral and introduce lattice in the non-relativistic quantum mechanics. The lattice artifacts that we are speaking about, emerge already there, as demonstrated in a couple of very simple

examples. Then I give a very brief introduction to lattice QCD and effective field theory methods, both only in order to set notations. Next, finally, I turn to the main topic of the lectures and consider the finite-volume effects, both in the properties of stable hadrons as well as in the scattering problems. In all cases, we shall illustrate the formalism with simple examples that help to better understand the material.

Finally, note that not all the material, contained in these lecture notes, will be covered during the lectures. I have however kept this additional material, which can be used for the in-depth understanding of the questions addressed in the lectures.

2 One-dimensional quantum mechanics on the lattice

2.1 Path integral formulation of quantum mechanics

The formulation of quantum field theory on he lattice is based on the path integral representation of Green functions. In order to make the presentation self-contained, below we shall briefly consider the essentials of the lattice formulation, starting from the simplest case of quantum mechanics in one dimension, described by the Hamiltonian

$$\hat{H} = \frac{\hat{p}^2}{2m} + \hat{V}(x)\,. \tag{1}$$

Here, $\hat{p}$ is the momentum operator of a particle with mas m, moving in the potential $\hat{V}(x)$. The evolution operator is given by:

$$U(t',t) = e^{-i\hat{H}(t'-t)}\,. \tag{2}$$

If the evolution operator is explicitly known for all times, one has found the complete solution of the problem: given any initial state of a system, described by the wave function $\Psi(x,t)$, the state at any other time t', with $t' > t$, is given by

$$\Psi(x',t') = \int_{-\infty}^{\infty} dx \langle x'|e^{-i\hat{H}(t'-t)}|x\rangle \Psi(x,t)\,. \tag{3}$$

In order to find the representation of the evolution operator in terms of path integrals, we divide the interval $[t',t]$ into N small intervals of a length a, so that $t'-t = Na$ (see Fig. 2). The evolution between t and t' is then represented, as a superposition of evolution between t and $t+a$, between $t+a$ and $t+2a$, and so on. Thus:

$$\langle x'|e^{-i\hat{H}(t'-t)}|x\rangle = \int_{-\infty}^{\infty} dx_1 \cdots dx_{N-1} \langle x'|e^{-i\hat{H}a}|x_{N-1}\rangle \cdots \langle x_1|e^{-i\hat{H}a}|x\rangle\,. \tag{4}$$

Taking a infinitesimally small, one can calculate matrix elements, entering this expression:

$$\begin{aligned} \langle x'|e^{-i\hat{H}a}|x\rangle &= \int \frac{dp}{2\pi} \langle x'|p\rangle\langle p|1 - ia\hat{H} + O(a^2)|x\rangle \\ &= \int \frac{dp}{2\pi} e^{ip(x'-x)} \left(1 - ia\left[\frac{p^2}{2m} + V(x)\right] + O(a^2)\right). \end{aligned} \tag{5}$$

If we had inserted the unit operator $1 = \int \frac{dp}{2\pi} |p\rangle\langle p|$ in front of the ket-vector $|x\rangle$, we would get $V(x')$ instead of $V(x)$. Bearing this in mind, we shall use the symmetric

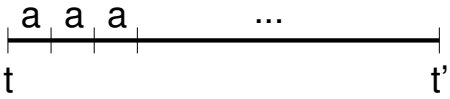

Figure 2: Discretization of the time interval: $t' - t = Na$.

expression:

$$\begin{aligned}\langle x'|e^{-i\hat{H}a}|x\rangle &= \int \frac{dp}{2\pi}\, e^{ip(x'-x)}\left(1 - ia\left[\frac{p^2}{2m} + \frac{1}{2}\left(V(x') + V(x)\right)\right] + O(a^2)\right) \\ &= \int \frac{dp}{2\pi}\, \exp\left(ip(x'-x) - ia\left[\frac{p^2}{2m} + \frac{1}{2}\left(V(x') + V(x)\right)\right] + O(a^2)\right).\end{aligned} \tag{6}$$

The difference between all above expressions in a quantity of order a^2.

Finally, performing the (Gaussian) integration in this formula by using

$$\int_{-\infty}^{\infty} dp \exp(-Ap^2) = \sqrt{\frac{\pi}{A}}\,, \tag{7}$$

we get

$$\langle x'|e^{-i\hat{H}a}|x\rangle = \left(\frac{m}{2\pi ia}\right)^{1/2} \exp\left(ia\left[\frac{m}{2}\left(\frac{x'-x}{a}\right)^2 - \frac{1}{2}\left(V(x') + V(x)\right)\right]\right). \tag{8}$$

In the limit $a \to 0$, we have $x' \to x$ and $\dfrac{x'-x}{a} \to \dot{x} = v$, where v is the velocity along the classical trajectory from x to x'. Consequently, the above expression can be rewritten as:

$$\begin{aligned}\langle x'|e^{-i\hat{H}a}|x\rangle &= \left(\frac{m}{2\pi ia}\right)^{1/2} \exp\left(ia\left[\frac{m\dot{x}^2}{2} - V(x)\right]\right) \\ &= \left(\frac{m}{2\pi ia}\right)^{1/2} \exp\Big(ia\mathcal{L}(x)\Big)\,.\end{aligned} \tag{9}$$

where $\mathcal{L}(x) = \dfrac{m\dot{x}^2}{2} - V(x)$ is the classical Lagrangian of a particle, moving in the external potential $V(x)$.

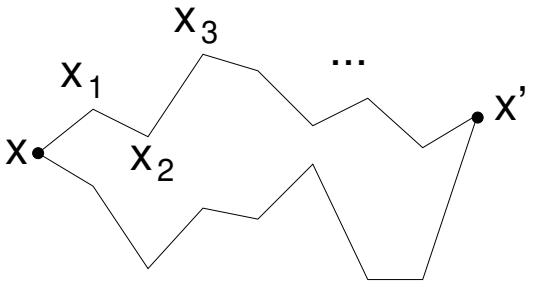

Figure 3: The path integral is performed over all trajectories, connecting the points x and x'.

The evolution operator at finite times is given by:

$$\begin{aligned}
\langle x'|e^{-i\hat{H}(t'-t)}|x\rangle &= \left(\frac{m}{2\pi i a}\right)^{N/2} \int_{-\infty}^{\infty} \prod_{i=1}^{N-1} dx_i \\
&\times \exp\left(ia \left[\frac{m}{2} \left(\frac{x'-x_{N-1}}{a} \right)^2 + \cdots + \frac{m}{2} \left(\frac{x_1 - x}{a} \right)^2 \right] \right) \\
&\times \exp\left(-ia \left[\frac{1}{2} V(x') + V(x_{N-1}) + \cdots + V(x_1) + \frac{1}{2} V(x) \right] \right) \\
&\doteq \int \mathcal{D}x \exp\left(i \int_t^{t'} d\tau \mathcal{L}(x(\tau)) \right) . \qquad (10)
\end{aligned}$$

Here the integration is carried out over all trajectories that go from x to x', see Fig. 3.

To summarize, path integrals provide an alternative formulation of quantum mechanics, completely equivalent to the Schrödinger and Heisenberg formulations. In this formulation, one obtains a representation of the evolution operator in terms of a path integral. The latter is defined as a multiple integral over $dx_1 \ldots dx_{N-1}$ in the limit, when $a \to 0$ and $N \to \infty$. This representation provides a basis for the calculations on the lattice. Schematically, the argument goes as follows. One can perform the integration over $dx_1 \ldots dx_{N-1}$ numerically and decrease a for fixed $t'-t$, until the calculated results become stable with respect to the further decrease. Then, one would claim that one is obtaining results already in the continuum limit.

Of course, the above argument is given for illustrative purpose only. To apply these ideas in practice, one has to refine them substantially.

2.2 Euclidean formulation

To start with, the path integral is rigorously defined in the Euclidean space only. In Minkowski space, the argument of the exponential is a wildly oscillating function

on the trajectories, which are far from the local minima of the action functional, coinciding with the solutions of the classical equations of motion:

$$\frac{d}{dt}\,\frac{\delta\mathcal{L}}{\delta\dot{x}(t)} - \frac{\delta\mathcal{L}}{\delta x(t)}\bigg|_{x(t)=x_{cl}(t)} = 0\,. \tag{11}$$

Consequently, in the strict mathematical sense, the limit $a \to 0$ does not exist in the Minkowski space, and an analytic continuation to the Euclidean space (Wick rotation) is necessary.

Below, for simplicity of the argument, we shall assume that the potential $V(x)$ is bound from below. Then, without losing generality, one may assume $V(x) > 0$. In Eq. (8) one may then perform the Wick rotation:

$$a = |a|e^{-i\varphi}\,, \qquad 0 \le \varphi \le \frac{\pi}{2}\,. \tag{12}$$

Then the real part of the argument takes the form:

$$\begin{aligned} &\mathrm{Re}\left(i\left[\frac{m}{2|a|e^{-i\varphi}}\,(x'-x)^2 - \frac{|a|e^{-i\varphi}}{2}\,(V(x')+V(x))\right]\right) \\ = \;& -\sin\varphi\left[\frac{m}{2|a|}\,(x'-x)^2 + \frac{|a|}{2}\,(V(x')+V(x))\right] < 0\,. \end{aligned} \tag{13}$$

Hence, the oscillating exponent transforms into the damping one, and the integral is convergent. This means that the analytic continuation is allowed. Taking $\varphi = \dfrac{\pi}{2}$, we arrive at the Euclidean evolution operator:

$$\langle x'|e^{-\hat{H}(t'-t)}|x\rangle = \int \mathcal{D}x \exp\Big(-S[x]\Big)\,, \tag{14}$$

where the Euclidean action functional is given by:

$$\begin{aligned} S[x] \;&=\; a\left[\frac{m}{2}\left(\frac{x'-x_{N-1}}{a}\right)^2 + \cdots + \frac{m}{2}\left(\frac{x_1-x}{a}\right)^2\right] \\ &+\; a\left[\frac{1}{2}\,V(x') + V(x_{N-1}) + \cdots + V(x_1) + \frac{1}{2}\,V(x)\right], \end{aligned} \tag{15}$$

and the integration measure takes the form

$$\mathcal{D}x = \left(\frac{m}{2\pi a}\right)^{N/2} \prod_{i=1}^{N-1} dx_i\,. \tag{16}$$

Note the change of sign in front of the potential.

2.3 The spectral representation

Suppose that $|n\rangle$ are the eigenvectors of the Hamiltonian, corresponding to the eigenvalue E_n. The set of states $|n\rangle$ obeys closure elation:

$$\sum_n |n\rangle\langle n| = 1\,. \tag{17}$$

Thus,

$$\langle x'|e^{-\hat{H}(t'-t)}|x\rangle = \sum_n \langle x'|n\rangle\langle n|x\rangle e^{-E_n(t'-t)} = \sum_n \Psi_n(x')\Psi_n^*(x)e^{-E_n(t'-t)}\,. \tag{18}$$

Note: the spectrum and the eigenvectors are the same in the Euclidean and Minkowski spaces, since the Hamiltonian does not depend on time.

At large Euclidean times, the ground-state $n = 0$ contribution dominates the sum, and we have:

$$\langle x'|e^{-\hat{H}(t'-t)}|x\rangle \sim e^{-E_0(t'-t)}\Psi_0(x')\Psi_0^*(x)\left\{1 + O(e^{-(E_1-E_0)(t'-t)})\right\}. \tag{19}$$

The state with the lowest energy $|n\rangle = |0\rangle$ is usually called the vacuum state.

2.4 The Green functions

The Green functions are the vacuum expectation values of the T-ordered products of operators:

$$G(t_1, \cdots, t_n) = \langle 0|T\hat{A}(t_1)\cdots\hat{A}(t_n)|0\rangle\,. \tag{20}$$

We assume that $\hat{A}(t) \doteq \hat{A}(x(t))$ are local operators, depending on $x = x(t)$ at time t only. The time-ordered product is defined as:

$$T\hat{A}(t_1)\hat{A}(t_2) = \begin{cases} \hat{A}(t_1)\hat{A}(t_2)\,, & t_1 > t_2 \\ \hat{A}(t_2)\hat{A}(t_1)\,, & t_2 > t_1 \end{cases} \tag{21}$$

The generalization to the case of more than two operators is straightforward.

In order to derive the path integral representation of Green functions, assume, for instance that $t_1 > t_2$. Next, let us consider

$$\begin{aligned} \langle x'|e^{-\hat{H}t'}\hat{A}(t_1)\hat{A}(t_2)e^{\hat{H}t}|x\rangle &= \int_{-\infty}^{\infty} dx_1 dx_2 \langle x'|e^{-\hat{H}(t'-t_1)}|x_1\rangle A(x_1)\langle x_1|e^{-\hat{H}(t_1-t_2)}|x_2\rangle \\ &\times\ A(x_2)\langle x_2|e^{-\hat{H}(t_1-t)}|x\rangle \\ &\doteq \int \mathcal{D}x A(x_1)A(x_2)e^{-S}\,. \end{aligned} \tag{22}$$

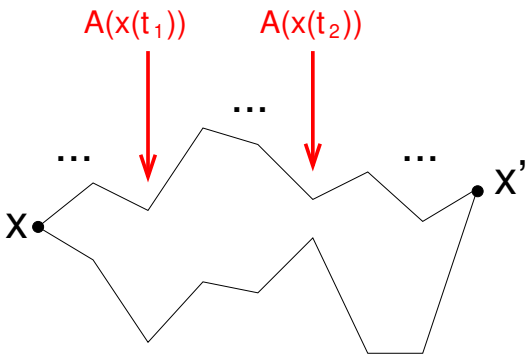

Figure 4: Two insertions in the path integral $\int \mathcal{D}x A(x(t_1))A(x(t_2))e^{-S}$.

This is a path integral with two insertions at $t = t_1$ and $t = t_2$, see Fig. 4.

Next, one can use closure relation. In the limit $t' \to \infty,\ t \to -\infty$, one gets:

$$\begin{aligned}\langle x'|e^{-\hat{H}t'}\hat{A}(t_1)\hat{A}(t_2)e^{\hat{H}t}|x\rangle &= \sum_{n'n}\langle x'|n'\rangle e^{-E_{n'}t'}\langle n'|\hat{A}(t_1)\hat{A}(t_2)|n\rangle e^{E_n t}\langle n|x\rangle \\ &\sim \Psi_0(x')\Psi_0^*(x)e^{-E_0(t'-t)}\langle 0|\hat{A}(t_1)\hat{A}(t_2)|0\rangle\,. \end{aligned} \tag{23}$$

Consequently,

$$\langle 0|\hat{A}(t_1)\hat{A}(t_2)|0\rangle = \lim_{t'\to\infty,\ t\to-\infty}\frac{\int \mathcal{D}x A(x(t_1))A(x(t_2))e^{-S}}{\int \mathcal{D}x e^{-S}}\,. \tag{24}$$

The same expression is obtained, when $t_1 < t_2$. Hence, the path integral representation of the two-point Euclidean Green function $\langle 0|T\hat{A}(t_1)\hat{A}(t_2)|0\rangle$ is given by the right-hand side of Eq. (24) for all times t_1, t_2. The generalization to the case of the Green functions with more external legs is straightforward.

The path integral, entering the above expression, still depends on x, x'. It is convenient to impose periodic boundary conditions $x' = x = x_0$ and integrate over x_0 as well. Using the normalization of the wave function

$$\int_{-\infty}^{\infty} dx|\Psi_0(x)|^2 = 1\,, \tag{25}$$

we finally get:

$$\langle 0|T\hat{A}(t_1)\hat{A}(t_2)|0\rangle = \lim_{t'\to\infty,\ t\to-\infty}\frac{\int \mathcal{D}x A(x(t_1))A(x(t_2))e^{-S}}{\int \mathcal{D}x e^{-S}}\,, \tag{26}$$

where, now,

$$S = \frac{m}{2a}\left[(x_0 - x_{N-1})^2 + \cdots + (x_1 - x_0)^2\right] + a\left[V(x_{N-1}) + \cdots + V(x_0)\right],$$

$$\mathcal{D}x \propto \prod_{i=0}^{N-1} dx_i\,, \tag{27}$$

and

$$A(x(t_1))A(x(t_2)) = \frac{1}{N}\sum_{i=0}^{N-1} A(x_{i+k})A(x_i)\,, \qquad t_1 - t_2 = ka\,. \tag{28}$$

Note also that, due to the translational invariance, the result does not depend on the choice of the starting point i. One may use this fact to average the expression over all i that improves the statistical error during the numerical evaluation of the integral (see below).

The energy spectrum of the Hamiltonian can be extracted directly from the Euclidean two-point Green functions without continuing analytically back to the Minkowski space. Indeed, using the closure relation, at large Euclidean times $t_1 - t_2 \to \infty$ we get:

$$\langle 0|T\hat{A}(t_1)\hat{A}(t_2)|0\rangle \sim e^{-(E_n - E_0)(t_1 - t_2)}|\langle 0|\hat{A}(0)|n\rangle|^2\,, \tag{29}$$

where $|n\rangle$ is the eigenvector of the Hamiltonian with the lowest eigenvalue, for which the matrix element $\langle 0|\hat{A}(0)|n\rangle$ does not vanish.

Consider, for example, the one-dimensional harmonic oscillator. Due to the invariance under parity, the following matrix element vanishes identically:

$$\langle 0|\hat{x}(0)|0\rangle = 0\,, \tag{30}$$

but the overlap of the vector $\hat{x}(0)|0\rangle$ with the first excited state does not vanish:

$$\langle 0|\hat{x}(0)|1\rangle \neq 0\,. \tag{31}$$

Consequently, calculating the Green function of two operators $\hat{x}(t)$, one may extract the difference between the energies of the first excited state and the ground state:

$$E_1 - E_0 = \lim_{t\to\infty}\frac{1}{t}\,\langle 0|T\hat{x}(t)\hat{x}(0)|0\rangle\,. \tag{32}$$

The quantity in the right-hand side of the above equation for finite values of t is called effective mass.

The determination of particle spectrum in lattice QCD (and, in general, in any lattice quantum field theory) follows exactly the same path. Namely, the Euclidean two-point functions of operators with pertinent quantum numbers is evaluated numerically, and the spectrum is determined by finding the plateaus of the effective mass at large Euclidean times.

2.5 Calculation of the path integral by using Monte-Carlo method

The discretized path integral on the lattice should be evaluated by using numerical methods. The usual numerical quadratures are hopelessly slow in case of a large number of integration variables, and so one has to invoke the Monte-Carlo method. We explain the essence of the method for the example of a simple one-dimensional integral:

$$\langle f \rangle = \int_a^b ds f(s) w(s) \,. \tag{33}$$

Here, we assume that the function $f(s)$ is smooth and slowly varying on the interval $[a, b]$. Further,

$$w(s) \in [0, 1] \,, \qquad \int_a^b ds w(s) = 1 \,. \tag{34}$$

The function $w(s)$ can be interpreted as the probability density. Consider now the set of points $s_1, \ldots, s_n \in [a, b]$ which, in the limit of large n, are distributed on this interval with the probability density $w(s)$. Then, it is clear that

$$\langle f \rangle = \lim_{n\to\infty} \frac{1}{n} \sum_{i=1}^{n} f(s_i) \,. \tag{35}$$

If n grows larger, the mean square deviation decreases like $\dfrac{1}{\sqrt{n}}$. Indeed,

$$\sigma^2 = \frac{1}{n}\left\{ \langle f^2 \rangle - \langle f \rangle^2 \right\} = \frac{1}{n} \left\{ \frac{1}{n} \sum_{i=1}^{n} f^2(s_i) - \left(\frac{1}{n} \sum_{i=1}^{n} f(s_i) \right)^2 \right\} . \tag{36}$$

Since both $\langle f^2 \rangle$ and $\langle f \rangle$ have finite limits at $n \to \infty$, one may conclude that $\sqrt{\sigma^2} \sim \dfrac{1}{\sqrt{n}}$.

In case of many integration variables, $s_k = (x_0^{(k)}, \ldots x_{N-1}^{(k)})$ denote the so-called configurations. The $\dfrac{1}{\sqrt{n}}$-rule holds in this case as well. Note that, in order to achieve reasonable accuracy, n need not be astronomically large and the calculations can be performed on modern computers.

Moreover, a typical path integral (say, for the two-point function) takes the following form:

$$\langle 0 | T \hat{A}(t_1) \hat{A}(t_2) | 0 \rangle \sim \int \mathcal{D}x A(x(t_1)) A(x(t_2)) e^{-S} \,. \tag{37}$$

An exponential factor rapidly vanishes away from the local minima of the Euclidean action. For this reason, distributing the configurations uniformly in the whole integration area would not be an optimal strategy: in this case, the integrand would be very small on most of the configurations. A better strategy assumes that $A(x(t_1))A(x(t_2))$ and e^{-S} play the role of the functions $f(s)$ and $w(s)$, respectively, so the most configurations are concentrated in the vicinity of Euclidean classical trajectories, which are minima of the action functional S.

There exist different algorithms that allow one to produce a sequence of configurations $s_1, \ldots, s_n$, distribute with a given probability $w(s)$. All these algorithms have to start at some arbitrary initial configuration s_1 and produce a chain $s_1 \to s_2 \to s_3 \to \ldots$ by defining a random update of a given configuration.

At the next step, one has to decide, whether one accepts the configuration, produced in the random update, or rejects it. We denote the acceptance probability by $w_{acc}(s \to s')$. If the configuration is accepted, it becomes a new member of the set and the process goes on.

In order to ensure that the configurations are distributed with the probability density $w(s)$, the acceptance probability should obey the equation of the detailed balance:

$$w(s)w_{acc}(s \to s') = w(s')w_{acc}(s' \to s)\,. \tag{38}$$

In practice, one deletes first few members of the set, in order to assume that the configurations have fully thermalized, i.e., all information about the initial configuration has been completely erased.

Various algorithms differ through choice of the update and acceptance criteria. Here, for illustrative purpose only, we briefly consider perhaps the simplest one, which goes under the name of the Metropolis algorithm. In this algorithm, the acceptance probability is given by the following expression:

$$w_{acc}(s \to s') = \min\left\{1, e^{-\Delta S}\right\}, \qquad \Delta S = S[s'] - S[s]\,. \tag{39}$$

Recalling that

$$w(s) = \frac{e^{-S[s]}}{\int \mathcal{D}x e^{-S}}\,, \tag{40}$$

it can be straightforwardly checked that the detailed balance is indeed obeyed.

If you decide to carry out a simple simulation in the one-dimensional quantum-mechanical problem, considered above, one may, for example, proceed along the following path:

- Choose some initial configuration, say, $x_i^{(1)} = 0$, $i = 0, \ldots N-1$.

- Define a random update. To this end, choose i randomly, produce a random number $0 < r < 1$ and define $x_i' = x_i + \Delta x_i = x_i + \beta(2r-1)$. Here, β is some fixed constant. If β is very small, the update is very slow. If β is large, acceptance rate will be very small. One has to choose an optimal value of β by trial and error method, in order to make the code faster.

- Calculate the change of the action under the update. Since the action is local, this expression contains only few terms:

$$\Delta S = -\Delta x_i \frac{x_{i+1} - 2x_i + x_{i-1}}{a} + \frac{(\Delta x_i)^2}{a} + a(V(x_i + \Delta x_i) - V(x_i))\,. \qquad (41)$$

- If $\Delta S < 0$, then the new configuration should be accepted. If $\Delta S > 0$, then it should be accepted with the probability $e^{-\Delta S}$. In order to do this, produce a new random number $0 < r' < 1$ and then accept, if $r' < e^{-\Delta S}$, otherwise reject.

- Continue, until the required number of configurations is produced.

Using this algorithm, you could write a simple code and try to extract the energy spectrum on the lattice yourself!

2.6 Numerical artifacts

The main aim of present lectures is not the lattice formulation of quantum mechanics and quantum field theory per se, but the introduction to what is called lattice artifacts and, most notably, to the finite-volume effects. The latter issue has attracted much attention lately. Moreover, the methods that are used to study finite-volume effects became the main tool for the extraction of the observables in the scattering sector from lattice calculations – in this sense, the finite-volume effects cannot be regarded as pure artifacts anymore.

To start with, any lattice calculation, even performed with a very large number of configurations (i.e., with an arbitrary small statistical error) still contains artifacts. In other words, the extracted quantity is not exactly equal to the same quantity in the continuum. For illustrative purposes, we shall first introduce these artifacts in the simple case of harmonic oscillator.

The Euclidean action in this example is given by (in order to ease notations, we have assumed $m = 1$):

$$S = \sum_{i=0}^{N-1} a\left\{\frac{1}{2}\left(\frac{x_{i+1} - x_i}{a}\right)^2 + \frac{\omega^2 x_i^2}{2}\right\}, \qquad x_N = x_0\,. \qquad (42)$$

Let us consider the quantity

$$\langle x|e^{-\hat{H}T}|x\rangle = \sum_n |\langle x|n\rangle|^2 e^{-E_n T} \sim |\Psi_0(x)|^2 e^{-E_0 T}\,, \qquad T \to \infty\,. \qquad (43)$$

From this, we obtain

$$Z(T) = \int_{-\infty}^{\infty} dx \langle x|e^{-\hat{H}T}|x\rangle = \sum_n e^{-E_n T} \sim e^{-E_0 T}\,, \qquad T \to \infty\,, \tag{44}$$

and

$$E_0 = -\lim_{T\to\infty} \frac{1}{T}\, Z(T)\,. \tag{45}$$

Moreover, at finite values of T,

$$E_0(T) = -\frac{1}{T} \ln Z(T) = E_0 - \frac{1}{T}\, \ln\biggl(1 + \sum_{n\neq 0} e^{-(E_n - E_0)T}\biggr) < E_0\,. \tag{46}$$

Consequently, carrying out calculations at finite values of T (that is always the case in practice), one gets the result which is smaller than the true value of E_0 in the continuum. If T is large, then,

$$E_0(T) = E_0 - \frac{1}{T}\, e^{-(E_1 - E_0)T} + \cdots\,, \tag{47}$$

where E_1 is the energy of the first excited state and the ellipses stand for even more suppressed terms. Here, one encounters the first example of a lattice artifact, which stems from the fact that T is not infinite in the lattice calculations.

Further, since the Gaussian integral can be calculated explicitly, it is possible to obtain a closed expression for $Z(T)$:

$$\begin{aligned} Z(T) &= \int \prod_{i=0}^{N-1} \frac{dx_i}{\sqrt{2\pi a}}\, \exp\biggl(-\frac{1}{2a}\biggl\{\frac{1}{2}\biggl(\frac{x_{i+1} - x_i}{a}\biggr)^2 + \frac{\omega^2 x_i^2}{2}\biggr\}\biggr) \\ &= \int \prod_{i=0}^{N-1} \frac{dx_i}{\sqrt{2\pi a}}\, \exp\biggl(-\frac{1}{2a} \sum_{i,j=0}^{N-1} x_i \mathcal{M}_{ij} x_j\biggr)\,, \end{aligned} \tag{48}$$

where the matrix $\mathcal{M}$ is given by

$$\mathcal{M} = \begin{pmatrix} z & -1 & 0 & 0 & \cdots & -1 \\ -1 & z & -1 & 0 & \cdots & 0 \\ 0 & -1 & z & -1 & \cdots & 0 \\ \cdots & \cdots & \cdots & \cdots & \cdots & \cdots \\ -1 & 0 & 0 & 0 & \cdots & z \end{pmatrix}, \qquad z = 2 + (a\omega)^2\,. \tag{49}$$

Performing Gaussian integration, we get:

$$E_0(T) = -\frac{1}{T}\, \ln\biggl(\det(\mathcal{M})^{-1/2}\biggr) = \frac{1}{2T}\, \ln\biggl(\det(\mathcal{M})\biggr)\,. \tag{50}$$

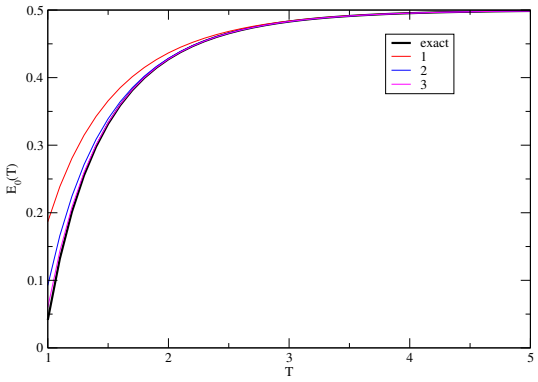

Figure 5: The quantity $E_0(T)$, calculated numerically and with the use of Eq. (46). The harmonic oscillator spectrum $E_0 = 1/2, E_1 = 3/2, E_2 = 5/2, \ldots$ is an input in these calculations. It is seen that Eq. (46) neatly converges to the exact result.

In order to calculate the determinant, let us first solve the eigenvalue equation for the matrix $\mathcal{M}$:

$$\sum_{i=0}^{N-1} \mathcal{M}_{ik} x_k^{(n)} = \lambda^{(n)} x_i^{(n)} \,, \tag{51}$$

or,

$$(z - \lambda^{(n)}) x_k^{(n)} = x_{k-1}^{(n)} + x_{k+1}^{(n)} \,, \qquad k = 0, \cdots, N-1 \,. \tag{52}$$

This equation is solved by the following ansatz:

$$x_k^{(n)} = c \exp\left(\frac{2\pi i}{N} nk\right) , \qquad n = 0, \cdots, N-1 \,. \tag{53}$$

The solution obeys the periodic boundary conditions:

$$x_N^{(n)} = c \exp(2\pi i n) = x_0^{(n)} \,. \tag{54}$$

Substituting this ansatz into the eigenvalue equation, we get:

$$\lambda^{(n)} = z - 2\cos\frac{2\pi n}{N} = 1 + (a\omega)^2 - 2\cos\frac{2\pi n}{N} \,, \tag{55}$$

and

$$E_0(T) = \frac{1}{2T} \sum_{n=0}^{N-1} \ln\left(1 + (a\omega)^2 - 2\cos\frac{2\pi n}{N}\right) . \tag{56}$$

For a fixed T, this expression can be rewritten as:

$$E_0(T) = \frac{1}{2T} \sum_{n=0}^{N-1} \ln\left(1 + \frac{(T\omega)^2}{N^2} - 2\cos\frac{2\pi n}{N}\right) . \tag{57}$$

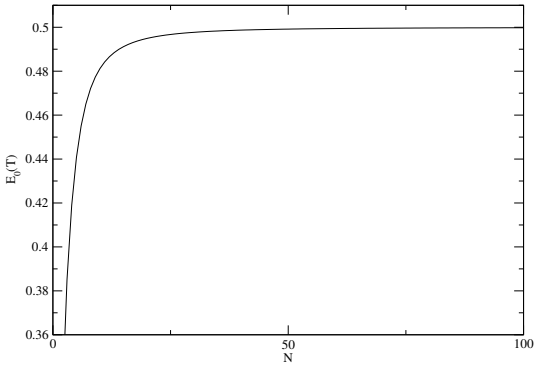

Figure 6: The N-dependence of the quantity $E_0(T)$, calculated at a fixed large value $T = 10$.

Calculating this expression for a fixed T and taking N very large, one should recover Eq. (46). This is nicely demonstrated in Fig. 5, which shows that, taking contributions from few excited states, one can nicely reproduce the exact result for all not very small values of T (in these calculations, we took $\omega = 1$).

Next, we study another limit, taking a fixed and sending T to infinity. In this manner, we may study the discretization effect in the ground state energy E_0. A straightforward calculation gives:

$$\begin{aligned} E_0 &= \lim_{T\to\infty} \frac{1}{T} \sum_{n=0}^{N-1} \ln\left(1 + (a\omega)^2 - 2\cos\frac{2\pi n}{N}\right) \\ &= \frac{1}{2a} \int_0^{2\pi} \frac{d\varphi}{2\pi} \ln\left(1 + (a\omega)^2 - 2\cos\varphi\right) \\ &= \frac{1}{2a} \ln\left(\sqrt{1 + \frac{(a\omega)^2}{2}} + (a\omega)\sqrt{1 + \frac{(a\omega)^2}{4}}\right) \\ &\simeq \frac{\omega}{2}\left(1 - \frac{a\omega}{4} + O((a\omega)^2)\right). \end{aligned} \tag{58}$$

This dependence is displayed in Fig. 6, where we display $E_0(T)$ at a large fixed $T = 10$ for different values of N.

In both cases of artifacts, considered above, the scale is set by a dynamical parameter ω. These artifacts are expressible in terms of the dimensional variables ωT and ωa, respectively.

2.7 Quantum mechanics on the torus

Up to now, we have considered one-dimensional quantum mechanics, where the time interval was restricted but the variable x could take any value $-\infty < x < \infty$. The

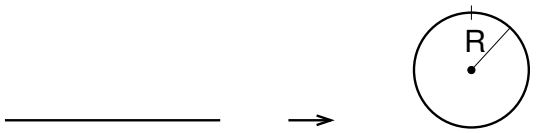

Figure 7: After imposing boundary condition, the linear x-axis folds into a circle with the radius $R = \dfrac{L}{2\pi}$.

situation is different in quantum field theory, where the space coordinate x, along with the time t, is the argument of a quantized field and, therefore, its range is also restricted. In practice, this restriction can be achieved by imposing the boundary conditions on the quantum fields. In most cases, the periodic boundary conditions are used in the spatial direction as well:

$$\varphi(x + nL, t) = \varphi(x, t)\,, \qquad n = \cdots, -2, -1, 0, 1, 2, \cdots\,. \tag{59}$$

Here, L denotes the size of a space "box." Geometrically, imposing the boundary condition transforms the x-axis into a torus with the radius $R = \dfrac{L}{2\pi}$, see Fig. 7 (in case of one dimension, a torus is just a circle). Here, we mention that the variable t is also defined in a restricted interval, $-\dfrac{T}{2} < t < \dfrac{T}{2}$. There is no reason, why L and T should be equal. On the contrary, in the most cases considered below, we will assume $T \gg L$ and will, eventually, take the limit $T \to \infty$ while leaving L finite.

In the context of quantum mechanics, could also study the effects coming from confining a system in a finite box. To this end, one imposes the similar boundary conditions on the wave function:

$$\Psi(x + nL, t) = \Psi(x, t)\,, \qquad \Psi'(x + nL, t) = \Psi'(x, t)\,. \tag{60}$$

in other words, the continuity of the wave function itself, together with its first derivative is required.

Consider first the free motion and start from the infinite space. The eigenfunctions of the free Hamiltonian are:

$$\Psi_k(x, t) = \exp\left(-\frac{k^2}{2m}\,t + ikx\right) = \exp\left(-\frac{k^2}{2m}\,t\right)\Phi_k(x)\,. \tag{61}$$

These obey the Schrödinger equation in the Euclidean space:

$$\frac{d}{dt}\Psi_k(x, t) = \frac{1}{2m}\,\frac{d^2}{dx^2}\Psi_k(x, t)\,. \tag{62}$$

The spectrum is continuous. The normalization condition takes the form:

$$\int_{-\infty}^{\infty} dx \Phi_k^*(x)\Phi_q(x) = 2\pi\delta(k - q)\,, \tag{63}$$

and the closure relation is given by

$$\int_{-\infty}^{\infty} \frac{dk}{2\pi}\, \Phi_k(x)\Phi_k^*(y) = \delta(x-y)\,. \tag{64}$$

On the torus, the eigenfunctions obey the same Schrödinger equation. Imposing the periodic boundary condition gives:

$$\Psi_k(x+nL,t) = \exp\!\left(-\frac{k^2}{2m}\,t + ik(x+nL)\right) = \Psi_k(x,t)\,. \tag{65}$$

From this we get:

$$e^{iknL} = 1 \qquad \text{and} \qquad k = \frac{2\pi}{L}\,n\,, \quad n \in \mathbb{Z}\,. \tag{66}$$

Thus, the spectrum is discrete. The normalization condition takes the form:

$$\int_{-L/2}^{L/2} dx\; \Phi_k^*(x)\Phi_q(x) = L\delta_{kq}\,, \tag{67}$$

and the closure relation is written as:

$$\frac{1}{L}\sum_k \Phi_k(x)\Phi_k^*(y) = \sum_{n\in\mathbb{Z}} \delta(x-y+nL)\,. \tag{68}$$

Can these results be obtained in the path integral formalism?

Consider first the case of the infinite space. As the path integral is Gaussian, modulo a constant factor, it is equal to the integrand evaluated at the solution of the classical equation of motion $x(t) = x + \dfrac{x'-x}{T}\,t$. Thus,

$$\begin{aligned}
\langle x'|e^{-\hat{H}T}|x\rangle &= \int \mathcal{D}x \exp\!\left(-\int_0^T dt \frac{m\dot{x}(t)^2}{2}\right) \\
&= \text{const}\, \exp\!\left(-\int_0^T dt \frac{m(x'-x)^2}{2T^2}\right) \\
&= \text{const}\, \exp\!\left(-\frac{m(x'-x)^2}{2T}\right).
\end{aligned} \tag{69}$$

The constant factor is determined from the requirement that

$$\lim_{T\to 0}\langle x'|e^{-\hat{H}T}|x\rangle = \langle x'|x\rangle = \delta(x'-x)\,. \tag{70}$$

This gives

$$\text{const} = \sqrt{\frac{m}{2\pi T}}\,, \tag{71}$$

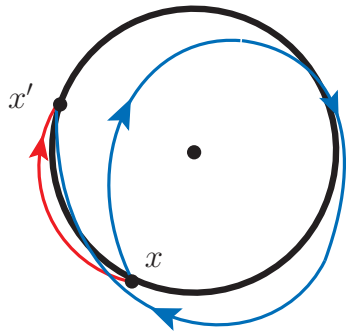

Figure 8: Two trajectories on the torus from x to x' with different winding numbers. The red trajectory corresponds to the winding number 0 and the blue one to the winding number 1.

and, finally,

$$\langle x'|e^{-\hat{H}T}|x\rangle = \sqrt{\frac{m}{2\pi T}}\exp\left(-\frac{m(x'-x)^2}{2T}\right). \tag{72}$$

Further, it can be seen that

$$\langle x'|e^{-\hat{H}T}|x\rangle = \int_{-\infty}^{\infty}\frac{dk}{2\pi}\exp\left(-\frac{k^2}{2m} - ik(x'-x)\right). \tag{73}$$

From the above formula we see that the spectrum is continuous, the stationary wave functions are $\Phi_k(x) = e^{ikx}$ and the energy is given by $E_k = \dfrac{k^2}{2m}$.

Next, let us derive the expression for the transition kernel $\langle x'|e^{-\hat{H}T}|x\rangle$ of the non-interacting particle on the torus. In this case, the topology of the torus plays a decisive role. Recall that the absolute value squared of the transition kernel gives the transition probability of a particle from x to x'. In the infinite space, we have just one classical trajectory – a straight line, connecting x and x', with a particle, moving along it with a constant velocity. On the opposite, on the torus we have a tower of trajectories that differ by a winding number. So, the particle can go from x to x' directly, or wind around the center of a circle any number of times (in either direction), see Fig. 8. Consequently, on the torus,

$$\langle x'|e^{-\hat{H}T}|x\rangle = \sum_{n\in\mathbb{Z}}\langle x'-nL|e^{-\hat{H}T}|x\rangle = \sum_{n\in\mathbb{Z}}\sqrt{\frac{m}{2\pi T}}\exp\left(-\frac{m(x'-nL-x)^2}{2T}\right). \tag{74}$$

Here, one may use the Poisson formula:

$$\sum_{n\in\mathbb{Z}}\delta(y-n) = \sum_{n\in\mathbb{Z}}e^{2\pi i n y}. \tag{75}$$

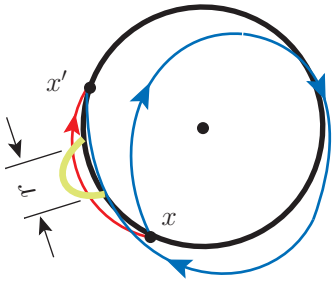

Figure 9: Two trajectories on the torus from x to x', passing through the area where the potential is non-zero. It is seen that the trajectory with the winding number 1 passes twice through this area.

and obtain:

$$\begin{aligned}
\langle x'|e^{-\hat{H}T}|x\rangle &= \sqrt{\frac{m}{2\pi T}}\sum_{n\in\mathbb{Z}}\int_{-\infty}^{\infty}\frac{dz}{L}\,\exp\left(-\frac{m(x'-z-x)^2}{2T}+\frac{2\pi i n z}{L}\right)\\
&= \frac{1}{L}\sum_{n\in\mathbb{Z}}e^{ik_n(x'-x)}\sqrt{\frac{m}{2\pi T}}\int_{-\infty}^{\infty}dz\exp\left(-\frac{mz^2}{2T}+ik_n z\right)\\
&= \frac{1}{L}\sum_{n\in\mathbb{Z}}\exp\left(-\frac{k_n^2}{2m}+ik_n(x'-x)\right), \qquad k_n=\frac{2\pi}{L}\,n\,. \qquad (76)
\end{aligned}$$

We see now that the spectrum is discrete, and the stationary wave function is given by $\Phi_n(x)=e^{ik_n x}$ with $k_n=\dfrac{2\pi}{L}\,n$.

2.8 Introducing a short-range potential

Now, let us consider a particle, moving in the short-range potential $V(x)$. The short-rangedness of the potential means that its range, r, is much smaller than L.

Consider again the path integral, which connects the points x and x'. As we have learned in the previous section, one has to sum up over all trajectories that go from x to x' – in other words, one has to take into account the trajectories with any winding number, going "around the world." Consider, for instance, the trajectory with a winding number one. It can be easily seen from Fig. 9 that the trajectory passes twice through the area where the potential is nonzero. The trajectories with larger winding numbers will pass through this area many times. Unfolding now a torus into the straight line, we get many copies if the potential, separated from each other by L. This is shown in Fig. 10. The points x and $x+nL$ on the linear axis are identified.

Putting differently, the short-range potential on the torus maps into the periodic

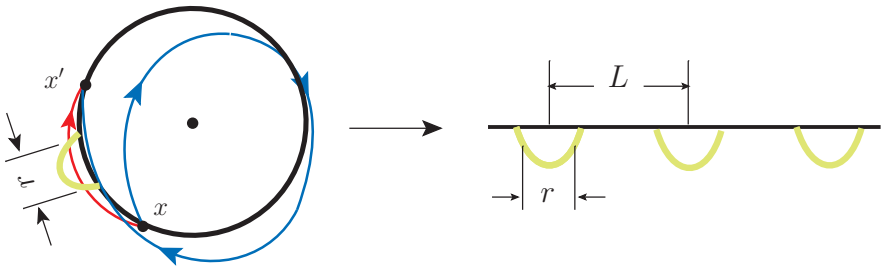

Figure 10: Unfolding the torus, we see that a short-range potential on the torus is equivalent to the periodic potential on a straight axis.

potential on the straight line:

$$V_L(x) = \sum_{n\in\mathbb{Z}} V(x+nL)\,. \tag{77}$$

Consequently, the spectrum of the particle on the torus, moving in the potential $V(x)$, is given by the solution of the Schrödinger equation in the infinite space

$$\left(-\frac{1}{2m}\frac{d^2}{dx^2} + V_L(x)\right)\Phi_k(x) = E_k\Phi_k(x)\,. \tag{78}$$

In addition, the wave functions are required obey periodicity (i.e., the points x and $x+nL$ should be physically equivalent):

$$\Phi_k(x+nL) = \Phi_k(x)\,, \qquad \Phi_k'(x+nL) = \Phi_k(x)\,. \tag{79}$$

The spectrum of Eq. (78) completely differs from the spectrum of a particle, scattered from the short-range potential in the infinite space. Namely, as it is well known, the spectrum in the infinite space is continuous and, in addition, can contain isolated bound states. On the other hand, the spectrum in the periodic potential has band structure and the eigenfunctions (Bloch wave functions) have the property:

$$\Phi_k(x+L) = e^{i\theta}\Phi_k(x)\,, \qquad 0 \le \theta < 2\pi\,. \tag{80}$$

Imposing the periodic boundary condition chooses one representative in each band. The spectrum becomes discrete.

It should be pointed out especially that the crucial point in the above discussion was the short-rangedness of the potential. Different mirror copies of the potential then do not overlap.

2.9 The energy shift of the bound state on the torus

Suppose that the potential $V(x)$ has a discrete spectrum. Further, assume that one or few bound states are shallow. This means that the binding momentum of the

bound state, which is defined by

$$\kappa_B = \sqrt{2mB}\,, \tag{81}$$

where E_B is the binding energy, obeys the following relations

$$\kappa_B^{-1} \gg r\,, \qquad \kappa_B^{-1} \ll L\,. \tag{82}$$

In other words, the characteristic length scale in such a bound state is much larger than the range of the potential. The fine details of the potential do not matter in this case.

Consider the stationary Schrödinger equation in the infinite space ($\hat{H}_0$ denotes the free Hamiltonian):

$$(\hat{H}_0 + \hat{V})|\Phi_B\rangle = -E_B|\Phi_B\rangle\,. \tag{83}$$

The bound-state wave function is normalized to unity:

$$\int_{-\infty}^{\infty} dx|\Phi_B(x)|^2 = 1\,. \tag{84}$$

The same equation on the torus takes the form:

$$(\hat{H}_0 + \hat{V}_L)|\Phi_L\rangle = -E_L|\Phi_L\rangle\,. \tag{85}$$

Define the trial wave function:

$$\langle x|\Phi_0\rangle = \sum_{n\in\mathbb{Z}} \Phi_B(x+nL)\,. \tag{86}$$

Then,

$$(\hat{H}_0 + \hat{V}_L)|\Phi_0\rangle = -E_B|\Phi_0\rangle + |\eta\rangle\,, \tag{87}$$

where

$$\langle x|\eta\rangle = \sum_{n,j\in\mathbb{Z}\ ,n\neq j} V(x+nL)\Phi_B(x+jL)\,. \tag{88}$$

Since both $V(x)$ and $\Phi_B(x)$ are localized, the vector $|\eta\rangle$ is very small in the whole space and can be considered as a perturbation. Applying the first-order perturbation theory, we get:

$$E_L - E_B = \delta E = -\frac{\langle\Phi_L|\eta\rangle}{\langle\Phi_L|\Phi_0\rangle} \simeq -\frac{\langle\Phi_0|\eta\rangle}{\langle\Phi_0|\Phi_0\rangle}\,. \tag{89}$$

There are many terms in the product $\langle\Phi_0|\eta\rangle$. Since the bound-state wave function falls off exponentially, the largest contribution comes from the terms, in which n and j differ by 1. There are two such terms. So, finally,

$$\delta E = -2\int_{-\infty}^{\infty} dx\Phi_B^*(x)V(x)\Phi_B(x+L)\,. \tag{90}$$

At large distances, the bound-state wave function falls off exponentially:

$$\Phi_B(x) \sim A_B e^{-\kappa_B |x|}\,, \tag{91}$$

where A_B is the so-called asymptotic normalization coefficient. Since $V(x)$ is short-ranged, one can replace $\Phi_B(x+L)$ by its asymptotic expression.Using Schrödinger equation, one gets:

$$\begin{aligned}
\delta E &= -2A_B e^{-\kappa_B L} \int_{-\infty}^{\infty} \left(\frac{1}{2m}\,\frac{d^2}{dx^2} - E_B \right) \Phi_B^*(x) \\
&= 2A_B E_B e^{-\kappa_B L} \int_{-\infty}^{\infty} dx \Phi_B^*(x) \\
&= 4|A_B|^2 \frac{E_B}{\kappa_B}\, e^{-\kappa_B L}\,,
\end{aligned} \tag{92}$$

where we have neglected the surface term and used the asymptotic expression to evaluate the integral $\int_{-\infty}^{\infty} dx \Phi_B^*(x)$. This is allowed, since only the large-distance behavior is relevant in this integral.

To summarize, if we take a shallow bound state that emerges in some attractive short-range potential, and restrict it on a torus, the energy changes. This change is however exponentially small for large L. The pertinent factor is $e^{-\kappa_B L}$ and does not depend on the details of the potential (except, of course, the value of κ_B). All information about the short-range details of the potential is concentrated in the asymptotic normalization constant A_B.

2.10 Scattering on the short-range potential

Again, consider first the infinite space. The reduced Schrödinger equation for the two-particle scattering is given by:

$$\left(-\frac{1}{2m}\,\frac{d^2}{dx^2} + V(x) \right) \Phi_k(x) = E_k \Phi_k(x)\,. \tag{93}$$

Assume, for simplicity, that the particles are identical. Then, the Bose-symmetry gives $\Phi_k(-x) = \Phi_k(x)$. Then, the asymptotic form of the solution at $|x| \gg r$ is:

$$\Phi_k(x) = e^{-ik|x|} + e^{2i\delta(k)} e^{ik|x|}\,, \tag{94}$$

where $k = \sqrt{2mE_k}$ and $\delta(k)$ is called the scattering phase.

On the torus, there is no scattering in the sense that there is no continuum spectrum. If the periodic boundary conditions are imposed:

$$\Phi_k\left(\frac{L}{2}\right) = \Phi_k\left(-\frac{L}{2}\right), \qquad \Phi_k'\left(\frac{L}{2}\right) = \Phi_k'\left(-\frac{L}{2}\right), \tag{95}$$

then, using the asymptotic form of the wave functions, we obtain:

$$e^{2i\delta(k)}e^{ikL} = 1\,, \tag{96}$$

and, finally,

$$kL = 2\pi n - 2\delta(k)\,, \qquad n = 0, 1, \ldots\,. \tag{97}$$

Here, we encounter the simplest example of the quantization condition, i.e., the equation that determines the spectrum of a particle on a torus, given the phase shift in the infinite space. One could put the argument other way around: measuring (numerically) the (discrete) energy levels E_n on the torus, it is possible to determine the phase shift $\delta(k)$ at $k_n = \sqrt{2mE_n}$, even there is no scattering on the torus!

The above equation represents a 1-dimensional version of Lüscher equation which, nowadays, plays a central role in the extraction of the scattering observables on the lattice. In the following, we shall consider this equation in detail.

3 Quantum field theory on the lattice

3.1 The scalar field

In the beginning, we shall consider the "latticization" of a single real scalar field $\varphi(x)$, which is described by an Euclidean action functional

$$S[\varphi] = \int d^4x \left\{ \frac{1}{2}\,\partial_\mu\varphi(x)\partial_\mu\varphi(x) + \frac{m^2}{2}\,\varphi^2(x) + \frac{\lambda}{4}\,\varphi^4(x) \right\}. \tag{98}$$

The generating functional is given by

$$Z(j) = \int \mathcal{D}\varphi\, \exp\left(-S[\varphi] + \int d^4x j(x)\phi(x) \right). \tag{99}$$

The Euclidean correlators are obtained by differentiating the above expression with respect to the external current $j(x)$ and setting it to zero at the end:

$$\langle 0|T\varphi(x_1)\cdots\varphi(x_n)|0\rangle = \frac{\delta}{\delta j(x_1)}\cdots\frac{\delta}{\delta j(x_n)}\,Z(j)\bigg|_{j=0}. \tag{100}$$

We shall discretize the path integral in Eq. (99) on the hypercubic Euclidean lattice, shown in Fig. 11. The lattice is a box of a size L, divided into N intervals of length a each, so $L = Na$ (In the following, it will be sometimes useful to consider the time and spatial directions separately, denoting the elongation of a box in time direction by T. In order to simplify the notations, we however stick to $T = L$ here.).

The fields $\varphi(x)$ become discrete variables, defined in the sites of the lattice. Any integral is replaced by the sum:

$$\int_{-L/2}^{L/2} d^4x f(x) \to a^4 \sum_x f(x) = a^4 \sum_{m_1=0}^{N-1} \cdots \sum_{m_4=1}^{N-1} f(m_1, m_2, m_3, m_4)\,. \tag{101}$$

Hence,

$$\int d^4x \left\{ \frac{m^2}{2}\,\varphi^2(x) + \frac{\lambda}{4}\,\varphi^4(x) \right\} \to a^4 \sum_x \left\{ \frac{m^2}{2}\,\varphi^2(x) + \frac{\lambda}{4}\,\varphi^4(x) \right\}. \tag{102}$$

Further, there are two equivalent definitions of the derivative that yield the same result in the continuum limit:

$$\begin{aligned} \partial_\mu\varphi(x) &= \frac{1}{a}\left(\varphi(x + a\hat{\mu}) - \varphi(x)\right), \\ \partial^*_\mu\varphi(x) &= \frac{1}{a}\left(\varphi(x) - \varphi(x - a\hat{\mu})\right). \end{aligned} \tag{103}$$

Here, $\hat{\mu}$ denotes a unit vector in the direction of μ.

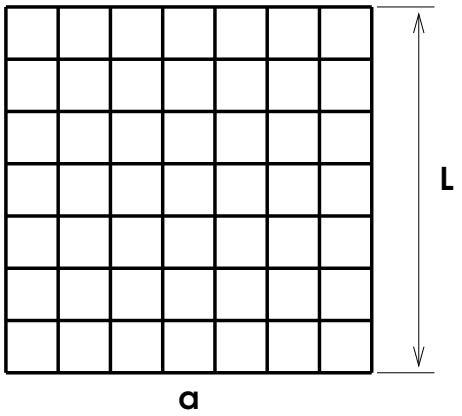

Figure 11: Hypercubic lattice. a denotes the lattice spacing and $L = Na$ is the size of the box.

In order to define the derivative in a consistent manner, one has to impose boundary conditions, i.e., one has to specify the value of $\varphi(x+Na\hat{\mu})$, corresponding to a field gone around the world once. The most widely used choice is to impose the so-called periodic boundary conditions:

$$\varphi(x + Na\hat{\mu}) = \varphi(x)\,. \tag{104}$$

In general, the twisted boundary conditions can be imposed

$$\varphi(x + Na\hat{\mu}) = e^{i\theta_\mu}\varphi(x)\,, \qquad 0 \le \theta_\mu < 2\pi\,. \tag{105}$$

For $\theta_\mu = 0$, this reduces to the periodic boundary conditions. Further, if not mentioned specially, the periodic boundary conditions are implicit by default.

The path integral measure is defined as:

$$\mathcal{D}\varphi = \text{const} \prod_x \int_{-\infty}^{\infty} d\varphi(x)\,. \tag{106}$$

and the Euclidean correlators are given by

$$\langle 0|T\varphi(x_1)\cdots\varphi(x_n)|0\rangle = \frac{1}{Z}\int \mathcal{D}\varphi\,\varphi(x_1)\cdots\varphi(x_n)e^{-S[\varphi]}\,, \tag{107}$$

where

$$Z = \int \mathcal{D}\varphi\, e^{-S[\varphi]}\,, \tag{108}$$

and

$$S[\varphi] = a^4 \sum_x \left\{ \frac{1}{2} \sum_\mu \left(\partial_\mu\varphi(x)\partial_\mu\varphi(x) \right) + \frac{m^2}{2}\,\varphi^2(x) + \frac{\lambda}{4}\,\varphi^4(x) \right\}. \tag{109}$$

3.2 Momentum space

Performing the Fourier transform on the lattice, one has to deal with a discrete set of momenta instead of a continuum, as in the infinite space. If the periodic boundary conditions are imposed, this set is given by

$$p_\mu = \frac{2\pi}{L}\, n_\mu\,, \qquad n_\mu \in \mathbb{Z}\,. \tag{110}$$

For fixed μ, x_μ takes the values

$$x_\mu = -\frac{L}{2} + m_\mu a\,, \qquad m_\mu = 0, \cdots, N-1\,. \tag{111}$$

Since the number of the degrees of freedom in the coordinate and momentum spaces should be the same, the values of n_μ should be also restricted. one may choose (taking N even for simplicity):

$$n_\mu = -\frac{N}{2} + 1, \cdots, \frac{N}{2}\,. \tag{112}$$

Then, the momentum cutoff on the lattice (the largest available momentum) is given by

$$p_{max} = \frac{\pi}{a} \tag{113}$$

Consequently, a finite lattice spacing acts as an ultraviolet regulator.

The Fourier transform for the fields takes the form:

$$\begin{aligned} \tilde\varphi(p) &= a^4 \sum_x e^{-ipx}\varphi(x)\,, \\ \varphi(x) &= (Na)^{-4} \sum_p e^{ipx}\tilde\varphi(p)\,. \end{aligned} \tag{114}$$

The momentum integration is replaced by a sum

$$(Na)^{-4} \sum_p \tilde f(p)\,. \tag{115}$$

There are two interesting limiting cases. Consider first the case of an infinite volume at a finite lattice spacing, i.e., $L \to \infty$ and $a = L/N = \text{const}$. In this case,

$$(Na)^{-4} \sum_p \tilde f(p) \to \int_{-\pi/a}^{\pi/a} \frac{d^4p}{(2\pi)^4}\, \tilde f(p)\,. \tag{116}$$

In other words, a finite lattice spacing indeed acts as a cutoff – the integration is restricted to the first Brillouin zone.

In the opposite case $a \to 0$ and $L = Na = \text{const}$, the sum over p runs over all discrete values from $-\infty$ to $+\infty$. This is the case of continuum physics in a finite volume, which will be considered in detail in our lectures.

In order to find the propagator of the scalar field, we shall rewrite the quadratic part of the action in the momentum space:

$$S_0[\varphi] = -\frac{1}{2}\, a^8 \sum_{xy} \varphi(x) S_{xy} \varphi(y)\,, \tag{117}$$

where

$$S_{xy} = -\frac{1}{4} \sum_z \left\{ \frac{1}{a^2} \sum_\mu (\delta_{z+a\hat{\mu},x} - \delta_{z,x})(\delta_{z+a\hat{\mu},y} - \delta_{z,y}) + m^2 \delta_{z,x} \delta_{z,y} \right\}, \tag{118}$$

and

$$S_p = \frac{a^4}{N^4} \sum_{xy} e^{-ip(x-y)} S_{xy} = -m^2 - \frac{4}{a^2} \sum_\mu \sin^2 \frac{a p_\mu}{2}\,. \tag{119}$$

Here, $\delta_{x,y}$ is the Kronecker's symbol, corresponding to the periodic boundary conditions, i.e.,

$$\delta_{x,y} = \begin{cases} 1, & \text{if} \quad x_\mu + n_\mu L = y_\mu\,, \quad n_\mu \in \mathbb{Z}\,, \\ 0, & \text{otherwise.} \end{cases} \tag{120}$$

From Eq. (119), one can read off the expression of the propagator on the lattice:

$$G(p) = \frac{1}{m^2 + \dfrac{4}{a^2} \sum\limits_\mu \sin^2 \dfrac{a p_\mu}{2}}\,. \tag{121}$$

In the continuum limit $a \to 0$, the standard expression for the scalar operator is restored

$$G(p) = \frac{1}{m^2 + \sum_\mu p_\mu^2 + O(a^2)} \to \frac{1}{m^2 + p^2}\,. \tag{122}$$

3.3 Perturbation theory

The perturbative expansion of Green functions can be constructed pretty much in the same manner as in the continuum. The vertices that describe the interactions are the same (in case of derivative vertices, one replaces these by the lattice derivatives, see Eq. (103)), whereas the propagators are replaced by lattice propagators. For the illustrative purposes, let us consider the calculation of the four-point function at

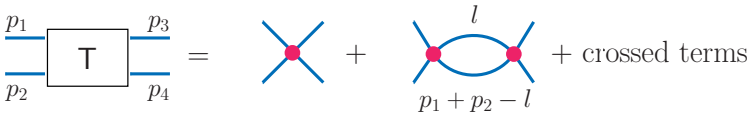

Figure 12: The scattering amplitude in the φ^4 theory at one loop.

one loop (the Feynman diagrams are shown in Fig. (12). The scattering amplitude is given by the familiar expression:

$$T(p_1,p_2;p_3,p_4) = -6\lambda + \frac{1}{2}(6\lambda)^2\Big[I(p_1+p_2)+I(p_1-p_3)+I(p_1-p_4)\Big]\,, \quad (123)$$

where

$$I(p) = (Na)^{-4}\sum_l \frac{1}{\left(m^2+\frac{1}{a^2}\sum\limits_\mu \sin^2\frac{al_\mu}{2}\right)}\,\frac{1}{\left(m^2+\frac{1}{a^2}\sum\limits_\mu \sin^2\frac{a(p_\mu-l_\mu)}{2}\right)}\,. \quad (124)$$

Consider the limit of the infinite volume $L\to\infty$ first. The above loop integral takes the form

$$I(p) = \int_{-\pi/a}^{\pi/a}\frac{d^4l}{(2\pi)^4}\,\frac{1}{\left(m^2+\frac{1}{a^2}\sum\limits_\mu \sin^2\frac{al_\mu}{2}\right)}\,\frac{1}{\left(m^2+\frac{1}{a^2}\sum\limits_\mu \sin^2\frac{a(p_\mu-l_\mu)}{2}\right)}\,. \quad (125)$$

This integral is well defined, because the ultraviolet divergences are regulated at a finite a. Moreover, it can be shown by direct calculation that it diverges logarithmically, as $a\to 0$:

$$I(p) = -\frac{1}{16\pi^2}\int_0^1 dx\,\ln\big[a^2(m^2+x(1-x)p^2)\big] + C_2 - \frac{1}{16\pi^2} + O(a^2)\,, \quad (126)$$

where $C_2 = 0.0303457\ldots$ is a numerical constant.

Next, in the limit $a\to 0$ (but still in a finite volume), the above loop takes the following form:

$$I(p) = \frac{1}{L^4}\sum_l \frac{1}{(m^2+l^2)}\,\frac{1}{(m^2+(p-l)^2)}\,. \quad (127)$$

Finally, we shall often refer to the "final volume effects" as to the one caused by a finite spatial elongation of a box. It is assumed that time elongation $T\gg L$ can be taken to infinity. In this case,

$$I(p) = \frac{1}{L^3}\int\frac{dk_4}{2\pi}\sum_{\mathbf{l}} \frac{1}{(m^2+l^2)}\,\frac{1}{(m^2+(p-l)^2)}\,. \quad (128)$$

It is important to note that ultraviolet divergences, arising in the above integrals at $L \neq \infty$ are the same as in the infinite volume. Intuitively, this is obvious, since the introduction of a box alters the infrared physics only. Hence, the above expressions, written down in the limit $a \to 0$, strictly speaking, make sense only together with an ultraviolet regulator. As we know, a can indeed act as such regulator. However, for convenience, it is more useful to use different regulators, say, the dimensional regularization or cutoff regularization. The calculations are much simpler in this case, and the physical results are the same. Such a separate treatment of finite-volume effects and the ultraviolet divergences is possible because the scales, which are relevant for these two cases, are vastly different.

3.4 Fermions on the lattice

QCD is formulated in terms of quarks and gluons. Therefore, in order to write down the generating functional of lattice QCD, we have to learn, how to define fermions and gauge bosons on the lattice. In this section we start with the fermions.

The free fermion action functional in the Euclidean space in the continuum is given by

$$S_F[\psi, \bar{\psi}] = \int d^4x \bar{\psi}(x)(\gamma_\mu \partial_\mu + m)\psi(x)\,, \tag{129}$$

where the relation between the gamma-matrices in the Euclidean and Minkowski spaces is given by:

$$\gamma_4(\text{Eucl}) = \gamma^0(\text{Mink})\,, \qquad \gamma_k(\text{Eucl}) = i\gamma^k(\text{Mink})\,. \tag{130}$$

Substituting this action functional into the path integral, one may explicitly perform the Grassmann integration. The free fermion correlator is given by

$$\langle 0|T\psi(x)\bar{\psi}(y)|0\rangle = \int \frac{d^4p}{(2\pi)^4} \frac{e^{ip(x-y)}}{m + i\gamma_\mu p_\mu}\,. \tag{131}$$

One may proceed with the "latticization" of the fermion field in analogy with the scalar field, placing the fields $\psi(x)$ and $\bar{\psi}(x)$ in the sites of a hypercubic box. The derivatives on the fermion fields are defined as:

$$\begin{aligned} \partial_\mu \psi(x) &= \frac{1}{a}\left(\psi(x + a\hat{\mu}) - \psi(x)\right), \\ \partial^*_\mu \psi(x) &= \frac{1}{a}\left(\psi(x) - \psi(x - a\hat{\mu})\right. \end{aligned} \tag{132}$$

(similarly for $\bar{\psi}(x)$). Further, taking into account the Hermiticity, a natural lattice generalization of the differential operator $\gamma_\mu \partial_\mu$ is

$$D_{naive} = \frac{1}{2}\gamma_\mu(\partial_\mu + \partial^*_\mu)\,. \tag{133}$$

The formulation, which uses the above differential operator, goes under the name of naive fermions, and is known to have the problem with the so-called doublers. To illustrate the problem, we display the fermion propagator, which can be directly obtained from the fermion action functional by performing the Fourier transform, as in case of the scalar field:

$$S_F(p) = \frac{m - i\sum\limits_{\mu} \gamma_\mu \hat{p}_\mu}{m^2 + \sum\limits_{\mu} \hat{p}_\mu^2}\,, \tag{134}$$

where

$$\hat{p}_\mu = \frac{1}{a}\,\sin ap_\mu\,. \tag{135}$$

Consider, for simplicity of the argument, the case with $m = 0$. The free fermion propagator has a pole at $p_\mu = 0$, corresponding to the massless particle in the continuum limit. However, besides this pole, the propagator has 15 additional poles at $p_\mu = \dfrac{\pi}{a}\,n_\mu$, where $n_\mu = (1,0,0,0),\ n_\mu = (0,1,0,0), \ldots, n_\mu = (1,1,1,1)$. These additional poles at different corners of the Brillouin zone are called doublers. It is clear that, in the continuum limit, the theory with naive fermion action converges to a theory with 16 fermion species instead of one. This, at the end, means that the naive fermion Lagrangian does not represent an appropriate lattice generalization of the Dirac Lagrangian.

There exist several ways to deal with the problem. Perhaps the simplest one was proposed by Wilson. The action with Wilson fermions contains the differential operator

$$D_W^0 = \frac{1}{2}\left(\gamma_\mu(\partial_\mu + \partial_\mu^*) - a\partial_\mu\partial_\mu^*\right). \tag{136}$$

It is clear that the last term (the Wilson term) vanishes, as $a \to \infty$, so, in fact, the above expression is a valid choice of a lattice generalization for the continuum differential operator. However, unlike the choice that has led to naive fermions, this choice does not give rise to the doublers. In order to see this, note that the propagator for Wilson fermions takes the form:

$$S_W(p) = \frac{-i\gamma_\mu\hat{p}_\mu + \dfrac{2}{a}\,\sin^2\dfrac{ap_\mu}{2} + m}{\hat{p}^2 + \left(\dfrac{2}{a}\,\sin^2\dfrac{ap_\mu}{2} + m\right)^2}\,. \tag{137}$$

It is straightforward to see that the expression

$$\frac{2}{a}\,\sin^2\frac{ap_\mu}{2} + m \tag{138}$$

plays the role of mass in case of Wilson fermions. This quantity is equal to m at the origin $p_\mu = 0$ and is equal to $m + \frac{2}{a}$,$m + \frac{2}{a}$, $m + \frac{4}{a}$, $m + \frac{6}{a}$, $m + \frac{8}{a}$ in the different corners of the Brillouin zone. Thus, in this approach the doublers get the masses of order of the ultraviolet cutoff $\frac{1}{a}$ and thus disappear in the continuum limit.

3.5 Gauge fields

In the continuum, the gauge fields G_μ ensure that the Lagrangian is invariant under local symmetry group $\mathcal{G}$. Namely, if $\Lambda(x) \in \mathcal{G}$ is an element of this group, the fermions and the gauge bosons transform as follows:

$$\begin{aligned} \psi(x) &\mapsto \Lambda(x)\psi(x)\,, \\ \bar{\psi}(x) &\mapsto \bar{\psi}(x)\Lambda(x)^{-1}\,, \\ G_\mu(x) &\mapsto \Lambda(x)G_\mu(x)\Lambda(x)^{-1} + i\Lambda(x)\partial_\mu\Lambda(x)^{-1}\,. \end{aligned} \tag{139}$$

In case of QCD, the group $\mathcal{G}$ coincides with the color group $SU(3)_c$.

The covariant derivative is defined as:

$$\nabla_\mu = \partial_\mu - iG_\mu\,. \tag{140}$$

It can be straightforwardly seen that the covariant derivatives of $\psi(x), \bar{\psi}(x)$ transform as the fields themselves:

$$\begin{aligned} \nabla_\mu\psi(x) &\mapsto \Lambda(x)\nabla_\mu\psi(x)\,, \\ \bar{\psi}(x)\overleftarrow{\nabla}_\mu &\mapsto \bar{\psi}(x)\overleftarrow{\nabla}_\mu\Lambda(x)^{-1}\,. \end{aligned} \tag{141}$$

Further, the field tensor

$$F_{\mu\nu}(x) = \partial_\mu G_\nu(x) - \partial_\nu G_\mu(x) - i[G_\mu(x), G_\nu(x)] \tag{142}$$

transforms as

$$F_{\mu\nu}(x) \mapsto \Lambda(x)F_{\mu\nu}(x)\Lambda(x)^{-1}\,. \tag{143}$$

The gauge invariant action functional in QCD is given by

$$S = \frac{1}{2g^2}\int d^4x \mathrm{tr}(F_{\mu\nu}(x)F_{\mu\nu}(x)) + \int d^4x\bar{\psi}(x)(\gamma_\mu\nabla_\mu + m)\psi(x)\,. \tag{144}$$

In order to generalize these expressions on the lattice, we start with the definition of the covariant derivative. The ordinary derivative does not transform covariantly:

$$\partial_\mu(x) = \frac{1}{a}\left(\psi(x + a\hat{\mu}) - \psi(x)\right) \mapsto \frac{1}{a}\left(\Lambda(x + a\hat{\mu})\psi(x + a\hat{\mu}) - \Lambda(x)\psi(x)\right). \tag{145}$$

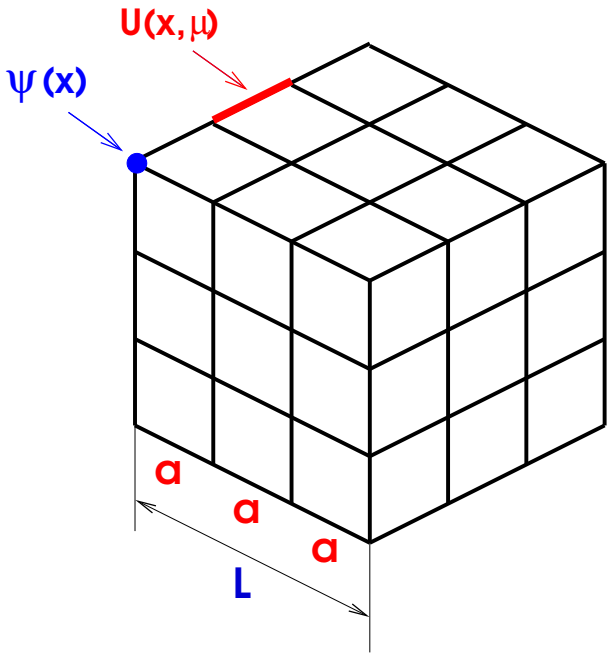

Figure 13: Quark and gluon fields on the lattice

We now define the link variable $U(x,\mu) \in SU(3)$, which transforms as:

$$U(x,\mu) \quad \mapsto \quad \Lambda(x) U(x,\mu) \Lambda(x+a\hat{\mu})^{-1} \,. \tag{146}$$

Physically, $U(x,\mu)$ can be interpreted as an operator that covariantly transports the color vector from point $x + a\hat{\mu}$ to point x. It is given by the expression

$$U(x,\mu) = P \exp\left(i \int dz_\mu G_\mu(z) \right) , \tag{147}$$

where the integral runs along the straight line from $x + a\hat{\mu}$ to x and $P\exp(\cdots)$ stands for the path-ordered exponent. To the lowest order in a, one can also write

$$U(x,\mu) = \exp(-iaG_\mu(x)) = 1 - iaG_\mu(x) + O(a^2) \,. \tag{148}$$

Hence, the fields $\psi(x), \bar{\psi}(x)$ live on the sites of a hypercubic lattice, whereas the gauge fields $U(x,\mu)$ live on the links between two sites. This is shown in Fig. 13.

The covariant derivative on the lattice is defined as:

$$\nabla_\mu \psi(x) = \frac{1}{a} \left(U(x,\mu)\psi(x+a\hat{\mu}) - \psi(x) \right) , \tag{149}$$

and it can be checked that

$$\nabla_\mu \psi(x) \quad \mapsto \quad \Lambda(x) \nabla_\mu \psi(x) \,. \tag{150}$$

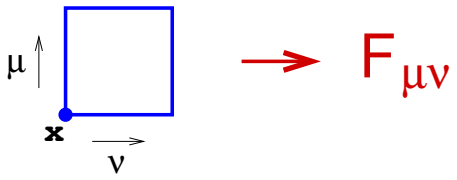

Figure 14: An elementary plaquette, with the sides looking in the directions $\hat{\mu}, \hat{\nu}$.

The covariant derivative ∇^*_μ can be constructed analogously.

In order to define the lattice analog of the field tensor $F_{\mu\nu}(x)$, we have to consider the elementary plaquette with an origin at point x. A plaquette is a collection of four lattice sites, which form a square with a side length a (see Fig. 14). The plaquette field is defined as:

$$P_{\mu\nu}(x) = U(x,\mu)U(x+a\hat{\mu},\nu)U(x+a\hat{\nu},\mu)^{-1}U(x,\nu)^{-1}\,. \tag{151}$$

It can be checked that

$$P_{\mu\nu}(x) \;\;\mapsto\;\; \Lambda(x)P_{\mu\nu}(x)\Lambda(x)^{-1}\,, \tag{152}$$

and, therefore, the quantity $\mathrm{tr}(P_{\mu\nu}(x))$ is gauge-invariant. The expansion of this quantity up to and including terms of order a^4 gives:

$$\mathrm{tr}\,(P_{\mu\nu}(x)) = N_c - \frac{a^4}{2}\,\mathrm{tr}(F_{\mu\nu}(x)F_{\mu\nu}(x)) + \cdots\,, \tag{153}$$

where $N_c = 3$ is the number of colors.

Thus, the generalization of the gluonic action functional on the lattice can be written as

$$S_G[U] = \frac{1}{g_0^2}\sum_x\sum_{\mu\nu}\mathrm{Re}\;\mathrm{tr}(1-P_{\mu\nu}(x)) = \frac{1}{2g_0^2}\,a^4\sum_x\sum_{\mu\nu}\mathrm{tr}(F_{\mu\nu}(x)F_{\mu\nu}(x)) + \cdots \tag{154}$$

and, finally, the QCD Lagrangian on the lattice with Wilson fermions takes the form:

$$S[\psi,\bar{\psi},U] = \frac{1}{g_0^2}\sum_x\sum_{\mu\nu}\mathrm{Re}\;\mathrm{tr}(1-P_{\mu\nu}(x)) + a^4\sum_x\bar{\psi}(x)(D_W+m_0)\psi(x)\,, \tag{155}$$

where

$$D_W = \frac{1}{2}\sum_\mu\Big(\gamma_\mu(\nabla_\mu+\nabla^*_\mu) - a\nabla_\mu\nabla^*_\mu\Big)\,. \tag{156}$$

Further, g_0 and m_0 here denote the "bare" coupling constant and bare mass, respectively.

3.6 Calculation of the spectrum

The asymptotic spectrum of QCD contains the following states:

- The vacuum state $|0\rangle$
- States, containing one particle, moving with a three-momentum $\mathbf{p}$: for example, the one-pion state $|\pi^+(\mathbf{p})\rangle$, or the one-nucleon state $|N(\mathbf{p})\rangle$.
- Multiparticle states (in- or out- states), for example, the two-pion state $|\pi^+(\mathbf{p}_1)\pi^-(\mathbf{p}_2)\rangle$.

These states are eigenstates of the total QCD Hamiltonian. For example,

$$\begin{aligned} H|0\rangle &= 0\,, \\ H|\pi^+(\mathbf{p})\rangle &= E_\pi(\mathbf{p})|\pi^+(\mathbf{p})\rangle\,, \\ H|\pi^+(\mathbf{p}_1)\pi^-(\mathbf{p}_2)\rangle &= (E_\pi(\mathbf{p}_1)+E_\pi(\mathbf{p}_2))|\pi^+(\mathbf{p}_1)\pi^-(\mathbf{p}_2)\rangle\,, \\ &\cdots \end{aligned} \tag{157}$$

Here, $E(\mathbf{p}) = \sqrt{M_\pi^2 + \mathbf{p}^2}$ is the energy of a one free pion with the three-momentum $\mathbf{p}$.

In order to calculate, say, the mass of a pion, one has first to choose an operator which carries the same quantum numbers as the pion. For example, π^+ can be described by the field

$$\phi_{\pi^+}(x) = \bar{d}(x)\gamma_5 u(x)\,. \tag{158}$$

It should be also pointed out that a specific choice of the field operator does not matter: any operator with appropriate quantum numbers will do the job.

Next, one calculates the Euclidean two-point correlator of these fields on the lattice:

$$\begin{aligned} \langle 0|T\phi_{\pi^+}(x)\phi^\dagger_{\pi^+}(y)|0\rangle &= \frac{1}{Z}\int \mathcal{D}\psi\mathcal{D}\bar{\psi}\mathcal{D}U\,\phi_{\pi^+}(x)\phi^\dagger_{\pi^+}(y)\exp(-S[\psi,\bar{\psi},U])\,. \\ Z &= \int \mathcal{D}\psi\mathcal{D}\bar{\psi}\mathcal{D}U\exp(-S[\psi,\bar{\psi},U])\,. \end{aligned} \tag{159}$$

On the other hand, using closure relation and the translational invariance, we get

$$\langle \phi_{\pi^+}(x)\phi^\dagger_{\pi^+}(y)\rangle = \sum_n e^{-E_n(x_4-y_4)}e^{i\mathbf{P}_n(\mathbf{x}-\mathbf{y})}|\langle 0|\phi_{\pi^+}(0)|n\rangle|^2\,, \tag{160}$$

where the sum runs over all eigenstates $|n\rangle$ of the Hamiltonian H. Projecting on a definite three-momentum $\mathbf{p}$ can be performed:

$$a^3\sum_x e^{-i\mathbf{p}\mathbf{x}}\langle \phi_{\pi^+}(x)\phi^\dagger_{\pi^+}(0)\rangle = \sum_n e^{-E_n x_4}L^3\delta_{\mathbf{p},\mathbf{P}_n}|\langle 0|\phi_{\pi^+}(0)|n\rangle|^2\,. \tag{161}$$

Here, $\mathbf{p} = \dfrac{2\pi}{L}\,\mathbf{n}$ denotes the quantized three-momentum on the lattice.[1]

At large Euclidean time separations, the term with the lowest possible energy dominates the sum. This is the contribution coming from the one-pion state (the vacuum contribution vanishes). Consequently, we have

$$a^3 \sum_x e^{-i\mathbf{px}} \langle \phi_{\pi^+}(x) \phi^\dagger_{\pi^+}(0) \rangle \sim e^{-E_\pi(\mathbf{p})x_4} |\langle 0|\phi_{\pi^+}(0)|\pi^+(\mathbf{p})\rangle|^2 + \cdots\,, \tag{162}$$

where ellipses stand for the (suppressed) contributions from higher eigenstates.Thus, at large Euclidean times x_4, one can extract the value of $E_\pi(\mathbf{p})$ from the two-point correlator, calculated on the lattice.

The situation is similar, if one wants to extract the energies of the multi-particle states. For example, in order to extract the energy of the two-pion state in the center-of-mass frame, one may, for example, use the operators

$$\phi_{\pi^+\pi^+}(x_4) = \sum_{\mathbf{xy}} e^{-i\mathbf{py}} \phi_{\pi^+}\left(\mathbf{x} + \frac{\mathbf{y}}{2}, x_4\right) \phi_{\pi^+}\left(\mathbf{x} - \frac{\mathbf{y}}{2}, x_4\right), \tag{163}$$

where, again, $\mathbf{p} = \dfrac{2\pi}{L}\,\mathbf{n}$ is a quantized three-momentum on the lattice. Choosing $\mathbf{n} = (0,0,0),\ (0,0,1), \ldots$ produces a set of operators, each having the correct quantum numbers. Therefore, each operator from this set can be used to extract the energy of the two-pion state[2].

As we have already seen from the quantum-mechanical examples already, the energies extracted in this manner contain various artifacts. Besides the statistical error, which – in principle – can be reduced by increasing the number of configurations, there are systematic effects as well. For example, there will be effects caused by the admixture of other states in the spectrum (thermal pollution), as well as the effects from a finite lattice spacing and finite volume.

In these lectures, we shall be primarily interested in the finite-volume effects, leaving aside other (otherwise also very interesting) problems. Namely, we assume that one has carefully eliminated the admixture to unwanted states in the correlators, singling out the states whose energies we wish to determine. Also, we assume that the calculations were performed at different values of the lattice spacing and the

[1] At this place, it is worth mentioning that the eigenstates $|n\rangle$ of the Hamiltonian in a finite volume do not coincide with those in the infinite volume given in Eq. (157). The free one-particle state is an exception, and even its mass is modified in a finite volume (this correction, is, however, exponentially suppressed in L). The reason for this is that one cannot completely neglect interactions between different hadrons in a finite volume, since the hadrons are never allowed to go at the asymptotically large distances. Hence, in fact, $|n\rangle$ denote *interacting* states and their interpretation as n-particle states is, strictly speaking, invalid. Below, we shall however sometimes allow ourselves such a slight abuse of language.

[2] In fact, to reduce the error, it is convenient to use the whole set of these operators simultaneously, solving the generalized eigenvalue problem. We shall not discuss this issue further, because it is not directly related to the topic of our lectures.

results were reliably extrapolated to the continuum limit. The results then still contain the effects, related to the finite spatial elongation of the lattice. These effects are of two types:

- One-particle states belong to the discrete spectrum. The energy of such state has a well-defined limit, when the volume becomes very large. The corrections to the infinite-volume limit are exponential (we have seen this in the example of the energy of the quantum-mechanical bound state).

- Multi-particle states belong to the continuum. When the volume becomes large, all these collapse towards the pertinent thresholds, so the meaningful infinite-volume limit does not exist. The corrections to the threshold energies go as inverse powers of L. Physical quantities one is interested in should be extracted at a finite volume (quantum-mechanical example: extracting the phase shift with the Lüscher equation). The infinite-volume limit should be performed for these quantities and not for the energies.

Below, a systematic calculation of the finite-volume effects in both cases will be addressed.

4 Effective field theories

4.1 Chiral symmetry

As already mentioned in the introduction, the asymptotic spectrum of QCD does not contain quarks and gluons but, rather, the mesons and baryons. These emerge as poles in the Green functions of composite operators with pertinent quantum numbers. For example, pions are described by the composite field

$$\varphi_\pi^a = \bar{\psi}(x) i\gamma_5 T^a \psi(x)\,, \tag{164}$$

where $\psi(x) = (u(x), d(x), s(x))^T$ is the light quark field, and T^a, $a = 1, 2, 3$ are the generators of the flavor $SU(3)$ group. The Green functions of the composite operators are obtained from the (Euclidean) generating functional:

$$Z(s,p,v,a) = \int \mathcal{D}G_\mu \mathcal{D}\psi \mathcal{D}\bar{\psi}\, \exp\biggl(-\int d^4x (\mathcal{L}_G + \mathcal{L}_F)\biggr)\,, \tag{165}$$

where $\mathcal{L}_G$ is the standard gluonic part of the Lagrangian (which may include, in the continuum, ghosts, gauge fixing term and all that), whereas $\mathcal{L}_F$ denotes the fermion part of the Lagrangian, equipped with the scalar, pseudoscalar, vector and axial-vector external sources:

$$\mathcal{L}_F = \bar{\psi}(\gamma_\mu(D_\mu - iv_\mu - i\gamma_5 a_\mu) + s - i\gamma_5 p)\psi\,, \qquad D_\mu = \partial_\mu - iG_\mu\,. \tag{166}$$

The Green functions of the quark bilinear operators are obtained by differentiating the generating functional Z with respect to the corresponding external sources s, p, v, a and, at the end, setting:

$$s = \mathcal{M}\,, \qquad p = v = a = 0\,, \tag{167}$$

where $\mathcal{M} = \mathrm{diag}\,(m_u, m_d, m_s)$ is the mass matrix of the light quarks. Using Eq. (167), it is seen that the fermion Lagrangian reduces to the conventional expression:

$$\mathcal{L}_F = \psi(\gamma_\mu D_\mu + \mathcal{M})\psi\,. \tag{168}$$

Hence, the above-described procedure indeed yields the Green functions of the composite quark bilinears in QCD.

The generating functional has a symmetry with respect to the transformations under the local $U(3)_L \times U(3)_R$ flavor group. In order to see this, one has to introduce the left- and right-hand components of the fermion fields:

$$\psi_L(x) = \frac{1}{2}(1 - \gamma_5)\psi(x)\,, \qquad \psi_R(x) = \frac{1}{2}(1 + \gamma_5)\psi(x)\,, \tag{169}$$

and rewrite the fermionic Lagrangian in the following form:

$$\mathcal{L}_F = \bar{\psi}_L\gamma_\mu(D_\mu - il_\mu)\psi_L + \bar{\psi}_R\gamma_\mu(D_\mu - ir_\mu)\psi_R + \psi_R(s + ip)\psi_L + \bar{\psi}_L(s - ip)\psi_R\,, \tag{170}$$

where

$$l_\mu = v_\mu - a_\mu\,, \qquad r_\mu = v_\mu + a_\mu\,. \tag{171}$$

It is now seen that the Lagrangian is invariant under local chiral $U(3)_L \times U(3)_R$ transformations:

$$\begin{aligned}
\psi_L(x) &\mapsto \psi'_L(x) = g_L(x)\psi_L(x)\,,\\
\psi_R(x) &\mapsto \psi'_R(x) = g_R(x)\psi_R(x)\,,\\
l_\mu(x) &\mapsto l'(x) = g_L(x)l_\mu(x)g_L(x)^\dagger - ig_L(x)\partial_\mu g_L(x)^\dagger\,,\\
r_\mu(x) &\mapsto r'(x) = g_R(x)r_\mu(x)g_R(x)^\dagger - ig_R(x)\partial_\mu g_R(x)^\dagger\,,\\
s(x)+ip(x) &\mapsto s'(x)+ip'(x) = g_R(x)(s(x)+ip(x))g_L(x)^\dagger\,,\\
s(x)-ip(x) &\mapsto s'(x)-ip'(x) = g_L(x)(s(x)-ip(x))g_R(x)^\dagger\,,
\end{aligned} \tag{172}$$

where $g_{L,R}(x) \in U(3)_{L,R}$. Note that these transformations act in the flavor space, leaving the gluonic part of the Lagrangian intact.

Assuming that the fermionic measure $\mathcal{D}\psi\mathcal{D}\bar{\psi}$ is invariant under chiral transformations[3], we immediately conclude that the generating functional is also invariant:

$$Z(s',p',v',a') = Z(s,p,v,a)\,. \tag{173}$$

Further, the chiral symmetry in QCD is broken down to the vector subgroup $SU(3)_V \times U(1)_V$. Almost massless octet of Goldstone bosons (pions, kaons and η) emerges in a result of this breaking (these would be exactly massless, if quark masses were exactly zero), whereas all other hadrons have nonzero masses in the chiral limit.

Now, we come to the crucial point in the discussion. As we said, the spectrum of QCD does not contain free quarks and gluons, i.e., QCD is an inherently non-perturbative theory. In order to calculate Green functions (e.g., to find the location of the poles), non-perturbative methods should be applied.

Let us now define the effective theory given by the generating functional:

$$Z_{eff}(s,p,v,a) = \int \mathcal{D}\Phi_{eff} \exp\biggl(-\int d^4x \mathcal{L}_{eff}[\Phi_{eff},s,p,v,a]\biggr)\,. \tag{174}$$

Here, Φ_{eff} denotes the set of fields which, by construction, correspond to the particles, observed in the experiment at low energies (i.e., mesons and baryons). Thus, the correct pole structure in the effective theory emerges in the perturbation theory, by definition.

[3]In fact, the statement about the invariance of the fermion measure should be refined due to the presence of anomalies. We shall, however, do not elaborate on this issue in the following.

Further, in order to ensure that the effective theory and the original theory are equivalent, one has to show that:

$$Z_{eff}(s,p,v,a) = Z(s,p,v,a)\,. \tag{175}$$

Below, we shall define a systematic procedure for constructing Z_{eff}, obeying Eq. (175), order by order in what is termed chiral expansion. The whole setting goes under the name of Chiral Perturbation Theory (ChPT).

There are two guiding principles that allow one to systematically construct Z_{eff}:

1) Symmetries: $Z_{eff}(s,p,v,a)$ has exactly the same symmetry properties as $Z(s,p,v,a)$. Along with the fact that they have the same asymptotic spectrum, this, according to the Weinberg's theorem, suffices to claim that both theories are equivalent.

2) Counting rules: A generic Lagrangian built of the effective fields Φ_{eff} contains infinitely many operators that obey required symmetry properties. If one could not introduce some hierarchy in these operators, the effective theory will possess no predictive power. In ChPT, various terms in the Lagrangian can be ordered according to the well-defined counting rules that take into account their relative importance at low energies. We shall give an illustration of the counting rules below.

Let us start with the octet of Goldstone bosons, which are hadrons with the lightest mass and thus dominate the low-energy spectrum. These can be collected in one matrix field:

$$U(x) = \exp\left(\frac{i}{F}\,\lambda^a\varphi^a(x)\right), \tag{176}$$

where λ^a are the Gell-Mann matrices for the $SU(3)$ group, and F will be seen to coincide with the pion decay constant in the chiral limit. The chiral transformation of the field U is defined as:

$$U \mapsto g_R U g_L^\dagger\,. \tag{177}$$

Further, one constructs the gauge-invariant building blocks, containing the field U:

$$\begin{aligned}
D_\mu U &= \partial_\mu U + i r_\mu U - i U l_\mu\,, \qquad D_\mu U \mapsto g_R D_\mu U g_L^\dagger\,,\\
r_{\mu\nu} &= \partial_\mu r_\nu - \partial_\nu r_\mu + i[r_\mu, r_\nu]\,, \qquad r_{\mu\nu} \mapsto g_R r_{\mu\nu} g_R^\dagger\,,\\
l_{\mu\nu} &= \partial_\mu l_\nu - \partial_\nu l_\mu + i[l_\mu, l_\nu]\,, \qquad l_{\mu\nu} \mapsto g_L l_{\mu\nu} g_L^\dagger\,,\\
\chi &= 2B(s+ip)\,, \qquad \chi \mapsto g_R \chi g_L^\dagger\,.
\end{aligned} \tag{178}$$

Here, B is a constant, proportional to the quark condensate in the chiral limit.

Assume now that we want to construct the effective Lagrangian $\mathcal{L}_{eff}$ with the Goldstone boson fields only (this is a valid procedure, because, as already said, Goldstone bosons are lightest hadrons in the QCD spectrum). This Lagrangian should be invariant under chiral $U(3)_L \times U(3)_R$ and thus should be constructed from the covariant building blocks, introduced above. In addition, this effective Lagrangian is meant to adequately describe the physics at small momenta only, i.e., when the components of the momenta of the Goldstone bosons p_μ are much smaller than a typical hadronic scale $\Lambda \simeq 1$ GeV (an estimate the latter is given, e.g., by the nucleon mass). Consequently, one may introduce a small parameter called p and uniquely assign different orders of this parameter to the various terms appearing in the Lagrangian. The resulting counting rules are given by:

- The matrix $U(x) = 1 + \dfrac{i}{F}\,\lambda^a \varphi^a(x) + \ldots$ is, obviously, $O(1)$ in chiral counting.
- The covariant derivative $D_\mu U(x)$ is $O(p)$. Since, apart from ordinary derivative, it contains the fields r_μ, l_μ, for consistency reason, the latter should be $O(p)$ as well.
- The tensors $r_{\mu\nu}, l_{\mu\nu}$ are then $O(p^2)$.
- According to the Gell-Mann-Oakes-Renner formula, the mass squared of the Goldstone boson is proportional to the quark mass. Consequently, the quantities s, p count at $O(p^2)$.

Using these counting rules, one can construct the terms of the chirally symmetric Lagrangian. There is only a finite number of terms at a given chiral order. A tree-level contribution from a term at $O(p^n)$ to a generic amplitude is then suppressed by a factor $\left(\dfrac{p}{\Lambda}\right)^n$.

4.2 The chiral Lagrangian with mesons and calculation of the observables

The mesonic Lagrangians contain only even powers in the parameter p:

$$\mathcal{L} = \mathcal{L}^{(2)} + \mathcal{L}^{(4)} + \cdots . \tag{179}$$

At $O(p^2)$, it is possible to construct only two chiral-invariant operators (we write down the Lagrangians in Minkowski space):

$$\mathcal{L}^{(2)} = \frac{F^2}{4}\,\mathrm{tr}\left(D_\mu U D^\mu U^\dagger + \chi^\dagger U + \chi U^\dagger\right). \tag{180}$$

This Lagrangian contains two unknown constants: F and B, which are not fixed by symmetry considerations.

At the next order, the Lagrangian contains 10 unknown low-energy constants $L_1, \dots L_{10}$:

$$\begin{aligned}\mathcal{L}^{(4)} &= L_1 \mathrm{tr}\,(D_\mu U D^\mu U^\dagger)^2 + L_2 \mathrm{tr}(D_\mu U D_\nu U^\dagger)\mathrm{tr}(D^\mu U D^\nu U^\dagger) + \cdots \\ &+ L_{10}\mathrm{tr}\,(U l_{\mu\nu} U^\dagger r^{\mu\nu})\,, \end{aligned} \tag{181}$$

and so on. At a fixed order in p, there is only a finite number of unknown couplings, which are not fixed by chiral symmetry.

Expanding the lowest-order Lagrangian in the fields φ^a, we get:

$$\mathcal{L}^{(2)} = \frac{1}{2}\sum_{a=1}^{8} \partial_\mu \varphi^a \partial^\mu \varphi^a - \sum_{a=1}^{8} \frac{M_a^2}{2}\,\varphi^a \varphi^a + O(\varphi^4)\,, \tag{182}$$

where M_a^2 denote the masses of Goldstone bosons. Assuming, for simplicity that the u- and d-quark masses are equal (the isospin is not broken),

$$m_u = m_d = \hat{m}\,, \tag{183}$$

at the lowest order we get:

$$\begin{aligned} M_\pi^2 &= 2B\hat{m}\,, \\ M_K^2 &= B(m_s + \hat{m})\,, \\ M_\eta^2 &= \frac{2}{3}\,B(2m_s + \hat{m})\,. \end{aligned} \tag{184}$$

The higher terms in the expansion of the Lagrangian in φ^a produce the vertices with $4, 6, 8, \dots$ Goldstone bosons. It is also seen that these vertices correspond to the derivative interactions, which become weak at low momenta, irrespective of the values of the couplings. This fact plays crucial role in establishing the counting rules.

Up to now, we have dealt with the counting rules at the level of tree diagrams, emerging from the Lagrangian. In the meson ChPT, the counting for the loop diagrams can be straightforwardly established, since the scaling behavior of the meson propagators are simple – namely, since both the Goldstone boson masses and momenta scale like p, the Goldstone boson propagators $\dfrac{1}{M_a^2 - p^2}$ scale at $O(p^{-2})$. Consider, for example the one-loop correction to the Goldstone boson mass, shown in Fig. 15a. The vertex, produced by the lowest-order Lagrangian, scales at $O(p^2)$, the propagator in the loop at $O(p^{-2})$, and the loop integration adds $O(p^4)$. In total, the self-energy part contributes at $O(p^{2-2+4}) = O(p^4)$ and, thus, at the same order as the tree contribution from the next-to-leading order chiral Lagrangian, shown in Fig. 15b. Moreover, the loop graph in Fig. 15a is ultraviolet-divergent. This divergence comes at order p^4 and can be canceled by the divergent counterterm in $\mathcal{L}^{(4)}$.

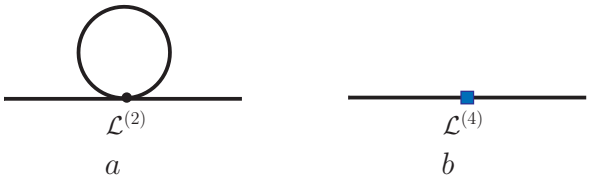

Figure 15: One-loop correction to the pion mass, together with the counterterms from $\mathcal{L}^{(4)}$.

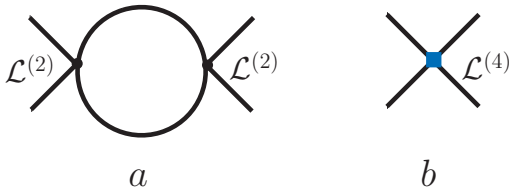

Figure 16: One-loop correction to the pion-pion scattering amplitude, together with the counterterms from $\mathcal{L}^{(4)}$.

The next example is the one-loop contribution to the scattering amplitude of the Goldstone bosons, shown in Fig. 16a. This diagram counts at $O(p^{2+2-2-2+4}) = O(p^4)$. The ultraviolet divergence, emerging in this loop, can be again eaten up by pertinent counterterms, contained in $\mathcal{L}^4$, see Fig. 16b. This pattern carries on consistently to the amplitudes with an arbitrary number of external legs, and to higher orders in chiral expansion.

To summarize, we have demonstrated, how the effective chiral Lagrangian can be constructed order by order in chiral expansion. One may further use this Lagrangian in order to calculate the Green functions with Goldstone boson fields at the same order. According to the Weinberg's theorem, these Green functions will coincide with those in QCD (at the same order). This, of course, does not really mean that we have "solved" QCD, since the Lagrangian of ChPT still contains a large number of couplings that are not fixed by symmetry (even so, this number is finite at any fixed chiral order). One has to determine these couplings somehow – e.g., matching a chosen set of calculated observables to the experiment or to the lattice results, and predicting the rest. We shall not enter this discussion, however, since the use of ChPT to study the hadron physics at low energy is not the primary goal of the present lectures. We are rather using the framework to study the finite-volume effects, taking for granted that these couplings are already determined elsewhere.

4.3 Baryon ChPT

Below, we give a very brief summary of the ChPT in the one-baryon sector. Here, both odd and even powers enter:

$$\mathcal{L} = \mathcal{L}^{(1)} + \mathcal{L}^{(2)} + \cdots . \tag{185}$$

The lowest-order pion-nucleon Lagrangian is given by

$$\mathcal{L}^{(1)} = \mathrm{tr}\,(\bar{B}(i\not{D} - m_0)B) - \frac{D}{2}\,\mathrm{tr}\,(\bar{B}\gamma_\mu\gamma_5\{u^\mu, B\}) - \frac{F}{2}\,\mathrm{tr}\,(\bar{B}\gamma_\mu\gamma_5[u^\mu, B])\,, \tag{186}$$

where B is the octet baryon field, m_0 denotes the baryon mass in the chiral limit, and

$$\begin{aligned} u_\mu &= i\Big[u^\dagger(\partial_\mu - ir_\mu)u - u(\partial_\mu - il_\mu)u^\dagger\Big]\,, \\ D_\mu B &= \partial_\mu B + [\Gamma_\mu, B]\,, \\ \Gamma_\mu &= \frac{1}{2}\Big[u^\dagger(\partial_\mu - ir_\mu)u + u(\partial_\mu - il_\mu)u^\dagger\Big]\,, \\ u &= \sqrt{U} = \exp\!\left(\frac{i}{2F}\,\lambda^a\varphi^a\right). \end{aligned} \tag{187}$$

The higher-order Lagrangians are constructed, using the covariant building blocks defined above.

The power counting in the baryon sector is a subtle issue, because the baryon propagator is no more a homogeneous function of momenta (namely, it contains a large scale, the baryon mass in the chiral limit, m_0, which scales at $O(1)$). There exist different prescriptions, how to formulate the power counting consistently in this case (infrared regularization, extended MOM scheme, heavy baryon ChPT). We do not dwell on these issues, because they are irrelevant in the calculation of the finite-volume artifacts.

4.4 The non-relativistic effective field theories

In the previous sections, we have discussed the construction of the effective theory of QCD, where all components of the four momenta of Goldstone bosons p_μ are of order of the Goldstone boson masses M_a. The relevant degrees of freedom in this case are the relativistic Goldstone boson fields φ^a together with the fields of other hadrons (e.g., the baryon field B). These fields form a basis for the non-linear realization of chiral symmetry of QCD, and the effective Lagrangian is constructed order-by-order in the chiral expansion. It should be however realized that, choosing different momentum scales, both the relevant degrees of freedom and relevant symmetries will look very different. Consider, for example, the processes with very high momentum

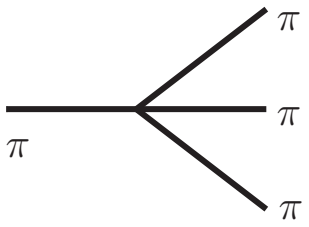

Figure 17: One pion producing three pions. Such processes are forbidden in NREFT.

transfer (e.g., deep inelastic ep scattering). Using hadronic degrees of freedom is very inconvenient here, because there are many different hadrons in a final state. In this case, using quark and gluon degrees of freedom is the best choice. Moreover, due to the asymptotic freedom, the color gauge symmetry, which played no explicit role in ChPT, comes now to the fore.

In many physical problems (on the lattice as well), we have to deal with the opposite situation. Namely, we have to consider slowly moving particles, whose three-momenta in magnitude are much smaller than their masses. In this case, one speaks of the non-relativistic effective field theories. It is also clear that the symmetry content is different here – namely, the chiral symmetry cannot play an explicit role. This happens because that all masses (including the masses of the Goldstone bosons) are now regarded as a heavy scale, the expansion in these masses is no more possible and various chiral orders mix up in the observables.

Another issue is the choice of the relevant degrees of freedom. At a first glance, we have the same particles as before. The crucial question is, however, whether the particles can be created and annihilated in the interaction vertices. For example, in a relativistic field theory, one pion can produce three pions through the vertex shown in Fig. 17. This is a perfectly allowed process in ChPT, since a mass gap here amounts to the two pion masses, and the pion mass represents a light scale for ChPT. On the contrary, in a theory where the pion mass is considered as a heavy scale, such processes cannot be included explicitly, and one has to set a framework, which conserves particle number in each interaction vertex. Such a framework goes under the name of the non-relativistic effective theory (NREFT).

There exist alternative formulations for NREFT. We start from the simplest one. Consider the system described by the free Lagrangian:

$$\mathcal{L}_0 = \phi^\dagger(x)\left(i\partial_t - m + \frac{\nabla^2}{2m}\right)\phi(x)\,. \tag{188}$$

Here, $\phi(x)$ is a scalar field. Its equation of motion (EOM) is given by:

$$\left(i\partial_t - m + \frac{\nabla^2}{2m}\right)\phi(x) = 0\,. \tag{189}$$

Note that the EOM is of the first order in the time derivative, in contrast to the Klein-Gordon equation. The solution of this equation is given by:

$$\phi(\mathbf{x},t) = \int \frac{d^3\mathbf{k}}{(2\pi)^3}\, e^{-iE_k t + i\mathbf{kx}} a(\mathbf{k})\,, \qquad E_k = \frac{\mathbf{k}^2}{2m}\,. \tag{190}$$

Note that the field $\phi(x)$ contains only annihilation operator and not the creation operator, i.e., it cannot be Hermitean.

The propagator of the non-relativistic field is given by:

$$i\langle 0|T\phi(x)\phi^\dagger(y)|0\rangle = \int \frac{d^4k}{(2\pi)^4} \frac{e^{-ikx}}{m + \dfrac{\mathbf{k}^2}{2m} - k_0 - i\varepsilon}\,. \tag{191}$$

It is seen that the dispersion law for this particle differs from the correct, relativistic dispersion law:

$$k_0 = \sqrt{m^2 + \mathbf{k}^2} = m + \frac{\mathbf{k}^2}{2m} - \frac{\mathbf{k}^4}{8m^3} + \cdots\,. \tag{192}$$

One may modify the free Lagrangian, adding above corrections:

$$\mathcal{L}_0 = \phi^\dagger(x)\left(i\partial_t - m + \frac{\nabla^2}{2m} + \frac{\nabla^4}{8m^3} + \cdots\right)\phi(x)\,. \tag{193}$$

The higher-order corrections are considered as a perturbation – their insertion in the diagrams corrects the non-relativistic dispersion law order by order.

Next, we consider the interactions. We write down all operators, which are rotationally invariant and obey discrete symmetries (the Lorentz-invariance or chiral symmetry are no more explicit in this framework). The small parameter in the counting rules are now provided by the magnitude of the three-momentum of a particle. Hence, the interaction Lagrangian contains a tower of operators with increasing number of space derivatives on the fields (time derivatives can be eliminated with the use of EOM). So, the Lagrangian takes the form:

$$\begin{aligned}\mathcal{L}_I &= c_0\phi^\dagger\phi^\dagger\phi\phi + c_1(\phi^\dagger \overset{\leftrightarrow}{\nabla}^2 \phi^\dagger\phi\phi + \text{h.c.}) + c_2(\phi^\dagger\phi^\dagger)\overset{\leftrightarrow}{\nabla}^2(\phi\phi) + \cdots \\ &+ d_0\phi^\dagger\phi^\dagger\phi^\dagger\phi\phi\phi + \cdots\,,\end{aligned} \tag{194}$$

where $a \overset{\leftrightarrow}{\nabla}^2 b = a\cdot\nabla^2 b + \nabla^2 a\cdot b$. The tree-level contribution from the higher-order terms of order p^{2n} is suppressed by a factor $\left(\dfrac{\mathbf{p}^2}{\Lambda^2}\right)^n$, where Λ is the hard scale of the non-relativistic theory (the lightest mass present).

It is seen that the interactions given in Eq. (194) indeed preserve the particle number. For this reason, one can consider the sectors with one, two, three, ...

particles individually: the sectors with lower number of particles do not talk to the sectors with more particles present.

The couplings $c_0, c_1, c_2, d_0, \ldots$ are the analogs of the low-energy couplings in ChPT. These should be determined from the matching of the physical observables. Due to the particle number conservation, the matching in the sectors with a given particle number can be done without considering the sectors containing higher number of particles.

4.5 Matching in NREFT

We shall give an example of matching in the two-particle sector. Consider the scattering amplitude of two identical non-relativistic particles $p_1 + p_2 \to q_1 + q_2$, and choose the center-of-mass (CM) frame $\mathbf{p}_1 = -\mathbf{p}_2 = \mathbf{p}$ and $\mathbf{q}_1 = -\mathbf{q}_2 = \mathbf{q}$. The total momentum in this frame is given by $P = (P_0, \mathbf{0}) = p_1 + p_2 = q_1 + q_2$. The non-relativistic scattering amplitude in the CM frame is denoted by $T^{NR}(\mathbf{p}, \mathbf{q})$.

Consider now the underlying relativistic theory, which reduces to our non-relativistic theory in the limit of small three-momenta. The same amplitude in the relativistic theory is denoted by $T^R(\mathbf{p}, \mathbf{q})$. The partial-wave expansion of this amplitude is given by:

$$T^R(\mathbf{p}, \mathbf{q}) = 4\pi \sum_{lm} Y_{lm}(\hat{p}) T_l^R(p, q) Y_{lm}^*(\hat{q})\,. \tag{195}$$

On the energy shell, $p = q$, the partial-wave amplitude $T_l^R(p, p) = T_l^R(p)$ obeys the unitarity relation:

$$\mathrm{Im}\, T_l^R(p) = \frac{p}{16\pi E(p)} \left|T_l^R(p)\right|^2, \qquad E(p) = 2\sqrt{m^2 + p^2}\,. \tag{196}$$

The scattering phase is defined as follows:

$$T_l^R(p) = \frac{16\pi E(p)}{p \cot \delta_l(p) - ip}\,. \tag{197}$$

The effective-range expansion for the S-wave phase shift $\delta_0(p) = \delta(p)$ reads:

$$p \cot \delta(p) = -\frac{1}{a} + \frac{1}{2}\, r p^2 + O(p^4) \tag{198}$$

(for simplicity, we restrict ourselves to the S-waves only). Here, a and r are the S-wave scattering length and the effective radius, respectively.

Next, let us turn to the matching. Our choice of the normalization of the one-particle states is different in the relativistic and the non-relativistic theories:

$$\begin{aligned} \text{Relativistic:} \qquad & \langle \mathbf{p}|\mathbf{q}\rangle = 2w(\mathbf{p})(2\pi)^3 \delta^3(\mathbf{p} - \mathbf{q})\,, \\ \text{Non-relativistic:} \qquad & \langle \mathbf{p}|\mathbf{q}\rangle = (2\pi)^3 \delta^3(\mathbf{p} - \mathbf{q})\,, \end{aligned} \tag{199}$$

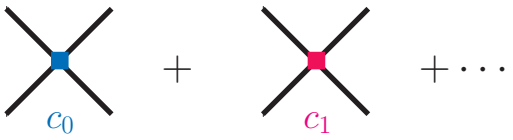

Figure 18: Tree diagrams in NREFT: no derivatives, two derivatives and so on.

where $w(\mathbf{p}) = \sqrt{m^2 + \mathbf{p}^2}$. Consequently, each external leg in the non-relativistic theory carries a factor $(2w(\mathbf{p}))^{-1/2}$, as compared to the relativistic theory. The matching condition for the on-shell amplitudes in the CM frame then reads:

$$T^R(\mathbf{p}, \mathbf{q}) = (2w(\mathbf{p}))^2 T^{NR}(\mathbf{p}, \mathbf{q}) \,, \qquad |\mathbf{p}| = |\mathbf{q}| \,. \tag{200}$$

More precisely, the above condition is assumed to hold, if the left- and right-hand sides are expanded in momenta $\mathbf{p}, \mathbf{q}$ up to a given order.

Let us now see, how the matching works in practice. The tree contribution to the non-relativistic on-shell S-wave amplitude is shown in Fig. 18:

$$T^{NR}_{tree}(p) = 4c_0 - 8c_1 p^2 + O(p^4) \,. \tag{201}$$

The one-loop contribution is shown in Fig. 19:

$$T^{NR}_{1-loop}(p) = 8c_0^2 \int \frac{d^D k}{(2\pi)^D i} \, \frac{1}{m + \dfrac{\mathbf{k}^2}{2m} - k_0 - i\varepsilon} \, \frac{1}{m + \dfrac{\mathbf{k}^2}{2m} - P_0 + k_0 - i\varepsilon} \,. \tag{202}$$

Note that the above integral is ultraviolet-divergent and should be regularized. Here, we use the dimensional regularization that leads to the much simpler formulae. Performing the integration over k_0, we get:

$$\begin{aligned} T^{NR}_{1-loop}(p) &= 8c_0^2 \int \frac{d^d \mathbf{k}}{(2\pi)^d} \, \frac{1}{2m - P_0 + \dfrac{\mathbf{k}^2}{m} - i\varepsilon} \\ &= 8c_0^2 (m(2m - P_0 - i\varepsilon))^{d/2-1} \int \frac{d^d \mathbf{k}}{(2\pi)^d} \, \frac{1}{\mathbf{k}^2 + 1} \,, \end{aligned} \tag{203}$$

where $d = D - 1$. Using now the formula:

$$\int \frac{d^d \mathbf{k}}{(2\pi)^d} \, \frac{1}{(\mathbf{k}^2 + 1)^n} = \frac{1}{(4\pi)^{d/2}} \, \frac{\Gamma\left(n - \dfrac{d}{2}\right)}{\Gamma(n)} \,, \tag{204}$$

and taking the limit $d \to 3$, we finally get[4]:

$$T^{NR}_{1-loop}(p) = \frac{ipm}{8\pi} \, (4c_0)^2 \,, \tag{205}$$

[4]In fact, the loop integral is ultraviolet-divergent. However, a linear divergence disappears in the dimensional regularization and we arrive at a finite answer.

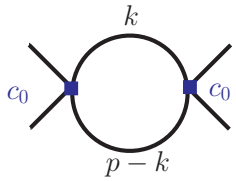

Figure 19: The simplest one-loop diagram in NREFT with non-derivative vertices.

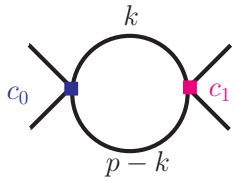

Figure 20: The one-loop diagram in NREFT with one derivative vertex.

where $p = \sqrt{m(P_0 - 2m)}$.

What happens, if the derivative vertex is inserted, see, e.g., Fig. 20? The corresponding loop integral is given by:

$$T^{NR}_{1-loop+derivative}(p) = (4c_0)(-4c_1)\frac{1}{2}\int \frac{d^d\mathbf{k}}{(2\pi)^d}\,\frac{\mathbf{p}^2+\mathbf{k}^2}{2m - P_0 + \dfrac{\mathbf{k}^2}{m} - i\varepsilon}\,. \tag{206}$$

The denominator of the above expression has the form $\dfrac{\mathbf{k}^2}{m} - \dfrac{\mathbf{p}^2}{m}$. Rewriting the numerator as $2\mathbf{p}^2 + (\mathbf{k}^2 - \mathbf{p}^2)$ and using the fact that, in the dimensional regularization,

$$\int \frac{d^d\mathbf{k}}{(2\pi)^d}\cdot 1 = 0\,, \tag{207}$$

we finally get:

$$T^{NR}_{1-loop+derivative}(p) = \frac{ipm}{8\pi}\,(4c_0)(-8c_1p^2)\,. \tag{208}$$

The pattern is crystal clear. At any given order, we shall have to deal with a bubble sum, shown in Fig. 21. Since the particle creation/annihilation is not allowed, the graphs in the non-relativistic theory will have only this topology. Here, V denotes the three-level matrix element, calculated to all orders[5]:

$$V = 4c_0 - 8c_1p^2 + \cdots\,. \tag{209}$$

[5] c_2 does not contribute to the matching in the CM frame. Galilean invariance allows to fix c_2 in terms on c_1.

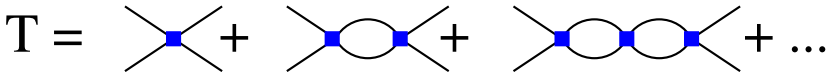

Figure 21: Lippmann-Schwinger equation in the NREFT. If dimensional regularization is used, the potential V coincides with the well-known two-body K-matrix and is expressed through the scattering phase.

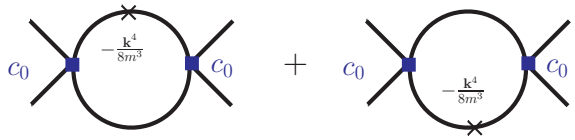

Figure 22: Relativistic insertions in the lowest-order loop diagram in NREFT.

Finally, we consider the relativistic insertions in the particle propagators. The insertions in the external propagators can be summed up easily – they just yield the relativistic dispersion law for the external particles. The insertions into the internal lines are shown in Fig. 22. The direct calculation yields:

$$\begin{aligned} T^{NR}_{1-loop+rel}(p) &= 16c_0^2 \int \frac{d^Dk}{(2\pi)^Di} \frac{1}{(m+\dfrac{\mathbf{k}^2}{2m}-k_0-i\varepsilon)} \frac{\mathbf{k}^4}{8m^3} \frac{1}{m+\dfrac{\mathbf{k}^2}{2m}-P_0+k_0-i\varepsilon} \\ &= \frac{5ip^3}{64\pi m}(4c_0)^2\,. \end{aligned} \tag{210}$$

Consequently,

$$\begin{aligned} & T^{NR}_{1-loop}(p)+T^{NR}_{1-loop+rel}(p) \\ &= \frac{im(4c_0)^2}{8\pi}\left((m(P_0-2m))^{1/2}+\frac{5}{8m^2}(m(P_0-2m))^{3/2}\right) \\ &= \frac{im(4c_0)^2}{8\pi}\left[\frac{P_0^2}{4}-m^2\right]^{1/2}\left(1+\frac{1}{2m^2}\left[\frac{P_0^2}{4}-m^2\right]\right). \end{aligned} \tag{211}$$

Thus, the relativistic insertions indeed correct the relativistic dispersion law to this order and, in addition, introduce some higher-order corrections in the amplitude.

At the end, we come to the matching condition. Using Eq. (200), we get:

$$\begin{aligned} \frac{32\pi w(\mathbf{p})}{-\dfrac{1}{a}+\dfrac{1}{2}rp^2+\cdots-ip} &= (2w(\mathbf{p}))^2\Bigg(4c_0-8c_1p^2+\frac{ipm}{8\pi}(4c_0)^2 \\ &+ \left(\frac{ipm}{8\pi}\right)^2(4c_0)^3+O(p^3)\Bigg)\,. \end{aligned} \tag{212}$$

Expanding the left-hand side in momentum p, we finally get:

$$\begin{aligned} c_0 &= -\frac{2\pi a}{m}\,, \\ -c_1 + \frac{c_0}{2m^2} &= -\pi a^2 r m\,. \end{aligned} \tag{213}$$

Thus, c_0 is given by the scattering length only, c_1 is given by the scattering length and the effective radius, and so on. The key property in the dimensional regularization is that the loop vanishes at threshold. Therefore, in order to perform an exact matching of the couplings $c_0, c_1, \ldots$, it suffices to carry out calculations at a given order. This statement does not hold, if another regularization is used.

4.6 "Relativized" non-relativistic effective theory

The approach, considered above, has one important drawback. As we have seen, the relativistic dispersion law in this approach is restored order by order, since the relativistic corrections are considered as a perturbation. This is very inconvenient, especially when moving reference frames are considered. Fortunately, it is possible to sum up all relativistic corrections in the propagators (but still do not allow for the particle creation/annihilation). In that vein, it is possible to generalize the definition of a non-relativistic effective theory, allowing three-momenta, comparable in magnitude with masses, provided that explicit creation/annihilation processes still do not have role at these momenta.

In order to achieve the above-mentioned generalization of the standard NREFT framework, we first rescale the field $\phi(x) \to \sqrt{2W}\phi(x)$, with $W = \sqrt{m^2 - \nabla^2}$, in order to avoid the non-covariant factors $\sqrt{2w(\mathbf{p})}$ in the matching condition. Further, as already said, we include all relativistic corrections into the free Lagrangian, rather than considering them as a perturbation. Consequently, the Lagrangian takes the form:

$$\mathcal{L} = \psi^\dagger (2W)(i\partial_t - W)\Phi + C_0 \phi^\dagger \phi^\dagger \phi\phi + \cdots\,, \tag{214}$$

and the free propagator is given by:

$$\langle 0|T\phi(x)\phi^\dagger(0)|0\rangle = \int \frac{d^4k}{(2\pi)^4}\, \frac{e^{-ikx}}{2w(\mathbf{k})(w(\mathbf{k}) - k_0 - i\varepsilon)}\,. \tag{215}$$

In addition to all this, one modifies Feynman rules, applying the so-called threshold expansion. The prescription consists in the following. One considers $(k_0 - m)$ and $\mathbf{k}$ as the quantities much smaller that m. Further, one expands the integrands in powers of these quantities, integrates in dimensional regularization and sums finally up. In this way, the original Feynman integral is modified that amounts to a change in the renormalization prescription.

In order to see, how the method works, consider the calculation of a single loop. In order to check the explicit relativistic invariance, we do calculation in a generic frame with $P_\mu = (P_0, \mathbf{P})$. The Feynman integral is given by:

$$\begin{aligned} J(P) &= \int \frac{d^D k}{(2\pi)^D i} \frac{1}{4w(\mathbf{k})w(\mathbf{P}-\mathbf{k})} \frac{1}{w(\mathbf{k}) - k_0 - i\varepsilon} \frac{1}{w(\mathbf{P}-\mathbf{k}) - P_0 + k_0 - i\varepsilon} \\ &= \int \frac{d^d k}{(2\pi)^d} \frac{1}{4w(\mathbf{k})w(\mathbf{P}-\mathbf{k})} \frac{1}{w(\mathbf{k}) + w(\mathbf{P}-\mathbf{k}) - P_0 - i\varepsilon} \,. \end{aligned} \tag{216}$$

One can now use the identity:

$$\begin{aligned} &\frac{1}{4w(\mathbf{k})w(\mathbf{P}-\mathbf{k})} \frac{1}{w(\mathbf{k}) + w(\mathbf{P}-\mathbf{k}) - P_0 - i\varepsilon} = \frac{1}{2P_0} \frac{1}{\mathbf{k}^2 - \frac{(\mathbf{kP})^2}{P_0^2} - q_0^2} \\ &+ \frac{1}{4w(\mathbf{k})w(\mathbf{P}-\mathbf{k})} \left(\frac{1}{w(\mathbf{k}) + w(\mathbf{P}-\mathbf{k}) + P_0} - \frac{1}{w(\mathbf{k}) - w(\mathbf{P}-\mathbf{k}) + P_0} \right. \\ &- \left. \frac{1}{-w(\mathbf{k}) + w(\mathbf{P}-\mathbf{k}) + P_0} \right) , \end{aligned} \tag{217}$$

where $q_0^2 = \frac{s}{4} - m^2$ and $s = P^2$.

Taking now into account the fact that $P_0 - 2m$ is a small quantity as compared to m, it is seen that the Taylor expansion of all terms except the first one gives polynomials in momenta. Since integrating the polynomials in dimensional regularization yields zero, only the first term survives the threshold expansion. The integral in this term can be evaluated explicitly, choosing the integration momentum as $\mathbf{k} = (k_\parallel, \mathbf{k}_\perp)$ with $\mathbf{k}_\perp \mathbf{P} = 0$, and rescaling $k_\parallel \to \gamma k_\parallel$ with $\gamma = \left(1 - \frac{\mathbf{P}^2}{P_0^2}\right)^{-1/2}$. The final result is given by:

$$J(P) = \frac{i}{16\pi} \left(1 - \frac{4m^2}{s}\right)^{1/2} . \tag{218}$$

Thus, the result for the loop in Lorentz-invariant (the result does not change, if the higher-order momentum insertions are considered in the vertices, provided the tree-level amplitude is invariant). The matching condition is also Lorentz-invariant. Consequently, the couplings $C_0, C_1, \ldots$, determined from the matching condition, do not depend on the reference frame.

5 Finite volume corrections to the stable particle masses

We finally start putting all pieces of the puzzle together, and show, how the effective field theories can be used for the calculation of the finite-volume artifacts on the lattice. The crucial point here is the observation that the size of a box, L, is much larger than the inverse of the hadronization scale Λ, which in QCD approximately equals to 1 GeV (the nucleon mass). Hence, the box "sees" hadrons and not quarks and gluons. Consequently, the properties of QCD *in a finite volume* will be described by the effective theories of hadrons *in a finite volume.* This observation lays ground for the approach we are pursuing.

It should be noted that, even $\Lambda L \gg 1$ should hold always, several different regimes are possible. These regimes can be characterized by the value of the parameter $M_\pi L$, where the pion mass M_π is the lightest mass in the system:

- $M_\pi L \gg 1$: This regime is relevant for the study of the processes in the multi-particle systems, like elastic and inelastic scattering, properties of the resonances, decay amplitudes. The condition $M_\pi L \gg 1$ means that the wave function of the system, reaching the boundary of the box, has taken the asymptotic form already and is determined solely through the on-shell S-matrix elements. NREFT is best suited to deal with this regime since, according to the above condition, the characteristic three-momenta of particles, given by integer multiples of $\dfrac{2\pi}{L}$, should be much smaller than the lightest mass in the system.

- $M_\pi L > 1$: This regime is relevant for calculation of the finite-volume artifacts to stable particle masses and spacelike form factors. ChPT is best suited for carrying out calculations in this regime.

- $M_\pi L < 1$: This regime is relevant for the study of the interplay between the chiral and infinite-volume limits. The so-called zero modes, corresponding to $\mathbf{p} = 0$, are non-perturbative in this regime and are described by the Lagrangian of a rigid rotator. Fast modes can be treated perturbatively.

Below, we shall consider all these regimes.

5.1 Particle mass in the φ^4-theory

As a warm-up example, we start from the calculation of the single particle mass in the φ^4-theory on the lattice. As seen from Fig. 23, this quantity exhibits quite a pronounced dependence on the box size L. We show below, how this dependence can be predicted. In the following, we shall neglect the artifacts, emerging from a finite lattice spacing, and concentrate on the finite-volume effects only. These two phenomena are well separated (short-distance vs. large distance) and can be treated separately.

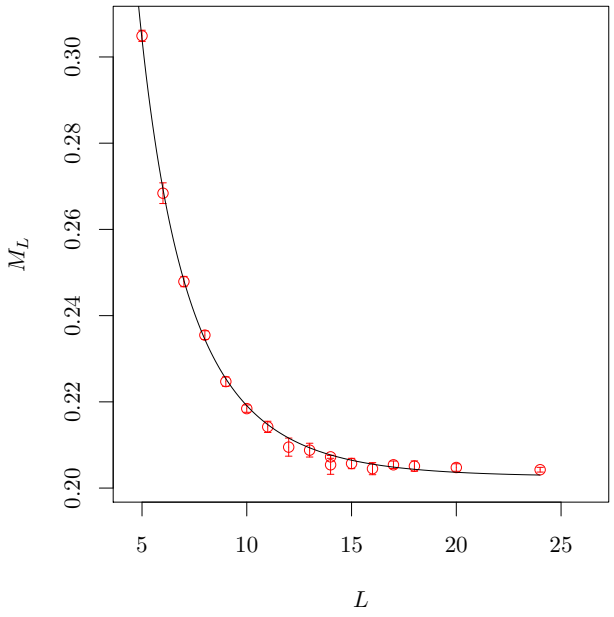

Figure 23: L-dependence of the particle mass in the φ^4 theory. The solid curve shows the result of the one-loop calculation. As seen, the agreement is almost perfect. The figure is taken from Ref. [19].

The Euclidean two-point function of the scalar field in the infinite volume is given by:

$$\langle 0|T\varphi(x)\varphi(0)|0\rangle = \int \frac{d^4p}{(2\pi)^4}\, e^{ipx} G(p)\,. \tag{219}$$

The two-point function is given through the self-energy part:

$$G^{-1}(p) = m^2 + p^2 - \Sigma(p)\,. \tag{220}$$

Due to $O(4)$-invariance in the infinite volume, both $G(p)$ and $\Sigma(p)$ are the functions of p^2 only. Further, m^2 is the physical mass. This means that:

$$\Sigma(p)\Big|_{p^2=-m^2} = 0\,, \qquad \frac{d}{dp^2}\,\Sigma(p)\Big|_{p^2=-m^2} = 0\,. \tag{221}$$

Consider now the same two-point function on the lattice, with the periodic boundary conditions imposed. Assume also that one has already extracted the mass from the large Euclidean time behavior of the two-point function. This implies that the effects that are related to the finite elongation of the lattice in the time direction (admixture of the contributions from the states other than the one-particle state of interest) are properly taken into account and we can forget about them. This corresponds to the situation when the Euclidean time elongation T is taken to infinity, whereas the

space elongation L stays finite. Hence, the two-point function on the lattice takes the form:

$$\langle 0|T\varphi(x)\varphi(0)|0\rangle_L = \frac{1}{L^3}\sum_{\mathbf{p}}\int\frac{dp_4}{2\pi}\,e^{ipx}G_L(p)\,, \tag{222}$$

where

$$G_L^{-1}(p) = m^2 + p^2 - \Sigma_L(p)\,. \tag{223}$$

This quantity has a pole at $p^2 = -m_L^2$, which is different from m^2. Our aim is to calculate the mass shift in a finite volume $m_L - m$. Note also that, due to breaking of the $O(4)$-symmetry by a finite cubic box, m_L depends on the frame it is calculated. We always imply the mass m_L to be the mass in the rest frame $\mathbf{p} = 0$.

The equation for m_L in the rest frame is given by:

$$m^2 + p_4^2 - \Sigma_L(p_4, \mathbf{0}) = 0\,, \qquad p_4 = im_L\,. \tag{224}$$

Since $m_L - m$ should be small, in the leading order in perturbation theory one obtains:

$$m_L - m \simeq -\frac{1}{2m}\,\Sigma_L(im, \mathbf{0})\,. \tag{225}$$

At the next step, we calculate the self-energy part in the φ^4 theory at lowest order. The (Euclidean) Lagrangian is given by:

$$\mathcal{L} = \frac{1}{2}\,\partial_\mu\varphi\partial_\mu\varphi + \frac{m_0^2}{2}\,\varphi^2 + \frac{\lambda_0}{4}\,\varphi^2\,. \tag{226}$$

Here, m_0 and λ_0 are bare parameters, which coincide with physical parameters m, λ only at tree level. Carrying out calculations in the infinite volume at $O(\lambda_0)$, we get:

$$G^{-1}(p) = m_0^2 + p^2 + 3\lambda_0\int\frac{d^Dk}{(2\pi)^D}\,\frac{1}{m_0^2 + k^2}\,. \tag{227}$$

from which we immediately conclude that

$$m^2 = m_0^2 + 3\lambda_0\int\frac{d^Dk}{(2\pi)^D}\,\frac{1}{m_0^2 + k^2}\,. \tag{228}$$

The inverse propagator in a finite volume is given by:

$$G_L^{-1}(p) = m_0^2 + p^2 + 3\lambda_0\frac{1}{L^3}\sum_{\mathbf{k}}\int\frac{dk_4}{2\pi}\,\frac{1}{m_0^2 + k^2}\,. \tag{229}$$

From this, we immediately get:

$$\Sigma_L(p) = -3\lambda_0\frac{1}{L^3}\sum_{\mathbf{k}}\int\frac{dk_4}{2\pi}\,\frac{1}{m_0^2 + k^2} + 3\lambda_0\int\frac{d^Dk}{(2\pi)^D}\,\frac{1}{m_0^2 + k^2}\,. \tag{230}$$

In order to calculate Σ_L, we use Poisson formula (75), generalizing it to d (non-integer) spatial dimensions (Alternatively, one could consider the replacement $dk_4 \to d^{1-\omega}k_4$ and $D = 4 - \omega \to 4$. The result is the same in both cases). We get:

$$\begin{aligned}\Sigma_L(p) &= -3\lambda_0 \int \frac{d^D k}{2\pi} \frac{1}{m_0^2 + k^2} \frac{1}{L^3} \sum_{\mathbf{n}\in\mathbb{Z}} \delta^d\left(\mathbf{k} - \frac{2\pi}{L}\,\mathbf{n}\right) + 3\lambda_0 \int \frac{d^D k}{(2\pi)^D} \frac{1}{m_0^2 + k^2} \\ &= -3\lambda_0 \int \frac{d^D k}{(2\pi)^D} \frac{1}{m_0^2 + k^2} \sum_{\mathbf{n}\in\mathbb{Z}} e^{iL\mathbf{nk}} + 3\lambda_0 \int \frac{d^D k}{(2\pi)^D} \frac{1}{m_0^2 + k^2}\,. \end{aligned} \tag{231}$$

The term with $\mathbf{n} = 0$ in the sum cancels the infinite-volume term exactly. Further, defining:

$$n_\mu = (0, \mathbf{n})\,, \tag{232}$$

and replacing m_0, λ_0 with m, λ in the terms which are already at $O(\lambda_0)$, we finally get:

$$m_L - m = \frac{3\lambda}{2m} \sum_{\mathbf{n}\neq 0} \int \frac{d^4 k}{(2\pi)^4} \frac{e^{iLnk}}{m^2 + k^2}\,. \tag{233}$$

Note that here we have already performed the limit $D \to 4$, since the integrals with $\mathbf{n} \neq 0$ are ultraviolet-convergent. These integrals can be calculated in the following manner:

$$\begin{aligned} m_L - m &= \frac{3\lambda}{2m} \sum_{\mathbf{n}\neq 0} \int_0^\infty d\lambda \int \frac{d^4 k}{(2\pi)^4}\, e^{iLnk - \lambda(m^2 + k^2)} \\ &= \frac{3\lambda}{2m} \sum_{\mathbf{n}\neq 0} \int_0^\infty d\lambda \int \frac{d^4 k}{(2\pi)^4}\, \exp\left(-\lambda k^2 - \lambda m^2 - \frac{n^2 L^2}{4\lambda}\right) \\ &= \frac{3\lambda}{32\pi^2 m} \sum_{\mathbf{n}\neq 0} \int_0^\infty \frac{d\lambda}{\lambda^2}\, \exp\left(-\lambda m^2 - \frac{n^2 L^2}{4\lambda}\right) \\ &= \frac{3\lambda}{8\pi^2} \sum_{\mathbf{n}\neq 0} \frac{1}{|\mathbf{n}|L}\, K_1(|\mathbf{n}|mL)\,. \end{aligned} \tag{234}$$

Here, $K_1(z)$ denotes the pertinent Bessel function, and we have used the formula:

$$\int_0^\infty d\lambda \lambda^{\nu-1} e^{-Z\lambda - Y/\lambda} = 2\left(\frac{Y}{Z}\right)^{\nu/2} K_\nu(2\sqrt{YZ})\,, \qquad K_{-\nu}(z) = K_\nu(z)\,. \tag{235}$$

Recalling now the asymptotic behavior of the Bessel functions:

$$K_\nu(z) \sim \sqrt{\frac{\pi}{2z}}\, e^{-z} \qquad z \to \infty\,, \tag{236}$$

we immediately see that the terms with $|\mathbf{n}| = 1$ give leading contribution to the mass shift – other contributions are exponentially suppressed with respect to this one. The leading contribution is also exponentially suppressed:

$$m_L - m \sim \frac{1}{L^{3/2}}\, e^{-mL}\,. \tag{237}$$

The argument of the exponent here is determined by the gap in the diagram. This is most easily seen from Eq. (233). Consider the term with $\mathbf{n} = (1, 0, 0)$ there. The integration contour in this integral can be deformed $k_1 \to k_1 + ic$ with $c \leq m$, and the denominator will not still be singular. After the deformation, the integral acquires the factor e^{-cL}, where c can be pushed maximally up to m. Finally, we arrive at the result shown in Eq. (237). On the contrary, the power-law prefactor $L^{-3/2}$ is non-universal (is different for the diagrams with different topology). In order to visualize, how the prediction works in practice, we refer to Fig. 23. The solid curve in this figure is given by Eq. (234), with the summation restricted to $|\mathbf{n}| = 1$ only. As seen, the agreement is almost perfect.

The argument with the gap applies to more complicated diagrams as well (and not only to the calculation of the finite-volume masses). In general, instead of m^2, the denominator contains an expression, denoted by $g(p, m, x)$, which is a polynomial in the external momenta, masses and the Feynman parameters x. Vanishing of this expression in the integration area over the Feynman parameters leads to the emergence of the imaginary parts in the diagrams (the intermediate particles can go on shell). However, if the quantity under consideration does not possess an imaginary part (say, the stable particle masses, or the spacelike form-factors), than $\min_x g(p, m, x)$ is always positive and determines the gap. Using the argument with the deformation of the contour again, we see that the same gap governs the volume dependence of this quantity at large values of L.

Let us briefly summarize the lessons learn in this simple example. The perturbation theory can be used to predict the volume dependence of the stable particle masses and other quantities away from the unitarity cuts. The quantity mL can be of order of 2 or 3 – then, the leading exponent is already small and the terms with large $|\mathbf{n}|$ in the sum are even more suppressed.

Note also that, for the stable particle masses, one can expand the argument to all orders in perturbation theory, showing that there is a lower bound on the gap in the diagrams with an arbitrary topology, and relate the coefficient at the leading exponential term to the two-particle scattering amplitude in the infinite volume. Moreover, the gap is bound from below by a positive number in all orders. Similar formulae can be obtained for some other quantities (say, the pion decay constant). We, however, do not consider this issue in detail.

5.2 Finite volume correction to the pion mass

Our primarily goal is to calculate the finite-volume artifacts in QCD, where perturbation theory in terms of quarks and gluons is no more applicable. The effective

field theories of QCD, considered above, help to achieve this goal. The conceptual argument goes here as follows. The finite-volume effects affect the dynamics at low momenta, where, in the infinite volume, QCD is described by an effective theory with meson and baryon degrees of freedom. Then, the behavior of the QCD Green functions in a finite volume should be also described by an effective theory in a finite volume. The difference can emerge only at short distances of order of $1/\Lambda \simeq 1\,\mathrm{GeV}^{-1}$ (Here Λ denotes the typical hadronic scale in ChPT, introduced earlier). However, if $\Lambda L \gg 1$, this effect will be exponentially small and can be safely neglected. In the scheme that we are describing, L^{-1} can be counted as a small quantity of $O(p)$, similar to the momenta of Goldstone bosons. This generalization leads to a consistent power-counting scheme in ChPT, rendering a systematic calculation of the finite-volume corrections possible.

At this point, it becomes clear, why we invested an effort in reviewing the low-energy effective theories first. As a demonstration, we consider calculation of the shift of the pion mass in ChPT in a finite volume at one loop. The calculations are very similar to the one carried out above for the φ^4-theory. For simplicity, we work in the $SU(2)$ version of ChPT, assuming isospin symmetry. Using the so-called σ-model parameterization

$$U = \sqrt{1 - \frac{\boldsymbol{\varphi}^2}{F^2}} + \frac{i}{F}\,\boldsymbol{\varphi}\boldsymbol{\tau}\,, \tag{238}$$

and expanding the lowest-order Lagrangian in fields[6], we get (in the Minkowski space):

$$\mathcal{L}^{(2)} = \frac{1}{2}\,\partial_\mu\boldsymbol{\varphi}\partial^\mu\boldsymbol{\varphi} - \frac{M^2}{2}\,\boldsymbol{\varphi}^2 + \frac{1}{2F^2}\,(\boldsymbol{\varphi}\partial_\mu\boldsymbol{\varphi})^2 - \frac{M^2}{8F^2}\,\boldsymbol{\varphi}^4 + \cdots\,. \tag{239}$$

Here, $M^2 = 2\hat{m}B$ is the lowest-order pion mass and the values of the couplings F, B differ in the $SU(3)$ and $SU(2)$ versions of ChPT.

The calculation of the pion mass in ChPT at one loop proceeds along the standard path, and we give only a final result here. Apart from the loop, produced from the lowest-order Lagrangian in Eq. (239), it contains one of the low-energy constants, l_3, which stems from the next-to-leading order Lagrangian $\mathcal{L}^{(4)}$ and cancels the divergence of the loop. Performing the Wick rotation in the loop integral, we finally get:

$$M_\pi^2 = M^2\left\{1 + \frac{1}{2F^2}\int\frac{d^Dk}{(2\pi D)}\,\frac{1}{M_\pi^2 + k^2} + \frac{2M_\pi^2}{F^2}\,l_3\right\}. \tag{240}$$

The expression for the mass in a finite volume is the same, except the integration over the space components $\mathbf{k}$ is replaced by summation. Thus,

$$M_{\pi,L}^2 - M_\pi^2 = M^2\left\{1 + \frac{1}{2F^2}\,\delta I_L\right\}, \tag{241}$$

[6]Here, τ^a are isospin matrices and $\boldsymbol{\varphi} = (\varphi^1, \varphi^2, \varphi^3)$ denotes the pion field

where

$$\delta I_L = \frac{1}{L^3}\sum_{\mathbf{k}}\int\frac{dk_4}{2\pi}\frac{1}{M_\pi^2+k^2} - \int\frac{d^Dk}{(2\pi)^D}\frac{1}{M_\pi^2+k^2}$$
$$= \frac{M_\pi}{4\pi^2F^2}\sum_{\mathbf{n}\neq 0}\frac{1}{|\mathbf{n}|L}\,K_1(|\mathbf{n}|M_\pi L)\,. \qquad (242)$$

Finally, we arrive at the following result:

$$M_{\pi,L} - M_\pi = \frac{M_\pi^2}{16\pi^2F^2}\sum_{\mathbf{n}\neq 0}\frac{1}{|\mathbf{n}|L}\,K_1(|\mathbf{n}|M_\pi L)\,. \qquad (243)$$

Note that this result does not depend on the low-energy constant l_3. In other words, renormalization in a finite and infinite volume is exactly the same, and no renormalization is needed in the difference.

The method described above can be used for other physical quantities as well. In calculating the nucleon mass, one need not care about the breaking of counting rules since this all concerns the self-energy in the infinite volume and the effect drops in the mass difference one is looking for. Moreover, the method can be successfully applied to calculate finite-volume effects in the spacelike form factors, subthreshold amplitudes, etc – in all quantities, where the intermediate particles in the Feynman diagrams cannot go on shell and thus the imaginary part vanishes.

6 Chiral limit in a finite volume

The formalism, described above, has a drawback. Namely, one cannot perform the chiral limit $M \to 0$ in the above expressions. To illustrate this, let us consider the quantity δI_L, given by Eq. (242). Since the infinite-volume integral vanishes, as $M \to 0$, the quantity δI_L at $M \to 0$ is given by:

$$\delta I_L = \frac{1}{L^3}\sum_{\mathbf{k}}\int\frac{dk_4}{2\pi}\frac{1}{k_4^2+\mathbf{k}^2} = \frac{1}{L^3}\sum_{\mathbf{k}}\frac{1}{2|\mathbf{k}|}\,. \qquad (244)$$

This quantity does not make sense, because the term with $\mathbf{k}=0$ diverges. Physically, it is no wonder that we encounter this difficulty: as $M \to 0$, the Compton wavelength of a pion becomes infinity and the pion does not fit a box anymore. So, a procedure for calculating the finite-volume artifacts within the effective field theory should be modified.

In order to move forward, let us note that, retaining only the zero modes with $\mathbf{k}=0$ in the expansion of the (interacting) pion field

$$\varphi^a(\mathbf{x},t) = \frac{1}{L^3}\sum_{\mathbf{k}}\left(e^{-iw(\mathbf{k})t+i\mathbf{kx}}c_a(\mathbf{k},t) + e^{iw(\mathbf{k})t-i\mathbf{kx}}c_a^\dagger(\mathbf{k},t)\right), \qquad (245)$$

we get a field that depends of the variable t only (here, $c_a(\mathbf{k},t), c_a^\dagger(\mathbf{k},t)$ are annihilation/creation operators for the interacting field $\varphi^a(x)$). This suggests the following splitting of the matrix $U(x)$:

$$\begin{aligned} U(x) &= \sqrt{U(t)}\tilde{U}(x)\sqrt{U(t)}\,, \\ \tilde{U}(x) &= \sqrt{1-\frac{\tilde{\boldsymbol{\varphi}}(x)^2}{F^2}}+\frac{i}{F}\,\tilde{\boldsymbol{\varphi}}(x)\,. \end{aligned} \tag{246}$$

Choosing $U(t)$ appropriately, one can always achieve that the expansion of $\tilde{\varphi}^a(x)$ does not contain a zero mode:

$$\tilde{\varphi}^a(\mathbf{x},t)=\frac{1}{L^3}\sum_{\mathbf{k}\neq 0}\left(e^{-iw(\mathbf{k})t+i\mathbf{kx}}\tilde{c}_a(\mathbf{k},t)+e^{iw(\mathbf{k})t-i\mathbf{kx}}\tilde{c}_a^\dagger(\mathbf{k},t)\right). \tag{247}$$

Thus the field $U(x)$ is split into two parts: the field $U(t)$ describing only zero modes and $\tilde{U}(x)$, describing only non-zero modes. The latter can be treated perturbatively, because their propagators never vanish. Fur the moment being, we neglect them completely and concentrate on the zero modes. The action functional for the latter in Minkowski space takes the form:

$$S=\int d^4x\,\frac{F^2}{4}\,\mathrm{tr}\left(\partial_\mu U(t)\partial^\mu U^\dagger(t)\right)=\frac{F^2L^3}{4}\int dt\mathrm{tr}\,(\dot{U}\dot{U}^\dagger)\,. \tag{248}$$

Here, we already work in the chiral limit. Introducing now the four-vector

$$s_\alpha=\left(\sqrt{1-\frac{\boldsymbol{\varphi}^2}{F^2}},\frac{\boldsymbol{\varphi}}{F}\right),\qquad s_\alpha s_\alpha=1\,, \tag{249}$$

we may rewrite the action functional in a well-known form, corresponding to the $O(4)$ quantum-mechanical rigid rotor:

$$S=\frac{\Theta}{2}\int dt\,\dot{s}_\alpha\dot{s}_\alpha\,, \tag{250}$$

where $\Theta=F^2L^3$ is the moment of inertia. The energy levels of the rigid rotor are well known:

$$E_n=\frac{n(n+2)}{2\Theta}\,. \tag{251}$$

The lowest energy level with $n=1$ corresponds to a single pion with $\mathbf{k}=0$ in a finite volume. Since the pion is massless in the infinite volume, we finally get:

$$M_{\pi,L}-M_\pi=\frac{3}{2\Theta}=\frac{3}{2F^2L^3}\,. \tag{252}$$

In case of N_f flavors, the above formula is modified to:

$$M_{\pi,L} - M_\pi = \frac{N_f^2 - 1}{N_f F^2 L^3} \,. \tag{253}$$

In order to carry out consistent calculations in ChPT in this regime, the power-counting rules should be modified. Introducing an abstract small parameter δ, one still counts the momenta as $O(\delta)$ and $1/L = O(\delta)$. However, one has to count $M_\pi = O(\delta^3)$, in difference to what was done previously. It can be seen that the propagators of zero and nonzero modes count differently in δ: whereas the contribution from the latter can be taken into account in the perturbation theory, the former has to be included by using non-perturbative methods, as in the example considered here.

Note, finally, that the regime $M_\pi L \ll 1$, considered is this section, goes under the name of the δ-regime, whereas the situation $M_\pi L > 1$, dealt in the previous section, is referred to as the p-regime.

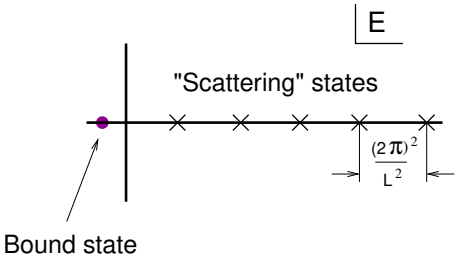

Figure 24: The bound and "scattering" states in a finite volume. When $L \to \infty$, the latter condense to the continuum.

7 Scattering processes in a finite volume

7.1 Maiani-Testa no-go theorem

The spectrum in a finite volume is always discrete – in difference to the infinite volume, where the spectrum consists of isolated states plus continuum (the scattering states). A correspondence between the infinite- and finite-volume spectra is schematically given in Fig. 24. The isolated states have their counterparts in a finite volume and the energy changes very little (the finite-volume effects are exponentially suppressed). On the contrary, the continuum is replaced by a tower of closely located states in a finite volume. Each chosen state in this tower collapses towards threshold, but there are infinitely many states that condense towards continuum, as $L \to \infty$.

This qualitative difference between isolated states and scattering states manifests itself in the Maiani-Testa no-go theorem. In the Euclidean space, one may directly extract the characteristics of the isolated states (e.g., the masses of stable particles, or the matrix elements of a current between stable particle states), without performing analytic continuation to the Minkowski space. However, one cannot deal in this way with the multiparticle states that correspond to the continuum in the infinite volume. In order to see this, consider, for example, the extraction of the timelike form factor from the Euclidean Green function, and take L very large (infinite):

$$G(t_1, t_2, \mathbf{q}, -\mathbf{q}) = \langle 0|\varphi_{\mathbf{q}}(t_1)\varphi_{-\mathbf{q}}(t_2)J(0)|0\rangle \,. \tag{254}$$

Here,

$$\phi_{\mathbf{q}}(t) = \int d^3\mathbf{x} e^{i\mathbf{q}\mathbf{x}}\varphi(\mathbf{x}, t) \,, \tag{255}$$

and $J(0)$ denotes the current operator (for simplicity, we assume that it is a scalar).

Consider first the limit $t_1 \to \infty$. Introducing the set of the intermediate states

gives:

$$\begin{aligned} G(t_1,t_2,\mathbf{q},-\mathbf{q}) &= \sum_n \langle 0|\varphi_{\mathbf{q}}(t_1)|n\rangle\langle n|\varphi_{-\mathbf{q}}(t_2)J(0)|0\rangle \\ &\to e^{-E_{\mathbf{q}}t_1}\langle 0|\varphi_{\mathbf{q}}(0)|\mathbf{q}\rangle\langle \mathbf{q}|\varphi_{-\mathbf{q}}(t_2)J(0)|0\rangle \\ &= e^{-E_{\mathbf{q}}t_1}\langle 0|\varphi_{\mathbf{q}}(0)|\mathbf{q}\rangle F_{\mathbf{q}}(t_2)\,. \end{aligned} \tag{256}$$

The one-particle state $|\mathbf{q}\rangle$ gives the leading contribution here.

Consider now the limit $t_2 \to \infty$ in the quantity $F_{\mathbf{q}}(t_2)$. introducing again the sum over all intermediate states, we get:

$$F_{\mathbf{q}}(t_2) = \sum_n (2\pi)^3\delta^3(\mathbf{P}_n)e^{-(E_n-E_{\mathbf{q}})t_2}\langle \mathbf{q}|\varphi_{-\mathbf{q}}(0)|n\rangle\langle n|J(0)|0\rangle\,. \tag{257}$$

The state with the lowest energy in this sum is $|\mathbf{0},\mathbf{0}\rangle$. However, the coefficient of the leading exponential does not provide a useful information. Namely, it is given by a product of the timelike form-factor at threshold $\langle \mathbf{0},\mathbf{0}|J(0)|0\rangle$ and the off-shell amplitude $\langle \mathbf{q}|\varphi_{-\mathbf{q}}(0)|\mathbf{0},\mathbf{0}\rangle$, which depends on the choice of the interpolating field. In brief, the extraction of the timelike form factor with a standard method fails, and one should be looking for the alternatives.

7.2 Perturbative shifts of the energy levels in the scattering sector

In the quest of the alternative approach, we again invoke the effective field theories in a finite volume. However, we put further restriction on the volumes that are used. Namely, in order to describe the scattering processes adequately, the size of the box must be much larger than the characteristic range of interactions,$r \ll L$. Only in this case, the discrete spectrum, which is determined by the boundary condition at the box surface, does not depend on the short-range details of interaction and can be expressed in terms of the physical observables. On the other hand, since the interaction range is usually given by the inverse mass of the lightest particle in the system (pion, in case of QCD), i.e., $r \simeq M_\pi^{-1}$, the exponential corrections that are proportional to $e^{-M_\pi L}$, are suppressed and can be neglected. Further, the characteristic momenta on a lattice are given in units of $\dfrac{2\pi}{L}$, very small as compared to M_π. Consequently, one finds himself/herself in the domain of applicability of the NREFT: the momenta are small, and the finite-volume corrections from the diagrams with a non-zero gap (these correspond to the particle creation/annihilation) are neglected. In the language of the NREFT, this is equivalent to the statement that the effective couplings to not depend on L.

Let is now see, how this works in practice. To this end, we write down the non-relativistic effective Lagrangian for a single spinless particle, already considered in

the previous sections:

$$\mathcal{L} = \phi^\dagger \left(i\partial_t - m + \frac{\nabla^2}{2m} \right) \phi + c_0 \phi^\dagger \phi^\dagger \phi \phi + \cdots \,, \tag{258}$$

where, from the matching, $c_0 = -\dfrac{2\pi a}{m}$.

Using canonical method, one can derive the Hamiltonian

$$H = H_0 + V \,, \tag{259}$$

where H_0 denotes the free Hamiltonian.

The matrix element of the potential in the momentum space, in the CM frame, takes the form:

$$\langle \mathbf{p}, -\mathbf{p}|V|\mathbf{k}, -\mathbf{k}\rangle = \frac{-2c_0}{L^3} \,. \tag{260}$$

Note that an additional factor $\dfrac{1}{2!}$ arises in the above matrix element, due to the fact that one has to deal with the identical particles.

We are now prepared to calculate the finite-volume shift of the ground two-particle state by using standard Raileigh-Schrödinger perturbation theory. The first- and the second-order corrections are given by:

$$\begin{aligned}
\delta E^{(1)} &= \langle 0|V|0\rangle = \frac{-2c_0}{L^3} \,, \\
\delta E^{(2)} &= \sum_{k\neq 0} \frac{|\langle 0|V|k\rangle|^2}{E_0^{(0)} - E_k^{(0)}} = \sum_{k\neq 0} \left(\frac{-2c_0}{L^3} \right)^2 \frac{1}{0 - \dfrac{\mathbf{k}^2}{m}} \\
&= -\frac{mL^2}{4\pi^2} \left(\frac{-2c_0}{L^3} \right)^2 \mathcal{I} \,,
\end{aligned} \tag{261}$$

where[7]

$$\mathcal{I} = \sum_{\mathbf{n}\neq 0} \frac{1}{\mathbf{n}^2} = -8.91363291781\cdots \,. \tag{262}$$

Using the matching condition, we finally get and expression for the ground-state energy shift:

$$E_0 = 0 + \delta E^{(1)} + \delta E^{(2)} + \cdots = \frac{4\pi a}{mL^3} \left\{ 1 - \left(\frac{a}{\pi L} \right) \mathcal{I} \right\} + O(L^{-5}) \,. \tag{263}$$

Few remarks are in order here:

[7]The calculation of the sum requires ultraviolet regularization. We give the answer in the dimensional regularization. This is consistent with the fact that dimensional regularization was also used to regulate divergences in the infinite volume.

- Using NREFT, we were able to calculate the energy shift of the ground state in the scattering sector up to $O(L^{-5})$. The Lagrangian represents a key link between the infinite- and finite-volume problems: its couplings are the same in both cases. For this reason, it was possible to relate the finite-volume shift to the parameters of the system in the infinite volume (the scattering length, in this case). Using the argument other way around, it is possible to extract the scattering length from the measured energy shift of the ground state, circumventing the Maiani-Testa no-go theorem. In doing so, we took and advantage of working in a finite volume: our energy level(s) have not collapsed towards threshold yet.

- As it can be easily seen, consecutive terms in the perturbative expansion correspond to the Feynman diagrams with no gap. For this reason, the corrections decrease as powers of L and not as exponentials.

- The counting rule in the NREFT states $\mathbf{p} \sim L^{-1}$. Thus, evaluating higher-order terms in perturbation theory and including derivative vertices in the Lagrangian, one can calculate corrections to Eq. (263) in higher orders in $1/L$ Up to now, the calculations are done, up to and including order L^{-7}. At higher orders, other effective-range parameters come into the play. For example, the effective range contributes to the ground-state shift at $O(L^{-6})$.

- Excited states can be treated on the equal footing.

- Relativistic corrections can be taken into account perturbatively, both in the matching condition and in the Raileigh-Schrödinger perturbation theory.

- States with three, four and more particles can be considered. More couplings come into play, but in the higher orders. For example, up to and including $O(L^{-5})$, all energies are determined by the couplings from the two-body sector. This imposes interesting constraints of the two-body effective-range parameters that are extracted through a global fit to the energy shifts.

7.3 The Lüscher equation for the two-body scattering

As we have seen, one may extract effective-range expansion parameters from the fit to the energy shifts in a finite volume. Below, we shall see that, in the two-body sector, one can afford more – namely, one can extract scattering phase shifts at a given energy and study the properties of resonances. We have already seen an example of this in the one-dimensional quantum mechanics, and we wish to derive an analog of the quantization condition for the scattering in three dimensions here. NREFT represents an ideal tool for this, as will be seen below. Moreover, for full generality, we shall derive the three-dimensional Lüscher equation in an arbitrary moving frame, using to this end the "relativized" version of NREFT, considered above and consider the case of non-identical particles with different masses $m_{1,2}$.

These particles are described by the non-relativistic fields $\phi_{1,2}$. The Lagrangian of the system is given by:

$$\mathcal{L} \;=\; \sum_{i=1,2} \phi_i^\dagger 2W_i(i\partial_t - W_i)\phi_i + C_0\phi_1^\dagger\phi_1\phi_2^\dagger\phi_2 + \cdots\,, \tag{264}$$

where $W_i = \sqrt{m_i^2 + \nabla^2}$ and the ellipses stand for the terms that contain at least two derivatives.

Let us start in the infinite volume. It is straightforward to ensure that the scattering T-matrix in the infinite volume in an arbitrary moving frame obeys the Lippmann-Schwinger (LS) equation:

$$T(\mathbf{p}_1,\mathbf{p}_2;\mathbf{q}_1,\mathbf{q}_2) = V(\mathbf{p}_1,\mathbf{p}_2;\mathbf{q}_1,\mathbf{q}_2) + \int \frac{d^d\mathbf{k}_1}{(2\pi)^d 2w_1(\mathbf{k}_1)} \frac{d^d\mathbf{k}_2}{(2\pi)^d 2w_2(\mathbf{k}_2)}$$

$$\times\;\; (2\pi)^d\delta^d(\mathbf{p}_1+\mathbf{p}_2-\mathbf{k}_1-\mathbf{k}_2)\, \frac{V(\mathbf{p}_1,\mathbf{p}_2;\mathbf{k}_1,\mathbf{k}_2)T(\mathbf{k}_1,\mathbf{k}_2;\mathbf{q}_1,\mathbf{q}_2)}{w_1(\mathbf{k}_1)+w_2(\mathbf{k}_2)-w_1(\mathbf{q}_1)-w_2(\mathbf{q}_2)-i\varepsilon}\,, \tag{265}$$

where $w_i(\mathbf{l}) = \sqrt{m_i^2 + \mathbf{l}^2}$ and the potential is given by the matrix element of the interaction Lagrangian between the two-particle states. As usual, the parameter d denotes the number of space dimensions (at the end of calculations, $d \to 3$).

By construction, the potential V is a Lorentz-invariant low-energy polynomial that depends only on scalar products of the 4-momenta. The first term in the expansion is given by

$$V(\mathbf{p}_1,\mathbf{p}_2;\mathbf{q}_1,\mathbf{q}_2) = C_0 + \cdots\,. \tag{266}$$

Next, let us define the CM and relative momenta, according to

$$\begin{aligned} P \;&=\; p_1 + p_2\,, \quad p = \mu_2 p_1 - \mu_1 p_2\,, \\ \mu_{1,2} \;&=\; \frac{1}{2}\left(1 \pm \frac{m_1^2 - m_2^2}{P^2}\right), \qquad p^2 = \frac{\lambda(P^2,m_1^2,m_2^2)}{4P^2}\,, \end{aligned} \tag{267}$$

and, similarly, for other pair of momenta. Here $\lambda(x,y,z)$ denotes the Källén triangle function.

Next, we define the momenta boosted to the CM frame (note that the boost velocity is different in the initial and the final states, because the potential is generally off the energy shell):

$$\mathbf{p}^* = \mathbf{p} + \mathbf{P}\left((\gamma-1)\frac{\mathbf{pP}}{\mathbf{P}^2} - \gamma v\frac{p_0}{|\mathbf{P}|}\right), \quad p_0^* = \gamma p_0 - \gamma v\frac{\mathbf{pP}}{|\mathbf{P}|} = 0\,,$$

$$P_\mu^* = (\sqrt{P^2},\mathbf{0})\,, \qquad v = \frac{|\mathbf{P}|}{P_0}\,, \quad \gamma = (1-v^2)^{-1/2}\,, \tag{268}$$

and, similarly, for other pair of momenta.

In the boosted frame, the potential can be expanded in partial waves:

$$V(\mathbf{p}_1,\mathbf{p}_2;\mathbf{q}_1,\mathbf{q}_2) = 4\pi \sum_{lm} V_l(|\mathbf{p}^*|,|\mathbf{q}^*|)\mathcal{Y}_{lm}(\mathbf{p}^*)\mathcal{Y}^*_{lm}(\mathbf{q}^*)\,. \tag{269}$$

Here, the function V_l is real and symmetric with respect to its arguments, i.e., Eq. (269) describes a Hermitean potential. The quantity $\mathcal{Y}_{lm}(\mathbf{p})$ is defined as $\mathcal{Y}_{lm}(\mathbf{p}) = |\mathbf{p}|^l Y_{lm}(\hat{\mathbf{p}})$, where Y_{lm} are the usual spherical harmonics.

Performing now the partial-wave expansion in the amplitude

$$T(\mathbf{p}_1,\mathbf{p}_2;\mathbf{q}_1,\mathbf{q}_2) = 4\pi \sum_{lm} T_l(|\mathbf{p}^*|,|\mathbf{q}^*|)\mathcal{Y}_{lm}(\mathbf{p}^*)\mathcal{Y}^*_{lm}(\mathbf{q}^*)\,, \tag{270}$$

substituting this expansion into the LS equation (265), it is seen that the equation diagonalizes in l due to unbroken rotational symmetry. Further, the denominator is proportional to $|\mathbf{k}^*|^2 - |\mathbf{q}^*|^2$. Hence, in the numerator one may replace

$$V_l(|\mathbf{p}^*|,|\mathbf{k}^*|)T_l(|\mathbf{k}^*|,|\mathbf{q}^*|) \to V_l(|\mathbf{p}^*|,|\mathbf{q}^*|)T_l(|\mathbf{q}^*|,|\mathbf{q}^*|)\,, \tag{271}$$

since the difference of these two quantities is proportional to $|\mathbf{k}^*|^2 - |\mathbf{q}^*|^2$ and the resulting integral vanishes in the dimensional regularization. Putting finally $|\mathbf{p}^*| = |\mathbf{q}^*| = \lambda^{1/2}(s,m_1^2,m_2^2)/(2\sqrt{s})$ on shell, we get an algebraic equation for the fully on-shell T-matrix and the potential:

$$T_l(s) = V_l(s) + V_l(s)|\mathbf{p}^*|^{2l} G(s) T_l(s)\,, \tag{272}$$

where the obvious shorthand notations for the on-shell quantities $V_l(s) = V_l(|\mathbf{p}^*|,|\mathbf{p}^*|)$ and $T_l(s) = T_l(|\mathbf{p}^*|,|\mathbf{p}^*|)$ are used. The quantity $G(s)$ is given by:

$$G(s) = \int \frac{d^d\mathbf{k}_1}{(2\pi)^d 2w_1(\mathbf{k}_1)} \frac{d^d\mathbf{k}_2}{(2\pi)^d 2w_2(\mathbf{k}_2)} \frac{(2\pi)^d\delta^d(\mathbf{P}-\mathbf{k}_1-\mathbf{k}_2)}{w_1(\mathbf{k}_1)+w_2(\mathbf{k}_2)-P_0-i0} = \frac{i|\mathbf{p}^*|}{8\pi\sqrt{s}}\,. \tag{273}$$

Further, unitarity gives:

$$T_l(s) = \frac{8\pi\sqrt{s}}{|\mathbf{p}^*|^{2l+1}}\, e^{i\delta_l(s)} \sin\delta_l(s)\,, \qquad V_l(s) = \frac{8\pi\sqrt{s}}{|\mathbf{p}^*|^{2l+1}}\, \tan\delta_l(s)\,, \tag{274}$$

where $\delta_l(s)$ is the scattering phase.

The transition to the finite volume is performed in the "lab frame". The momenta are discretized according to

$$\mathbf{k}_i = \frac{2\pi}{L}\,\mathbf{n}_i\,, \qquad \mathbf{n}_i \in \mathbb{Z}^3\,. \tag{275}$$

The partial-wave expansion of the potential does not change. However, since the introduction of a cubic box breaks rotational symmetry, the partial-wave expansion of the scattering amplitude has to be modified:

$$T(\mathbf{p}_1,\mathbf{p}_2;\mathbf{q}_1,\mathbf{q}_2) = 4\pi \sum_{lm,l'm'} T_{lm,l'm'}(|\mathbf{p}^*|,|\mathbf{q}^*|;\mathbf{P})\mathcal{Y}_{lm}(\mathbf{p}^*)\mathcal{Y}^*_{l'm'}(\mathbf{q}^*)\,. \tag{276}$$

Substituting this expression into the Lippmann-Schwinger equation, on the energy shell we obtain:

$$T_{lm,l'm'}(s;\mathbf{P}) = \delta_{lm,l'm'}V_l(s) + 4\pi \sum_{l''m''} V_l(s)\mathcal{X}_{lm,l''m''}(s,\mathbf{P})T_{l''m'',l'm'}(s;\mathbf{P})\,, \quad (277)$$

where

$$\mathcal{X}_{lm,l'm'}(s,\mathbf{P}) = \frac{1}{L^3}\sum_{\mathbf{k}_1} \frac{\mathcal{Y}^*_{lm}(\mathbf{k}^*)\mathcal{Y}_{l'm'}(\mathbf{k}^*)}{2w_1(\mathbf{k}_1)2w_2(\mathbf{P}-\mathbf{k}_1)(w_1(\mathbf{k}_1)+w_2(\mathbf{P}-\mathbf{k}_1)-P_0)}\,. \quad (278)$$

Next, we use the identity given in Eq. (217). As we already know, all terms in the right-hand side, except the first term, do not become singular in the physical region. For regular functions, the Lüscher's regular summation theorem holds:

$$\frac{1}{L^3}\sum_{\mathbf{k}} f(\mathbf{k}) = \int \frac{d^3\mathbf{k}}{(2\pi)^3}\, f(\mathbf{k}) + \cdots\,, \quad (279)$$

where ellipses stand for the terms, exponentially suppressed at large L. Moreover, using dimensional regularization and threshold expansion, it is seen that this integral indeed vanishes. So, like in the infinite volume, only the first term survives in a finite volume, and

$$\mathcal{X}_{lm,l'm'}(s,\mathbf{P}) = \frac{1}{2P_0}\,\frac{1}{L^3}\sum_{\mathbf{k}=\mathbf{k}_1+\mu_1\mathbf{P}} \frac{\mathcal{Y}^*_{lm}(\mathbf{k}^*)\mathcal{Y}_{l'm'}(\mathbf{k}^*)}{\mathbf{k}^2 - \dfrac{(\mathbf{kP})^2}{P_0^2} - (\mathbf{p}^*)^2}\,. \quad (280)$$

In order to transform this equation further, let us define the parallel and perpendicular components of the three vectors with respect to the CM momentum $\mathbf{P}$. In particular, one may write $\mathbf{k}^* = (k^*_\parallel, \mathbf{k}^*_\perp)$, where $k^*_\parallel = (\gamma^*)^{-1}k_\parallel$, $\mathbf{k}^*_\perp = \mathbf{k}_\perp$ and $\gamma^* = (1-(v^*)^2)^{-1/2}$, $v^* = |\mathbf{P}|/E^* = |\mathbf{P}|/(w_1(\mathbf{k}^*)+w_2(\mathbf{k}^*))$. Consequently, on the energy shell $E^* = P_0$ we obtain: $\mathbf{k}^* = \mathbf{r} = (\gamma^{-1}k_\parallel, \mathbf{k}_\perp)$ with $\gamma = (1-\mathbf{P}^2/P_0^2)^{-1/2}$. Up to exponentially suppressed terms, Eq. (280) now takes the form

$$\mathcal{X}_{lm,l'm'}(s,\mathbf{P}) = \frac{(p^*)^{l+l'+1}}{32\pi^2\sqrt{s}}\, i^{l-l'}\,\mathcal{M}_{lm,l'm'}(s,\mathbf{P})\,,$$

$$\mathcal{M}_{lm,l'm'}(s,\mathbf{P}) = \frac{(-)^l}{\pi^{3/2}\gamma}\sum_{j=|l-l'|}^{l+l'}\sum_{s=-j}^{j}\frac{i^j}{\eta^{j+1}}\,Z^{\mathbf{d}}_{js}(1;s)C_{lm,js,l'm'}\,, \quad (281)$$

and the coefficients $C_{lm,js,l'm'}$ are expressed in terms of Wigner $3j$-symbols:

$$\begin{aligned} C_{lm,js,l'm'} &= (-)^{m'}i^{l-j+l'}\sqrt{(2l+1)(2j+1)(2l'+1)} \\ &\times \begin{pmatrix} l & j & l' \\ m & s & -m' \end{pmatrix}\begin{pmatrix} l & j & l' \\ 0 & 0 & 0 \end{pmatrix}\,, \end{aligned} \quad (282)$$

where

$$\mathbf{d} = \frac{2\pi}{L}\,\mathbf{P}\,, \qquad \eta = \frac{|\mathbf{p}^*|L}{2\pi}\,, \tag{283}$$

and $Z^{\mathbf{d}}_{lm}(1;s)$ stands for the so-called Lüscher zeta-function in the moving frame, characterized by the CM momentum $\mathbf{d}$ (in units of $\frac{2\pi}{L}$).

$$\begin{aligned} Z^{\mathbf{d}}_{lm}(1;s) &= \sum_{\mathbf{r}\in P_d} \frac{\mathcal{Y}_{lm}(\mathbf{r})}{\mathbf{r}^2-\eta^2}\,, \\ P_d &= \{\mathbf{r}=\mathbb{R}^3\,|\,r_\parallel = \gamma^{-1}(n_\parallel - \mu_1|\mathbf{d}|),\ \mathbf{r}_\perp = \mathbf{n}_\perp, \quad \mathbf{n}\in\mathbb{Z}^3\}\,. \end{aligned} \tag{284}$$

Note that $Z^{\mathbf{d}}_{lm}(1;s)$ is a function of s and not merely η^2. This happens because the kinematical factor γ depends on s.

The Eq. (277) is a system of linear equations that determines unknown $T_{lm,l'm'}$ through V_l. Since the rotational symmetry on a cubic lattice is broken, it mixes all values of l, m. Consequently, in order to have a tractable system of equations, one has to make a cutoff on l at some l_{max}, assuming that the partial waves with $l > l_{max}$ are negligibly small at low energies we are considering. Suppose, the cutoff is done. Than, the above equation determines the spectrum of a system in a finite box through the known phase shifts. To see this, recall that the finite-volume spectrum is determined by the pole positions of the scattering matrix. The poles emerge when the determinant of the system of linear equations (277) vanishes. Taking into account Eqs. (274,281), the equation determining the the energy spectrum can be written in the following form:

$$\det\Big(\delta_{ll'}\delta_{mm'} - \tan\delta_l(s)\mathcal{M}_{lm,l'm'}(s;\mathbf{P})\Big) = 0\,. \tag{285}$$

This is Lüscher's equation in a moving frame, or the Gottlieb-Rummukainen formula, or the quantization condition for the two-particle system. It looks quite complicated at a first glance. For illustration, let us consider the rest frame $\mathbf{d}=\mathbf{0}$ and restrict ourselves to the S-waves only. Then, Eq. (285) simplifies to an equation

$$p\cot\delta_0(p) = \frac{2}{\pi^{1/2}L}\,Z_{00}(1;\eta)\,, \quad Z_{00}(1,\eta^2) = \frac{1}{\sqrt{4\pi}}\sum_{\mathbf{n}\in\mathbb{Z}^3}\frac{1}{\mathbf{n}^2-\eta^2}\,, \quad \eta = \frac{pL}{2\pi}\,. \tag{286}$$

Given the phase shift $\delta_0(s)$, this equation determines a tower of solutions η_n, giving a finite-volume spectrum of the system, see Fig. 25. Putting the argument other way around, one can measure the energy spectrum η_n on the lattice and then calculate the phase shift $\delta_0(s)$ exactly at these energies. This method is widely used nowadays to determine the two-body phase shift for different physical systems. As a simple illustration, in Fig. 26 we show the S-wave phase shift, extracted in the φ^4-theory with the use of this method.

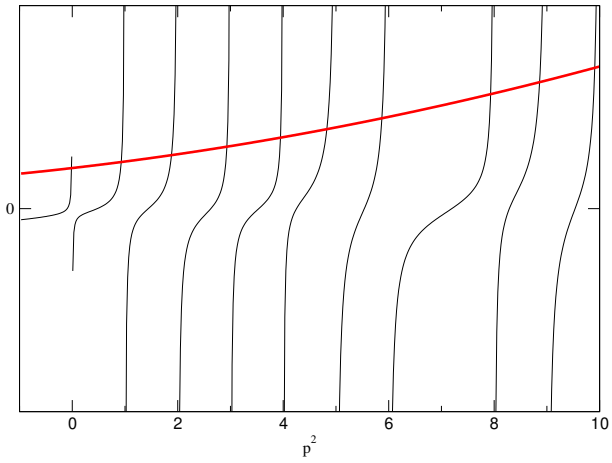

Figure 25: The Lüscher zeta-function (thin black lines) has a very irregular dependence on the momentum p for a fixed L. The intersection points with the function $p \cot \delta(p)$ (thick red line) define the spectrum of a system at a finite L.

The method,described in this section, can be trivially generalized to the multichannel scattering, if each channel contains only two particles. Than, the Lippmann-Schwinger equation one started with, is a matrix equation in the channel space. We refrain here from displaying explicit (rather cumbersome) formulae. Also, instead of working with Lippmann-Schwinger equation in the dimensional regularization, one could rewrite the equations of unitary ChPT, that usually uses cutoff regularization, in a finite volume. Physically, this approach is equivalent to the Lüscher approach (the difference amounts to only exponentially suppressed terms).

7.4 Resonances

In the vicinity of the resonances, the phase shift rapidly goes through $\pi/2$. This is seen very well in Fig. 27, which shows the P-wave phase shift in $\pi\pi$ scattering, extracted on the lattice with the use of the Lüscher method.

It is interesting to note that the energy levels behave in a peculiar wave in the vicinity of a narrow resonance. Solving the Lüscher equation with input resonance phase shift, we observe an avoided level crossing in the energy levels, see Fig. 28. Thus, the avoided level crossing, observed in data, may be a signature of a resonance at this energy[8].

However, in order to extract a resonance pole position from lattice data, an additional effort is needed. In a rigorous manner, a resonance is identified with a pole in the complex energy plane, so one has to define way, how our results could be analytically continued to the complex energies. To this end, one may invoke

[8]A caution is needed here, however. Something like avoided level crossing emerges as well, if a new threshold is open.

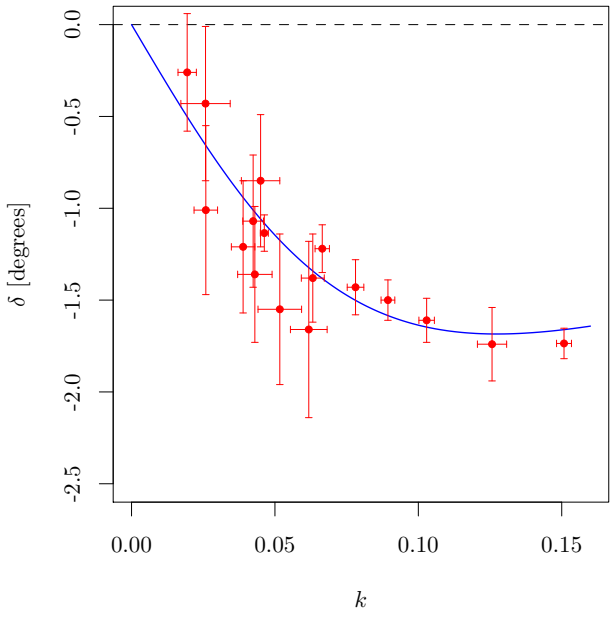

Figure 26: The S-wave scattering phase, extracted in the φ^4-theory with the help of the Lüscher equation. The solid curve corresponds to the effective-range expansion with the parameters determined on the lattice. The figure is taken from Ref. [19].

effective-range expansion, assuming, e.g., that the effective range expansion is valid up to the resonance energy. This assumption works rather well, e.g., for the physical Δ-resonance. The effective-range expansion for the scattering phase shift is written as:

$$p^{2l+1}\cot\delta_l(p) = -\frac{1}{a_l} + \frac{1}{2}\,r_l p^2 + O(p^4)\,, \qquad p^2 = \frac{\lambda(s,m_1^2,m_2^2)}{4s}\,. \tag{287}$$

This means that the lattice data allow one to determine the scattering length a_l, the effective range r_l, etc. The pole position p_R (on the second sheet) is then determined by solving an algebraic equation with known coefficients:

$$p_R^{2l+1}\cot\delta_l(p_R) = -\frac{1}{a_l} + \frac{1}{2}\,r_l p_R^2 + \cdots = -ip_R^{2l+1}\,. \tag{288}$$

It should be stressed that, in order to justify the application of this procedure, the data should cover the energy range where the resonance mass is located. There exist alternative strategies, which may be applied, if the use of the effective-range expansion is questionable.

7.5 Shallow bound states

The Lüscher method can be used to study the shallow bound states, which were considered previously in the context of the one-dimensional quantum mechanics.

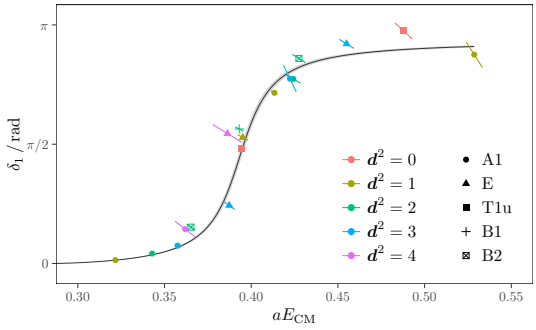

Figure 27: ETM Collaboration: ρ-resonance, seen in the P-wave $\pi\pi$ phase shift. The figure is taken from arXiv:1907.01237.

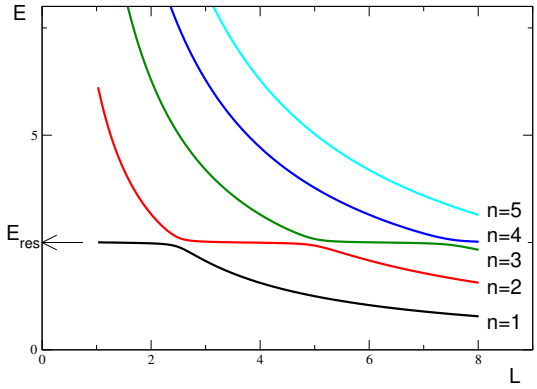

Figure 28: Avoided level crossing in the vicinity of the resonance energy.

For illustrative purpose, let us concentrate on the S-wave bound state and neglect the mixing to other partial waves completely. Further, for the bound state we have $\eta^2 = -\kappa_0^2 < 0$. For negative values of η^2, the Poisson formula can be applied and we have

$$\begin{aligned} Z_{00}(1,\eta^2) &= \frac{1}{\sqrt{4\pi}} \sum_{\mathbf{n}\in\mathbb{Z}^3} \frac{1}{\mathbf{n}^2+\kappa_0^2} = \frac{1}{2\pi^{1/2}} \int \frac{d^d\mathbf{k}}{\mathbf{k}^2+\kappa_0^2} \sum_{\mathbf{n}\in\mathbb{Z}^3} e^{2\pi i \mathbf{n}\mathbf{k}} \\ &= -\pi^{3/2}\kappa_0 + \pi^{1/2} \sum_{\mathbf{n}\neq 0} \frac{1}{n} \int_0^\infty \frac{kdk}{2\pi i} \frac{e^{2\pi i n k} - e^{-2\pi i n k}}{k^2+\kappa_0^2}\,, \end{aligned} \tag{289}$$

where $n = |\mathbf{n}|$. Changing the integration variable $k \to -k$ in the second term of the integral, and using Cauchy theorem, the integral can be evaluated:

$$Z_{00}(1,\eta^2) = -\pi^{3/2}\kappa_0 + \pi^{1/2} \sum_{\mathbf{n}\neq 0} \frac{1}{2n}\, e^{-2\pi n \kappa_0}\,. \tag{290}$$

Using $\kappa_0 = \dfrac{\kappa L}{2\pi}$, where κ is the bound-state momentum in physical units, from the Lüscher equation we get:

$$p \cot \delta_0(p) = -\kappa + \sum_{\mathbf{n}\neq 0} \frac{1}{nL} e^{-\kappa n L}\,, \qquad p = i\kappa\,. \tag{291}$$

Using the effective-range expansion for the phase shift:

$$p \cot \delta_0(p) = -\frac{1}{a} + \frac{1}{2}\, p^2 + O(p^4)\,, \tag{292}$$

The above equation can be solved iteratively:

$$\begin{aligned} \kappa &= \frac{1}{a} + \frac{r^2}{2a} + \left(1 + \frac{r}{a}\right) \sum_{\mathbf{n}\neq 0} \frac{1}{nL} e^{-\kappa n L} + \cdots \\ &= \kappa_B \left\{ 1 + \frac{1}{1 - r\kappa_B} \sum_{\mathbf{n}\neq 0} \frac{1}{n\kappa_B L} e^{-\kappa_B n L} \right\} + \cdots\,, \end{aligned} \tag{293}$$

where

$$\kappa_B = \frac{1}{a} + \frac{r^2}{2a} + \cdots \tag{294}$$

is the bound-state momentum in the infinite volume,

$$A_B = \frac{1}{(1 - r\kappa_B)^{1/2}} \tag{295}$$

is the asymptotic normalization coefficient, and ellipses stand for the higher-order terms.

At the leading order, only the term with $n = 1$ contributes to the sum, and for the shallow bound-state energy in a finite volume we get:

$$E = \frac{\kappa^2}{2m} = \frac{\kappa_B^2}{2m} \left\{ 1 + \frac{12}{\kappa_B L} \frac{1}{1 - r\kappa_B}\, e^{-\kappa_B L} \right\}. \tag{296}$$

Analogy to the case of the one-dimensional quantum mechanics is complete.

7.6 Projecting on the irreps of the cubic group

As already mentioned, the cubic lattice breaks rotational symmetry. In a result of this, the different partial waves do not decouple in the Lüscher equation.

The rotational symmetry is not broken down completely, however. In case of scattering in the rest frame, the symmetry of the box is the octahedral group (rotations + inversions), which leave a cube invariant. This group consists of 48 elements:

24 rotations, and each of them combined with an inversion. These rotations are given in Table 1. The octahedral group is a finite subgroup of the rotation group combined with the inversion of all axes. Consequently, the irreducible representations of the rotation group are also representations of the octahedral group but, in general, not irreducible anymore.

In case of scattering in the moving frame, the system is invariant under some subgroup of the octahedral group (the so-called little group), which leaves the CM vector $\mathbf{d}$ invariant. Different choices of $\mathbf{d}$ on the lattice correspond to the different little groups. In the following, we restrict ourselves to the discussion of the rest frame only, albeit the argument applies to moving frames as well without any modification.

The octahedral group has ten irreducible representations (irreps), which include 4 one-dimensional, 2 two-dimensional and 4 three-dimensional ones. They are:

- A_1 is the trivial representation, where all elements of O_h are 1.
- A_2 is the trivial representation for O times -1 when an inversion is present.
- B_1 assigns $R_i = -1$ to rotations in the conjugacy classes $6C_4$ and $6C_2'$ and $R = 1$ otherwise.
- B_2 is the same as B_1 multiplying by -1 when an inversion is present.
- E labels a two-dimensional representation. For the octahedral group, the superscript $E^{\pm}$ means whether an inversion multiplies the element by ± 1.
- $T_1^{\pm}$ is a three-dimensional representation which coincides with the Wigner matrices: $R_i = \exp(-in^i J\omega_i)$, with J the group generators and n^i and ω_i as listed in Table 1. The superscript $\pm$ labels whether spatial inversion are assigned always $+1$ or ± 1.
- $T_2^{\pm}$ is the same as T_1 with a change of sign in the conjugacy classes $6C_4$ and $6C_2'$.

Class	R_i	n	ω	$R_i(E^{\pm})$
I	1	any	0	$\mathbf{1}$
$8C_3$	2	$(1,1,1)$	$-2\pi/3$	$-\frac{1}{2}\mathbf{1}+\frac{i\sqrt{3}}{2}\sigma_2$
	3	$(1,1,1)$	$2\pi/3$	$-\frac{1}{2}\mathbf{1}-\frac{i\sqrt{3}}{2}\sigma_2$
	4	$(-1,1,1)$	$-2\pi/3$	$-\frac{1}{2}\mathbf{1}-\frac{i\sqrt{3}}{2}\sigma_2$
	5	$(-1,1,1)$	$2\pi/3$	$-\frac{1}{2}\mathbf{1}+\frac{i\sqrt{3}}{2}\sigma_2$
	6	$(-1,-1,1)$	$-2\pi/3$	$-\frac{1}{2}\mathbf{1}+\frac{i\sqrt{3}}{2}\sigma_2$
	7	$(-1,-1,1)$	$2\pi/3$	$-\frac{1}{2}\mathbf{1}-\frac{i\sqrt{3}}{2}\sigma_2$
	8	$(1,-1,1)$	$-2\pi/3$	$-\frac{1}{2}\mathbf{1}-\frac{i\sqrt{3}}{2}\sigma_2$
	9	$(1,-1,1)$	$2\pi/3$	$-\frac{1}{2}\mathbf{1}+\frac{i\sqrt{3}}{2}\sigma_2$
$6C_4$	10	$(1,0,0)$	$-\pi/2$	$-\frac{1}{2}\sigma_3-\frac{\sqrt{3}}{2}\sigma_1$
	11	$(1,0,0)$	$\pi/2$	$-\frac{1}{2}\sigma_3-\frac{\sqrt{3}}{2}\sigma_1$
	12	$(0,1,0)$	$-\pi/2$	$-\frac{1}{2}\sigma_3+\frac{\sqrt{3}}{2}\sigma_1$
	13	$(0,1,0)$	$\pi/2$	$-\frac{1}{2}\sigma_3+\frac{\sqrt{3}}{2}\sigma_1$
	14	$(0,0,1)$	$-\pi/2$	σ_3
	15	$(0,0,1)$	$\pi/2$	σ_3
$6C_2'$	16	$(0,1,1)$	$-\pi$	$-\frac{1}{2}\sigma_3-\frac{\sqrt{3}}{2}\sigma_1$
	17	$(0,-1,1)$	$-\pi$	$-\frac{1}{2}\sigma_3-\frac{\sqrt{3}}{2}\sigma_1$
	18	$(1,1,0)$	$-\pi$	σ_3
	19	$(1,-1,0)$	$-\pi$	σ_3
	20	$(1,0,1)$	$-\pi$	$-\frac{1}{2}\sigma_3+\frac{\sqrt{3}}{2}\sigma_1$
	21	$(-1,0,1)$	$-\pi$	$-\frac{1}{2}\sigma_3+\frac{\sqrt{3}}{2}\sigma_1$
$3C_2$	22	$(1,0,0)$	$-\pi$	$\mathbf{1}$
	23	$(0,1,0)$	$-\pi$	$\mathbf{1}$
	24	$(0,0,1)$	$-\pi$	$\mathbf{1}$

Table 1: Pure rotations belonging to the octahedral group. The first column indicates the conjugacy class, to which a given rotation belongs. Last column includes the element of the two dimensional irreducible representation for the cubic group.

Since the system in a finite box is invariant under the octahedral group (instead of the group of rotations), it follows from the Wigner-Eckart theorem that the quantization condition can be diagonalized in the basis belonging to different irreps, rather that in the partial-wave basis. In order to achieve the diagonalization, one introduces the projectors:

$$(P^{\Gamma,l}_{\alpha\beta})_{mm'} = \sum_{\mathcal{S}\in O_h} (R^{\Gamma}_{\alpha\beta}(\mathcal{S}))^* D^l_{mm'}(\mathcal{S})\,. \tag{297}$$

Here, $\mathcal{S}$ runs over all 48 elements of the octahedral group, $R^{\Gamma}_{\alpha\beta}(\mathcal{S})$ are matrices, belonging to the particular irrep Γ of O_h, and $D^l_{mm'}(\mathcal{S})$ ale usual Wigner matrices. If $\mathcal{S}=I\bar{\mathcal{S}}$ consists of a pure rotation and an inversion, then, by definition, $D^l_{mm'}(\mathcal{S})=$

$(-1)^l D^l_{mm'}(\bar{\mathcal{S}})$. Acting now with these projectors on the basis vectors $|lm\rangle$ of the rotation group, we get the (unnormalized) basis vectors of the irrep Γ:

$$|\Gamma, \alpha, l, n\rangle = \sum_{m'} (P^{\Gamma,l}_{\alpha\beta})_{mm'} |lm'\rangle \,, \qquad m \text{ and } \beta \text{ fixed}, \tag{298}$$

where n labels the multiple occurrences of Γ for a given l. Acting in this manner, we can determine all coefficients in the expansion of the basis vectors $|\Gamma, \alpha, l, n\rangle$:

$$|\Gamma, \alpha, l, n\rangle = \sum_{m} c^{\Gamma\alpha n}_{lm} |lm\rangle \,. \tag{299}$$

The matrix elements of the operator $\mathcal{M}$ from Eq. (285) in the new basis are given by:

$$\langle \Gamma\alpha ln|\mathcal{M}|\Gamma'\alpha' l' n'\rangle = \sum_{mm'} (c^{\Gamma\alpha n}_{lm})^* c^{\Gamma'\alpha' n'}_{l'm'} \mathcal{M}_{lm,l'm'} \,. \tag{300}$$

According to the Wigner-Eckart theorem,

$$\langle \Gamma\alpha ln|\mathcal{M}|\Gamma'\alpha' l' n'\rangle = \delta_{\Gamma\Gamma'}\delta_{\alpha\alpha'} \mathcal{M}^{\Gamma}_{ln,l'n'} \tag{301}$$

and the Eq. (285) in a particular irrep Γ reduces to (in the rest frame)

$$\det\left(\delta_{ll'}\delta_{nn'} - \tan\delta_l(s) \mathcal{M}^{\Gamma}_{ln,l'n'}(s, \mathbf{0}) \right) = 0 \,. \tag{302}$$

The dimension of the matrix in this equation is much smaller that in the original one – for example, the indices m, m' do not appear at all. Moreover, these equations allow one to study the spectrum in a particular irrep Γ, whereas the original equation contained the spectrum from all irreps.

Few remarks are in order:

- As mentioned already, the same method applies in case of the moving frame as well. In this case, when constructing the projection operators, the sum runs over the elements of a little group instead of O_h. Further, Γ and $R^{\Gamma}_{\alpha\beta}(\mathcal{S})$ stand for a particular irrep of a little group and the matrices in this irrep, respectively.

- The formalism can be extended in case of particles with spin. In case of the half-integer total spin, the symmetry group is the double cover of the octahedral group (and the little groups thereof).

- Using the method of projection operators, one may systematically construct the operators that belong to a particular irrep Γ.

7.7 Lellouch-Lüscher formula

As a next illustration of the might and beauty of the effective field theory approach, we discuss the extraction of the timelike scalar form factor on the lattice (this is exactly the place where the approach a la Maiani and Testa fails). The main conceptual problem, that is also the reason for that failure, can be reformulated as follows: on the lattice, one may extract the matrix element of the current operator between the vacuum and a two-pion state in a finite volume. Increasing now L continuously, we see that a given state collapses toward threshold, so a trivial result emerges in the infinite volume limit. If we instead fix the energy of two pions and increase L, the measured matrix element will oscillate wildly and does not show sign of converging at $L \to \infty$. So, how does one extract this matrix element on the lattice?

The NREFT can rescue the situation. Here, the bridge between the finite- and infinite-volume cases is provided by the Lagrangian, which is the same in both cases. So, carrying out calculations twice, in a finite and in the infinite volume, one can express the infinite-volume matrix element through its finite-volume counterpart and perform the infinite-volume limit.

Below, we shall demonstrate, how does this approach work. For simplicity, we consider the rest frame, albeit the treatment can be carried out in arbitrary moving frames. Also, to ease notations, we consider the case of non-identical particles with the same mass (e.g., π^+ and π^- in the calculation of the timelike electromagnetic form factor of the pion). We in addition assume that all particles and currents are scalar. Generalizations are obvious.

In order to study the form factor, the non-relativistic Lagrangian in Eq. (264) should be equipped by the part that describes the interaction with the external field $A(x)$. This part of the Lagrangians takes the form

$$\mathcal{L}_{\mathsf{A}} = eA(x)j(x) = eA\phi_1^\dagger\phi_2^\dagger + \text{terms with derivatives} + \text{h.c.}\,, \tag{303}$$

where the low-energy constants $e, \cdots$ describe the coupling of the field $A(x)$ to $\phi_{1,2}$.

Define now the two-particle operators

$$\mathcal{O}(x_0;\mathbf{k}) \;=\; \int_{-L/2}^{L/2} d^3\mathbf{x}\, d^3\mathbf{y}\, e^{-i\mathbf{k}(\mathbf{x}-\mathbf{y})}\, \phi_1(x_0,\mathbf{x})\phi_2(x_0,\mathbf{y})\,, \tag{304}$$

where $\mathbf{k} = \dfrac{2\pi}{L}\,\mathbf{n},\ \mathbf{n} \in \mathbb{Z}^3$, and consider the following matrix element in Euclidean space for $x_0 > y_0$:

$$\langle 0|T\mathcal{O}(x_0;\mathbf{k})\mathcal{O}^\dagger(y_0;\mathbf{k})|0\rangle = \sum_n |\langle 0|\mathcal{O}(0;\mathbf{k})|E_n\rangle|^2 e^{-E_n(x_0-y_0)}\,, \tag{305}$$

where the E_n denote the energy eigenvalues.

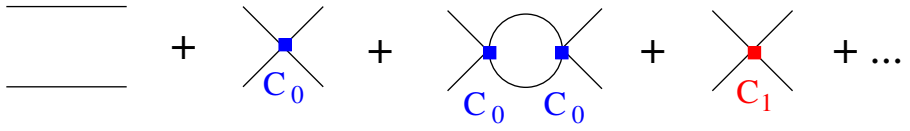

Figure 29: Diagrams contributing to the matrix element on the l.h.s of Eq. (305) in perturbation theory. The first diagram corresponds to the free propagation of the fields $\phi_{1,2}$.

Note that in the non-relativistic EFT the above matrix element can be calculated in perturbation theory. The pertinent diagrams are shown in Fig. 29. Using the Euclidean-space propagator in the non-relativistic EFT

$$\langle 0|T\phi_i(x)\phi_i^\dagger(y)|0\rangle = \int \frac{dp_0}{2\pi}\,\frac{1}{L^3}\sum_{\mathbf{p}}\frac{e^{ip_0(x_0-y_0)+i\mathbf{p}(\mathbf{x}-\mathbf{y})}}{2w(\mathbf{p})(w(\mathbf{p})+ip_0)}\,, \tag{306}$$

for this matrix element we get:

$$\begin{aligned}\langle 0|T\mathcal{O}(x_0;\mathbf{k})\mathcal{O}^\dagger(y_0;\mathbf{k})|0\rangle &= L^3\int\frac{dP_0}{2\pi}\,e^{iP_0(x_0-y_0)}\\ \times\ &\left\{\frac{-iL^3}{4w^2(\mathbf{k}))(P_0-2iw(\mathbf{k}))}-\frac{T}{(4w^2(\mathbf{k}))^2(P_0-2iw(\mathbf{k}))^2}\right\},\end{aligned} \tag{307}$$

where T is the forward scattering amplitude (see Fig. 29):

$$\begin{aligned}T &= C_0+C_0^2\frac{1}{L^3}\sum_{\mathbf{l}}\frac{1}{4w^2(\mathbf{l})(2w(\mathbf{l})+iP_0)}+\cdots\,.\\ &= C_0+C_0^2\frac{p}{8\pi^{5/2}\sqrt{s}\eta}\,Z_{00}(1;\eta^2)+\cdots\,,\\ &\qquad s=-P_0^2\,,\qquad p=\sqrt{\frac{s}{4}-m^2}\,,\qquad \eta=\frac{pL}{2\pi}\,,\end{aligned} \tag{308}$$

where we have used Eqs. (278,281), and where we have retained only the S-wave contribution in the scattering matrix in order to simplify the discussion of the scalar form factor. Using Eqs. (266,274), the tree-level and bubble diagrams in Fig. 29 can be summed up to all orders. The result on the energy shell is given by

$$T=\frac{8\pi\sqrt{s}}{p\cot\delta(p)+p\cot\phi(p)}\,,\qquad \tan\phi(p)=-\frac{\pi^{3/2}\eta}{Z_{00}(1;\eta^2)}\,, \tag{309}$$

where $\delta(s)=\delta_0(s)$ denotes the S-wave phase shift.

The poles of the T-matrix are determined by the Lüscher equation:

$$\delta(p_n)=-\phi(p_n)+\pi n\,,\qquad s_n=E_n^2=4(m^2+p_n^2)\,. \tag{310}$$

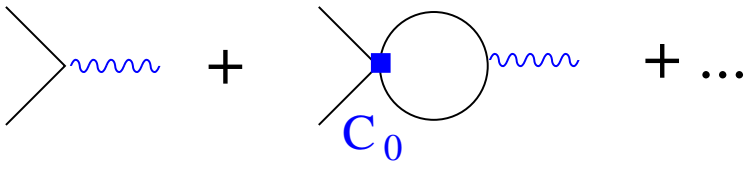

Figure 30: Diagrams contributing to the vertex function. The wiggly line corresponds to the external field $A(x)$.

The quantity T defined by Eq. (309) has poles at at $P_0 = iE_n$. In the vicinity of this pole, the quantity T behaves as:

$$T \to \frac{32\pi \sin^2 \delta(p_n)}{\delta'(p_n) + \phi'(p_n)} \frac{1}{E_n + iP_0} + \text{regular terms}\,, \tag{311}$$

where the derivative is taken with respect to the variable p. Substituting now this expression into Eq. (307), performing the integral over P_0 and taking into account the fact that the "free" poles at $P_0 = 2iw(\mathbf{k})$ cancel in the integrand, the final expression for the matrix element in Eq. (307) for $x_0 - y_0 > 0$ reads:

$$\langle 0|T\mathcal{O}(x_0;\mathbf{k})\mathcal{O}^\dagger(y_0;\mathbf{k})|0\rangle = L^3 \sum_n \frac{32\pi \sin^2 \delta(p_n)}{\delta'(p_n) + \phi'(p_n)} \frac{e^{-E_n(x_0-y_0)}}{(4w^2(\mathbf{k}))^2(E_n - 2w(\mathbf{k}))^2}\,. \tag{312}$$

Comparing this expression with Eq. (305), one reads off:

$$|\langle 0|\mathcal{O}(0;\mathbf{k})|E_n\rangle| = L^{3/2} \frac{32\pi \sin^2 \delta(p_n)}{|\delta'(p_n) + \phi'(p_n)|} \frac{1}{4w^2(\mathbf{k})} \frac{1}{|E_n - 2w(\mathbf{k})|}\,. \tag{313}$$

Next, we turn to the determination of the form factor in the time-like region. To this end, we have to consider the amplitude of pair creation from the vacuum in the presence of an external field $A(x)$, at the first order in the coupling e. This matrix element is described by

$$\langle 0|\mathcal{O}(x_0;\mathbf{k})\,\mathcal{L}_{\mathsf{A}}(0)|0\rangle = eA(0)F[\mathbf{k};x_0]\,, \qquad x_0 > 0\,. \tag{314}$$

We evaluate the quantity F in perturbation theory. The pertinent diagrams are shown in Fig. 30. Summing up all bubbles yields:

$$F[\mathbf{k};x_0] = \bar{F}(t) \int \frac{dP_0}{2\pi i} \frac{e^{iP_0x_0}}{4w^2(\mathbf{k})(P_0 - 2iw(\mathbf{k}))} \frac{p\cot\delta(p)}{p\cot\delta(p) + p\cot\phi(p)}\,, \tag{315}$$

where the quantity $\bar{F}(t)$ is a low-energy polynomial that is obtained from the Lagrangian in Eq. (303) at tree level.

Using Eq. (311), we may now perform the integration over the variable P_0 in Eq. (315), with the result

$$F[\mathbf{k};x_0] = \bar{F}(t) \sum_n \frac{e^{-E_nx_0}}{4w^2(\mathbf{k})(2w(\mathbf{k}) - E_n)} \frac{4p\cot\delta(p_n)\sin^2\delta(p_n)}{(\delta'(p_n) + \phi'(p_n))E_n}\,. \tag{316}$$

On the other hand, the matrix element in Eq. (314) has the following representation:

$$\langle 0|T\mathcal{O}(x_0;\mathbf{k})\,\mathcal{L}_{\mathsf{A}}(0)|0\rangle = eA(0)\sum_n e^{-E_n x_0}\langle 0|\mathcal{O}(0;\mathbf{k})|E_n\rangle\langle E_n|j(0)|0\rangle\,. \tag{317}$$

Using Eqs. (313), (316) and (317), we get

$$|\langle E_n|j(0)|0\rangle| = L^{-3/2}|\bar{F}(t)|\frac{p|\cos\delta(p_n)|}{(2\pi E_n^2)^{1/2}}\,\frac{1}{|\delta'(p_n)+\phi'(p_n)|^{1/2}}\,. \tag{318}$$

This is the expression of the matrix element in a finite volume. It should be compared with its counterpart in the infinite volume, which is obtained by using Watson's theorem:

$$\langle k_1,k_2;\mathsf{out}|j(0)|0\rangle = F(t)\,,\qquad |F(t)| = |\bar{F}(t)\cos\delta(s)|\,. \tag{319}$$

From Eqs. (318) and (319) we finally get:

$$|F(t)|^2 = |L^{3/2}\langle E_n|j(0)|0\rangle|^2\frac{2\pi E_n^2}{p^2}\,|\delta'(p_n)+\phi'(p_n)|\,. \tag{320}$$

This expression allows one to extract the absolute value of a scalar form factor in the time-like region from the measured matrix element $\langle E_n(\mathbf{P})|j(0)|0\rangle$ in a finite volume. The factor proportional to $|\delta'(p_n)+\phi'(p_n)|$, known as Lellouch-Lüscher factor, rescues the situation. It is an irregular function of L, like the finite-volume matrix element $\langle E_n|j(0)|0\rangle$. However, the combination, which is present in Eq. (320) has a smooth limit that coincides with the absolute value of the infinite-volume form factor squared. Since the phase of this form factor, which is determined by Watson's theorem, is also measurable on the lattice, we finally conclude that the real and imaginary parts of the form factor can be measured on the lattice in the elastic region.

7.8 Three particles

There are quite a few reasons that justify our interest to the study of the three-particle problem in a finite volume:

- The presence of the multi-particle inelastic channels imposes a major limitation on the applicability of the Lüscher approach for 2 particles. One would like to have a framework that allows to include these channels explicitly.

- There are quite some resonances that decay (predominately or to a large part), into the three-particle final states. These are both the well-known decays, like $K\to 3\pi\,,\ \eta\to 3\pi\,,\ \omega\to 3\pi$ or the decay of the Roper resonance, as well as the decays of exotic particles. In this respect, one would like to ask:

Figure 31: The dimer propagator, as a sum over bubbles.

  - How does one extract the mass and width of a resonance?
  - Is there an analog of the Lellouch-Lüscher formula for three particles?

- Three-particle dynamics is needed to study nuclear physics on the lattice, e.g., the reaction like $nd \to nd$.

Let us explain in more detail, what are the requirements to the framework we are looking for. In the infinite volume, we have a host of observables: the characteristics of the three-body bound states, the amplitudes for the elastic scattering, rearrangement and breakup reactions, the matrix elements with the interaction in a final state, like the one that describes the weak decay of a kaon into three pions, $\langle K|H_W|\pi\pi\pi\rangle$. In a finite volume, however, one could measure the two- and three-particle energy levels, and the counterparts of the displayed matrix elements in a finite volume. Hence, we need a framework that "translates" the input finite-volume data into the infinite volume output. Based on our experience in the two-particle sector, one expects this to be a tough job.

Still, as we shall demonstrate below, the methods of the NREFT, with small modifications, apply in the three-particle sector as well, and enable one to achieve the goal. The link is again provided by the couplings in the Lagrangian – these are the same in a finite and in the infinite volume. In other words, these couplings, determined from the lattice data, possess a smooth infinite-volume limit, unlike the amplitudes and the matrix elements, which wildly oscillate in this limit.

This defines the general two-step strategy in the three-particle sector: only the couplings (or equivalent quantities) are determined from lattice data. All physical observables in the scattering sector are obtained by solving the integral equations with given values of the couplings. A direct relation of the amplitudes with the measured spectrum (like the Lüscher equation in the two-particle sector) is, in general, not possible.

Let us now see, how does this strategy work. We again start with the NREFT in the two-particle sector and write down the familiar Lagrangian:

$$\mathcal{L}_2 = \phi^\dagger \left(i\partial_t - m + \frac{\nabla^2}{2m} \right) \phi + c_0\, \phi^\dagger \phi^\dagger \phi \phi + \cdots \,. \tag{321}$$

To apply the formalism to the three-particle sector, it is useful to introduce an auxiliary dimer field T in the Lagrangian:

$$\mathcal{L}_2^{\text{dimer}} = \phi^\dagger \left(i\partial_0 - m + \frac{\nabla^2}{2m} \right) \phi + \sigma T^\dagger T + \left(T^\dagger \left[f_0 \phi\phi + \cdots \right] + \text{h.c.} \right). \tag{322}$$

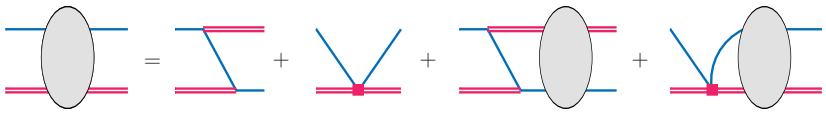

Figure 32: Bethe-Salpeter equation for the particle-dimer amplitude.The three-particle amplitude is obtained from the particle-dimer amplitude by multiplying each external dimer leg with the two-particle-dimer vertex.

Here, $\sigma = \pm 1$. Integrating out the field T, we arrive at the Lagrangian in Eq. (321) with $c_0 = -\dfrac{f_0^2}{\sigma}$. Physically, a dimer propagator, shown in Fig. 31, corresponds to the sum of all bubble diagrams that yield the two-body scattering amplitude. For example, in the rest frame,

$$\begin{aligned} D(P_0, \mathbf{0}) &= \frac{1}{\sigma} + \frac{1}{\sigma^2}\, 2f_0^2\, J + \frac{1}{\sigma^3}\, (2f_0^2\, J)^2 + \cdots = \frac{\sigma}{1 - \dfrac{2f_0^2}{\sigma}\, J + \cdots} \\ &= \frac{z}{p \cot \delta(p) - ip}\,, \end{aligned} \tag{323}$$

where

$$z = \frac{2\pi}{m f_0^2} + \cdots\,, \qquad p = \sqrt{m(P_0 - 2m)}\,. \tag{324}$$

Here J denotes a bubble:

$$J = \int \frac{d^D k}{(2\pi)^D i}\, \frac{1}{m + \dfrac{\mathbf{k}^2}{2m} - k_0 - i\varepsilon}\, \frac{1}{m + \dfrac{\mathbf{k}^2}{2m} - P_0 + k_0 - i\varepsilon} = \frac{imp}{4\pi}\,. \tag{325}$$

Note also that, in order to simplify the notations, we introduced here an S-wave dimer only. This restriction can be easily lifted.

Similar to this, the three-body Lagrangian

$$\mathcal{L}_3 = d_0\, \phi^\dagger \phi^\dagger \phi^\dagger \phi \phi \phi + \cdots \tag{326}$$

can be easily rewritten by using the auxiliary dimer field:

$$\mathcal{L}_3^{\mathsf{dimer}} = h_0 T^\dagger T \psi^\dagger \psi + \cdots\,, \tag{327}$$

with

$$d_0 = f_0^2 h_0\,. \tag{328}$$

The particle-dimer scattering amplitude obeys the Bethe-Salpeter equation, see Fig. 32:

$$\mathcal{M}(\mathbf{p},\mathbf{q};E) = Z(\mathbf{p},\mathbf{q};E) + \int^{\Lambda} \frac{d^3\mathbf{k}}{(2\pi)^3}\, Z(\mathbf{p},\mathbf{k};E)\tau(\mathbf{k};E)\mathcal{M}(\mathbf{k},\mathbf{q};E)\,, \tag{329}$$

where

$$Z(\mathbf{p},\mathbf{q};E) = \frac{1}{\mathbf{p}^2+\mathbf{q}^2+\mathbf{pq}-mE} + H_0 + \cdots\,, \tag{330}$$

and

$$H_0(\Lambda) = \frac{h_0}{mf_0^2}\,. \tag{331}$$

Note also that here only the leading particle-dimer interaction is taken into account. At higher orders, one has to replace:

$$H_0(\Lambda) \to H_0(\Lambda) + H_1(\Lambda)(\mathbf{p}^2+\mathbf{q}^2) + \cdots\,. \tag{332}$$

Further, the two-body amplitude (the dimer propagator) is not in the rest-frame anymore. The expression for this quantity takes the form:

$$\tau^{-1}(\mathbf{k};E) = k^*\cot\delta(k^*) + ik^*\,, \tag{333}$$

where

$$ik^* = \sqrt{\frac{3}{4}\,\mathbf{k}^2 - mE} \tag{334}$$

Next, let us consider the three-particle system in a finite volume. The Bethe-Salpeter equation remains the same, except that the momenta are now discretized:

$$\mathcal{M}_L(\mathbf{p},\mathbf{q};E) = Z(\mathbf{p},\mathbf{q};E) + \frac{8\pi}{L^3}\sum_{\mathbf{k}}^{\Lambda} Z(\mathbf{p},\mathbf{q};E)\tau_L(\mathbf{k};E)\mathcal{M}_L(\mathbf{k},\mathbf{q};E) \tag{335}$$

and

$$\tau_L^{-1}(\mathbf{k};E) = k^*\cot\delta(k^*) - \frac{4\pi}{L^3}\sum_{\mathbf{l}}\frac{1}{\mathbf{k}^2+\mathbf{l}^2+\mathbf{kl}-mE} \tag{336}$$

In a complete analogy with the two-particle case, the energy levels are determined by the zeros of the determinant of the above linear equation. Consequently, the quantization condition in the three-particle case is given by:

$$\det(\tau_L^{-1} - Z) = 0\,. \tag{337}$$

Note that this is a matrix in the space of the discrete three-momentum $\mathbf{k}$. As in the two-particle case, one can use the symmetry with respect to the octahedral group and obtain the quantization condition in different irreps. We shall not pursue this issue anymore.

The workflow in analyzing data from the three-particle sector can be schematically represented as follows: the scattering phase $\delta(p)$ can be determined separately in the two-particle sector, using the Lüscher equation. What remains unknown are the couplings $H_0(\Lambda), H_1(\Lambda), \ldots$. These should be determined from the fit to the measured energy shift in the three-particle sector. At the end, the particle-dimer scattering amplitude is obtained from the solution of the Bethe-Salpeter equation in the infinite volume by using the values of $H_0(\Lambda), H_1(\Lambda), \ldots$, determined on the lattice. all other amplitudes can be then expressed from the particle-dimer amplitude.

8 Literature

Disclaimer: the given list of literature does not pretend to include everything. I decided to give only few references, which were directly related to the issues considered in the lectures.

- For the lattice formulation of quantum mechanics, I would recommend Refs. [1, 2].
- There exist several good textbooks on lattice quantum field theory and lattice QCD, which I also recommend, see Refs. [3–6].
- For the introduction to Chiral Perturbation Theory, you may consult Refs. [7, 8].
- The introduction to the NREFT can be found, e.g., in Ref. [9] (standard approach) and in Ref. [10] (relativized NREFT).
- Corrections to the stable particle masses, to the binding energies, the shift of the ground-state energy and the scattering on the torus is considered in Refs. [11–13].
- The chiral limit is considered, e.g., in Ref. [14].
- The perturbative shift of the ground state is considered, e.g., in Ref. [15].
- For the derivation of the Lüscher equation in NREFT, see, e.g., Refs. [16, 17].
- The group-theoretical analysis of the Lüscher equation is given in Ref. [18], see also references therein.

- The finite-volume aspects of the φ^4-theory on the lattice in considered in Ref. [19].
- The formalism to treat three particles in a finite volume, which is based on NREFT, is given in Ref. [20], see also [21] for the relativistic-invariant formulation. Alternative approaches are discussed, e.g., in Refs. [22, 23].
- The three-particle analog of the Lellouch-Lüscher equation is considered, e.g., in Refs. [24–26].

References

[1] G. P. Lepage, "Lattice QCD for novices," hep-lat/0506036.

[2] M. Creutz and B. Freedman, "A Statistical Approach To Quantum Mechanics," Annals Phys. **132** (1981) 427.

[3] J. Smit, "Introduction to quantum fields on a lattice: A robust mate," Cambridge Lect. Notes Phys. **15** (2002) 1.

[4] I. Montvay and G. Munster, "Quantum fields on a lattice,"

[5] C. Gattringer and C. B. Lang, "Quantum chromodynamics on the lattice," Lect. Notes Phys. **788** (2010) 1.

[6] H. J. Rothe, "Lattice gauge theories: An Introduction," World Sci. Lect. Notes Phys. **43** (1992) 1 [World Sci. Lect. Notes Phys. **59** (1997) 1] [World Sci. Lect. Notes Phys. **74** (2005) 1] [World Sci. Lect. Notes Phys. **82** (2012) 1].

[7] S. Scherer, Adv. Nucl. Phys. **27** (2003) 277 [hep-ph/0210398].

[8] S. Scherer, "Chiral Perturbation Theory: Introduction and Recent Results in the One-Nucleon Sector," Prog. Part. Nucl. Phys. **64** (2010) 1 [arXiv:0908.3425 [hep-ph]].

[9] J. Gasser, V. E. Lyubovitskij and A. Rusetsky, "Hadronic atoms in QCD + QED," Phys. Rept. **456** (2008) 167 [arXiv:0711.3522 [hep-ph]].

[10] J. Gasser, B. Kubis and A. Rusetsky, "Cusps in K –¿ 3pi decays: a theoretical framework," Nucl. Phys. B **850** (2011) 96 [arXiv:1103.4273 [hep-ph]].

[11] M. Lüscher, "Volume Dependence of the Energy Spectrum in Massive Quantum Field Theories. 1. Stable Particle States," Commun. Math. Phys. **104** (1986) 177.

[12] M. Lüscher, "Volume Dependence of the Energy Spectrum in Massive Quantum Field Theories. 2. Scattering States," Commun. Math. Phys. **105** (1986) 153.

[13] M. Lüscher, "Two particle states on a torus and their relation to the scattering matrix," Nucl. Phys. B **354** (1991) 531.

[14] H. Leutwyler, "Energy Levels of Light Quarks Confined to a Box," Phys. Lett. B **189** (1987) 197.

[15] S. R. Beane, W. Detmold and M. J. Savage, "n-Boson Energies at Finite Volume and Three-Boson Interactions," Phys. Rev. D **76** (2007) 074507 [arXiv:0707.1670 [hep-lat]].

[16] S. R. Beane, P. F. Bedaque, A. Parreno and M. J. Savage, "Exploring hyperons and hypernuclei with lattice QCD," Nucl. Phys. A **747** (2005) 55 [nucl-th/0311027].

[17] V. Bernard, D. Hoja, U.-G. Meißner and A. Rusetsky, "Matrix elements of unstable states," JHEP **1209** (2012) 023 [arXiv:1205.4642 [hep-lat]].

[18] M. Göckeler, R. Horsley, M. Lage, U.-G. Meißner, P. E. L. Rakow, A. Rusetsky, G. Schierholz and J. M. Zanotti, "Scattering phases for meson and baryon resonances on general moving-frame lattices," Phys. Rev. D **86** (2012) 094513 [arXiv:1206.4141 [hep-lat]].

[19] F. Romero-Lopez, A. Rusetsky and C. Urbach, "Two- and three-body interactions in φ^4 theory from lattice simulations," Eur. Phys. J. C **78** (2018) no.10, 846 [arXiv:1806.02367 [hep-lat]].

[20] H.-W. Hammer, J.-Y. Pang and A. Rusetsky, "Three particle quantization condition in a finite volume: 2. general formalism and the analysis of data," JHEP **1710** (2017) 115 [arXiv:1707.02176 [hep-lat]].

[21] F. Müller, J. Y. Pang, A. Rusetsky and J. J. Wu, "Relativistic-invariant formulation of the NREFT three-particle quantization condition," JHEP **02** (2022), 158 [arXiv:2110.09351 [hep-lat]].

[22] M. T. Hansen and S. R. Sharpe, "Relativistic, model-independent, three-particle quantization condition," Phys. Rev. D **90** (2014) no.11, 116003 [arXiv:1408.5933 [hep-lat]].

[23] M. Mai and M. Döring, "Three-body Unitarity in the Finite Volume," Eur. Phys. J. A **53** (2017) no.12, 240 [arXiv:1709.08222 [hep-lat]].

[24] F. Müller and A. Rusetsky, JHEP **03** (2021), 152 doi:10.1007/JHEP03(2021)152 [arXiv:2012.13957 [hep-lat]].

[25] F. Müller, J. Y. Pang, A. Rusetsky and J. J. Wu, "Three-particle Lellouch-Lüscher formalism in moving frames," JHEP **02** (2023), 214 [arXiv:2211.10126 [hep-lat]].

[26] M. T. Hansen, F. Romero-López and S. R. Sharpe, JHEP **04** (2021), 113 doi:10.1007/JHEP04(2021)113 [arXiv:2101.10246 [hep-lat]].